INAUGURAL-DISSERTATION

submitted to the

Combined Faculties of Natural Sciences and Mathematics

of the Ruperto-Carola University of Heidelberg/Germany

for the degree of

Doctor of Natural Sciences (Doctor rerum naturae)

A novel function for the eukaryotic translation elongation factor 1A

presented by the

Diploma-Biologist Udo Többen

from Börger

Day of oral examination:_____

INAUGURAL-DISSERTATION

submitted to the

Combined Faculties of Natural Sciences and Mathematics

of the Ruperto-Carola University of Heidelberg/Germany

for the degree of

Doctor of Natural Sciences (Doctor rerum naturae)

presented by the

Diploma-Biologist Udo Többen

from Börger

Day of oral examination: _____

A novel function for the eukaryotic translation elongation factor 1A

Referees: Prof. Dr. Felix T. Wieland

Prof. Dr. Martin Wiedmann

Forsan et haec olim meminisse iuvabit !

Vos igitur, doctrinae et sapientiae filii, perquirite in hoc libro colligendo meam dispersam intentionem quam in diversis locis proposui et quod occultam est a me in uno loco, manifestum feci illud in alio, ut sapientibus vobis patefiat.

Acknowledgements

I would like to thank everybody, who supported me in one or another way, actively or passively, and thus contributed to the succesful ending of this enterprise.

Particular thanks are due to Prof. Dr. Felix T. Wieland for giving me the opportunity to pursue this work and Prof. Dr. Martin Wiedmann for providing all the freedom I wanted and advice I needed to explore Life, the Universe and Everything … of the ribosome. For as long as one can say that *"In the end of the day we learned something"*, we are on the right track. Or to quote a source with a profound influence on me: "*Even the most lunatic experiments can produce strange side effects, stimulating research that proves perhaps less amusing but scientifically more serious.*"

I have to single out the former and current members of the Wiedmann- and Lauring-lab. Their scientific (and by times not so scientific) input was decisive in putting forward this work, although some explanations will remain mysterious to me forever – despite intense efforts shall I never find the famous "Anywhere" nor understand Cricket.

Furthermore, I would like to give a big **Thank you!** to all the current and former colleagues and friends in the Rothman-, Söllner-, Massague-, Patel-, and Tempst-lab for the fruitful discussions about scientific issues as well as anything else. All other friends and acquaintances be thanked for keeping me sane by diverting my mind to issues other than science.

I deeply apologize for forgetting to mention anybody, who should have been named here. This is solely attributable to my current limited mental capacity and happens by no means intentionally.

New York, June 2004

A novel function for the eukaryotic translation elongation factor 1A

2 Summary

The eukaryotic translation elongation factor 1A, eEF1A, a homolog of the bacterial EF1A (formerly known as EF-Tu), is a well-characterized ribosome associated factor, responsible for the delivery of aminoacyl-tRNA^{aa} to the ribosomal A site.

In contrast to this indirect interaction with the nascent polypeptide chain it is shown here for the first time that eEF1A also associates directly with the nascent polypetide chain distal to the peptidyl transferase center of the ribosome. This is demonstrated for a variety of nascent polypeptide chains of different length and sequence. Interestingly, unlike other ribosome associated factors, eEF1A also interacts with polypeptides after their release from the ribosome. It is further demonstrated that eEF1A does not bind to correctly folded full-length proteins, but interacts specifically with proteins that are unable to fold correctly in a cytosolic environment. This association was demonstrated both by photo-crosslinking and by a functional refolding assay.

Furthermore, it is shown that the interaction of the nascent polypeptide chain with eEF1A can be competed out with a variety of short peptides. However, the found minimum length of 20-30 amino acids for these short peptides is significantly longer than typical binding sites in molecular chaperones or MHCs which is about seven to nine amino acids in length. The presence of charged aa-tRNA^{aa} or uncharged tRNA^{aa} in crosslinking experiments elicited a dose-dependent response similar to that seen in the competition experiments with short peptides.

Gel-filtration demonstrated that eEF1A exhibits “quasi chaperone” activities, because eEF1A seems to be able to dissolve large complexes of oligomerized peptides and co-migrates with the dissolved peptide.

Based upon the results of this work a model describing a novel function for eEF1A is presented.

2 Zusammenfassung

Der eukaryontische Translations-Elongationsfaktor 1A (eEF1A) ist ein sehr gut charakterisierter Ribosom-assoziierter Faktor, der für die Lieferung von Aminoacyl-tRNA^{aa} zur ribosomalen A Stelle verantwortlich ist. Er ist homolog zum bakteriellen EF1A (früher EF-Tu genannt).

Der Elongationsfaktor 1A ist nicht nur für die indirekte Interaktion über die aa-tRNA^{aa} mit der naszierenden Polypeptidekette verantwortlich, sondern er tritt, wie hier zum ersten Mal gezeigt wird, auch direkt mit der naszierenden Polypeptidekette distal des Peptidyltransferasezentrums des Ribosoms in Kontakt. Dies wird mit einer Vielzahl von naszierenden Polypeptidketten von verschiedener Länge und Sequenz demonstriert. Interessanterweise interagiert eEF1A im Gegensatz zu anderen Ribosom-assoziierten Faktoren auch mit Polypeptidketten, nachdem diese vom Ribosom losgelöst sind. Weiterhin wird gezeigt, daß eEF1A präferentiell an nicht korrekt gefaltete Proteine bindet, wenn diese sich nach erreichen der vollen Länge vom Ribosom lösen. Dieser enge Kontakt wurde sowohl mittels Photoquervernetzung als auch durch funktionale Rückfaltungsexperimente demonstriert.

Es wird zudem gezeigt, daß die Interaktion der naszierenden Polypeptidekette mit eEF1A durch verschiedene kurze Peptide kompetitiert werden kann. Im Verlaufe der Arbeit wurde klar, daß eine Minimumlänge von 20-30 Aminosäuren für die Verdrängung benötigt wird. Dies ist jedoch signifikant länger als die sieben bis neun Aminosäuren von Peptiden, die typischerweise an molekulare Chaperone oder MHCs binden. Ein ähnlicher Verdrängungseffekt wurde mit geladener aa-tRNA^{aa} und ungeladener tRNA^{aa} in Quervernetzungsexperimenten in Dosisabhängigkeit hervorgerufen.

Mit Gelfiltration wurde nachgewiesen, daß eEF1A in der Lage ist, große Komplexe aus oligomerisierten Peptiden aufzulösen. In diesem Verhalten ähnelt eEF1A einem molekularem Chaperone.

Basierend auf den Ergebnissen dieser Arbeit wird ein Modell vorgestellt, daß eine neuartige Funktion für eEF1A beschreibt.

3 Introduction

3.1 The ribosome – a short historical account

Ribosomes are and have been for a long time a prominent object of genetical, biochemical and molecular studies. The high interest is due to the eminent role protein synthesis plays for living entities: life as we know it is on a cellular level functionally based on proper interactions of proteins – and ribosomes are the resource for protein production.

Starting with studies of the Rous sarcoma (1,2) in the late 1930s and early 1940s, Claude tried to isolate tumor-inducing fractions. He termed particles known since 1958 as ribosomes (3) first "small granules" and later on "microsomes". In the 1940s, Jeener and Brachet isolated microsomes and showed that they always contain RNA. They put forward the hypothesis that microsomes play a crucial role in protein synthesis (4). Also in the 1940s Luria, Delbrück and Anderson (5) came up with an approximate molecular weigth of 10^6, deduced from the ~15 nm diameter for the regular shaped granular material of bacterial lysates they saw in their electron microscopy pictures. Palade confirmed with his electron microscopy studies in the 1950s earlier proposals of Claude about the presence of microsomes in the cell (6,7). A clear demonstration that ribosomes were the site where amino acids were assembled to form proteins came from the laboratory of Zamecnik (8,9). In the late 1960s and early 1970s, attempts were made to reconstitute the small and large ribosomal subunits from its isolated components (10) in order to get insight into the internal organization of the ribosome.

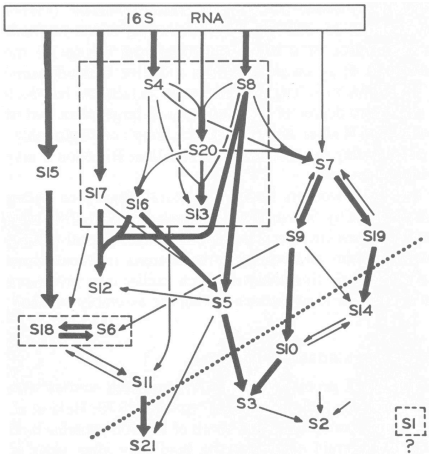

Figure 3.1: Map of *E. coli* 30S ribosomal proteins.
Arrows indicate the facilitating effect of one component on the binding of another – a thick arrow indicates a major facilitating effect. Reproduced from Nomura and Held.

Over time a plethora of biochemical experiments have been conducted in order to reach a functional map of the ribosome. More recently, several techniques like X-ray crystallography (11,12), cryo-electron microscopy (13), and fluorescence spectroscopy (14) have provided opportunities for

studying the molecular basis of translation in great detail. In addition, new ribosome associated factors or RAFs are still discovered (15) and new functions can be assigned to already identified RAFs (this work).

3.2 Mechanism of ribosomal translation

All events in protein synthesis are catalyzed on the ribosome, hence the ribosome is referred to as a ribozyme (16,17). Initiation of translation starts by binding several initiation factors to the small ribosomal subunit. They occupy the A and the E site, whereas the P site is occupied by the initiator tRNA. After the mRNA and initiator tRNA bind, the initiation factors leave the initiation complex upon association with the large ribosomal subunit. Thus, the elongation cycle starts with an aminoacylated initiator tRNA in the P site and an empty A site. The process of polypeptide chain elongation on a ribosome can be described as a cycle with three discrete steps.

Firstly, a ternary complex of aa-tRNA^{aa}•elongation factor 1A•GTP delivers the aa-tRNA^{aa} to the ribosome where it binds to the empty A site adjacent to the occupied P site by forming base pairs with the exposed mRNA codon on the small ribosomal subunit. Interactions of the correct cognate codon with the anticodon result in a conformational change in the ribosome, which stabilizes aa-tRNA^{aa}-binding and triggers GTP hydrolysis by the elongation factor 1A. The aa-tRNA^{aa} then accommodates itself into the peptidyl transferase site of the large subunit (see Figures 3.3 and 3.4).

Secondly, the peptidyl transferase activity of the major rRNA molecule in the large subunit allows peptide bond formation essentially spontaneously. The reason for the catalytic power of the peptidyl transferase site lies in the precise alignment of the substrates (18-20). The peptidyl transferase site is at the bottom of a large cleft in the small-subunit-binding surface of the large subunit (18,20). The Figure 3.2 shows a hypothetical but generally accepted mechanism derived from the crystal structure of the ribosome from *Haloarcula marismortui*.

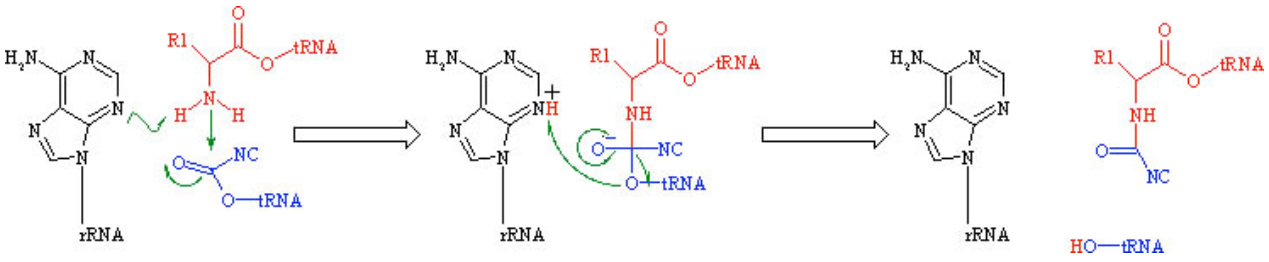

Figure 3.2: A proposed mechanism of peptide bond formation.
An adenosine residue (reference: A2451 in *E. coli* 23S rRNA) of the large rRNA of the large ribosomal subunit highly conserved across all species is shown in black, the aa-tRNA^{aa} in the A site with the amino acid sidechain represented by R1 is depicted in red, and the peptidyl-tRNA carrying the growing nascent polypeptide chain NC is in blue. Green arrows show the proposed resonance and directions of attacks. This suggested mechanism is based upon the complete atomic structure of the large ribosomal subunit (11,16). Note that some controversial discussion (21-23) as well as supportive evidence (17,19,24,25) exists. For details see main text.

In this working model (Figure 3.2) the N3 of the adenosine residue, which is the only titratabel general base within 5 Å of the nascent peptide bond, abstracts a proton from the □-amino group of the aa-tRNA^{aa} in the A site. The □-amino group itself is positioned in a way that it can perform a nucleophilic attack on the carbonyl carbon of the ester linking the nascent polypeptide chain to the peptidyl-tRNA bound in the P site. Through shifting of a bond the carbonyl oxygen becomes a negatively charged oxyanion. The protonated N3 stabilizes the tetrahedral carbon intermediate by hydrogen bonding to the oxyanion. Through rearrangement of bonds and charges the proton is transferred to the peptidyl-tRNA as the newly elongated nascent polypeptide chain transfers to the A site tRNA by deacylation.

Thirdly, the new peptidyl-tRNA in the A site is translocated to the P site as the ribosome moves ~50 Å to the next codon of the mRNA molecule. The widely accepted hybrid state model (26,27) outlined in Figure 3.3 is based on chemical footprinting experiments and was proposed as a hypothesis about 20 years earlier (28). At the start of each cycle there is a peptidyl-tRNA (blue) with an attached nascent chain in both parts of the P site forming the P/P state. An aa-tRNA^{aa} (red) enters the A site as part of a ternary complex (not depicted) and is therefore in an A/T state. The acceptor arm of the aa-tRNA^{aa} accommodates its proper position at the peptidyl transferase site and reaches the A/A state. After formation of the new peptide bond, the two tRNAs are in a hybrid state. Due to the movement of the large ribosomal subunit relative to the mRNA, the deacylated tRNA^{aa} (blue) with its anticodon is still in the P site of the small ribosomal subunit, but the 3' CCA-terminus is in the E site of the large ribosomal subunit (P/E state). Correspondingly, the former aa-tRNA^{aa} switches from an A/A state into an A/P state and becomes the new peptidyl-tRNA with the attached nascent polypeptide chain.

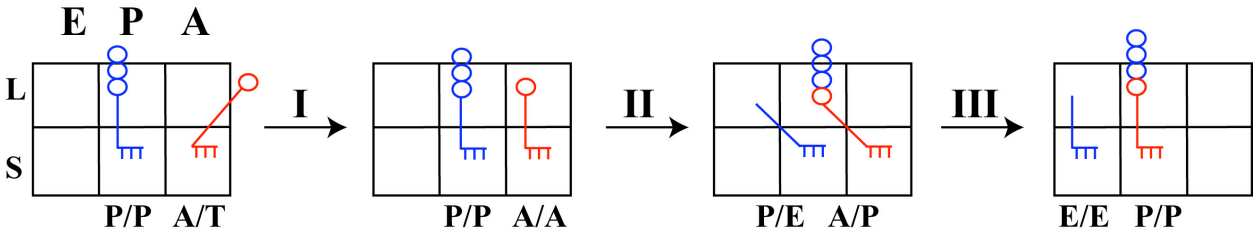

Figure 3.3: The modified hybrid state model for translocation after Moazed and Noller(26,27).
The three binding sites are depicted on top as exit site (E), peptidyl-tRNA-binding site (P) and aminoacyl-tRNA-binding site (A). Each binding site is a composite in which both, the small (S) and the large (L) ribosomal subunit contribute to the complete site. The decoding site (20,29,30) was left out for the sake of clarity. Step I shows the accommodation of the aa-tRNA^{aa} into the proper position, step II refers to the peptidyl transferase reaction and step III indicates the translocation step. See the main text for detailed description.

In a next step translocation of the small ribosomal subunit to the next codon on the mRNA is facilitated by the action of a GTP-dependent translation elongation factor which results in an empty A

site. The new peptidyl-tRNA is in a P/P state and the deacylated tRNA in an E/E state from which it subsequently leaves the ribosome.

This model explains with ease the mechanistic aspect of both, the peptidyl transferase reaction as well as the translocation. It also conveniently explains the existence of two ribosomal subunits in all known species and the high degree of conservation with respect to the adenosine residue. The translocation requires energy in form of GTP and is driven by a series of conformational changes on the ribosome with the help of the translation elongation factor eEF2 in eukaryotes or EF2, formerly known as EF-G in prokaryotes.

As soon as a stop codon is exposed in the ribosomal A site a release factor RF (eukaryotes have one, prokaryotes have three) will bind to the A site and triggers hydrolysis of the peptidyl-tRNA ester and release of the peptide chain from $tRNA^{aa}$ in the P site (31). After release of the peptide chain, the ribosome is left with the mRNA and a deacylated $tRNA^{aa}$ in the P site. Ribosome recycling factors (RRF) in concert with elongation factor 2 disassemble the remaining complex into the ribosomal subunits and mRNA (32). The deacylated $tRNA^{aa}$ can only be removed from the small ribosomal subunit by help of an initiation factor. Interestingly, the structure of RRF is the closest in shape and charge distribution to an aminoacyl-$tRNA^{aa}$ of any factor involved in protein synthesis determined so far, suggesting that it takes advantage of molecular mimicry at the ribosomal A site (33).

3.3 The eukaryotic translation elongation factor 1A

While the *modus operandi* for the description in 3.1 and 3.2 was to give general background information about basic events happening on an actively translating ribosome, the following part will focus on the eukaryotic translation elongation factor 1A (eEF1A) from *Saccharomyces cerevisiae*, which was predominantly used in this study.

The elongation factor 1A from *Saccharomyces cerevisiae* consists of 458 aa and has a molecular weight of 50.03 kDa for the unmodified protein. The isoelectric point of eEF1A from yeast (pI = 9.14) is much higher than the one of EF1A from *E. coli* (pI = 5.30). The protein has a blocked N-terminus and four lysine residues are methylated (34). The unique glyceryl-phosphorylethanolamine modification observed commonly in mammalian eEF1As is missing in the yeast eEF1A (34). The sequence is deposited at the ExPASy database (at *http://us.expasy.org/cgi-bin/niceprot.pl?P02994*), with the SwissProt accession number P02994. Published cellular concentrations across several eukaryotic species are in the range of ~2 µM, which corresponds to ~1-2 % of the total soluble cellular protein (35-37). This represents roughly ten times the concentration of ribosomes in the cell. In view of its relative abundance, it is not suprising to find eEF1A involved in other activities. It was reported to be involved in actin and tubulin binding (35,38-41). Further acitivities were suggested: association with the centrosphere (42) and

the mitotic apparatus (43), bundling of microtubules (44,45), and involvement in the degradation of N-acetylated proteins (46,47).

3.3.1 Canonical function of the eukaryotic translation elongation factor 1A

The translation elongation factor 1A or eEF1A plays a crucial part in protein synthesis. Figure 3.4 illustrates one life-cycle of eEF1A in protein synthesis. The canonical function of eEF1A in protein synthesis is to recruit charged tRNA (aa-tRNA^{aa}) via a ternary complex with GTP at the A site of the ribosome. The pairing of the cognate anticodon of the aa-tRNA^{aa} with the codon of the mRNA positions the cognate aa-tRNA^{aa} into the A site of the small ribosomal subunit. Non-cognate aa-tRNA^{aa}s are rejected at this point in an initial selection step. A conformational change within the ribosome stabilizes the binding of aa-tRNA^{aa}, and eEF1A hydrolyzes its bound GTP to GDP and P_i. eEF1A has, like other translation factors, a rather low intrinsic rate of GTP hydrolysis.

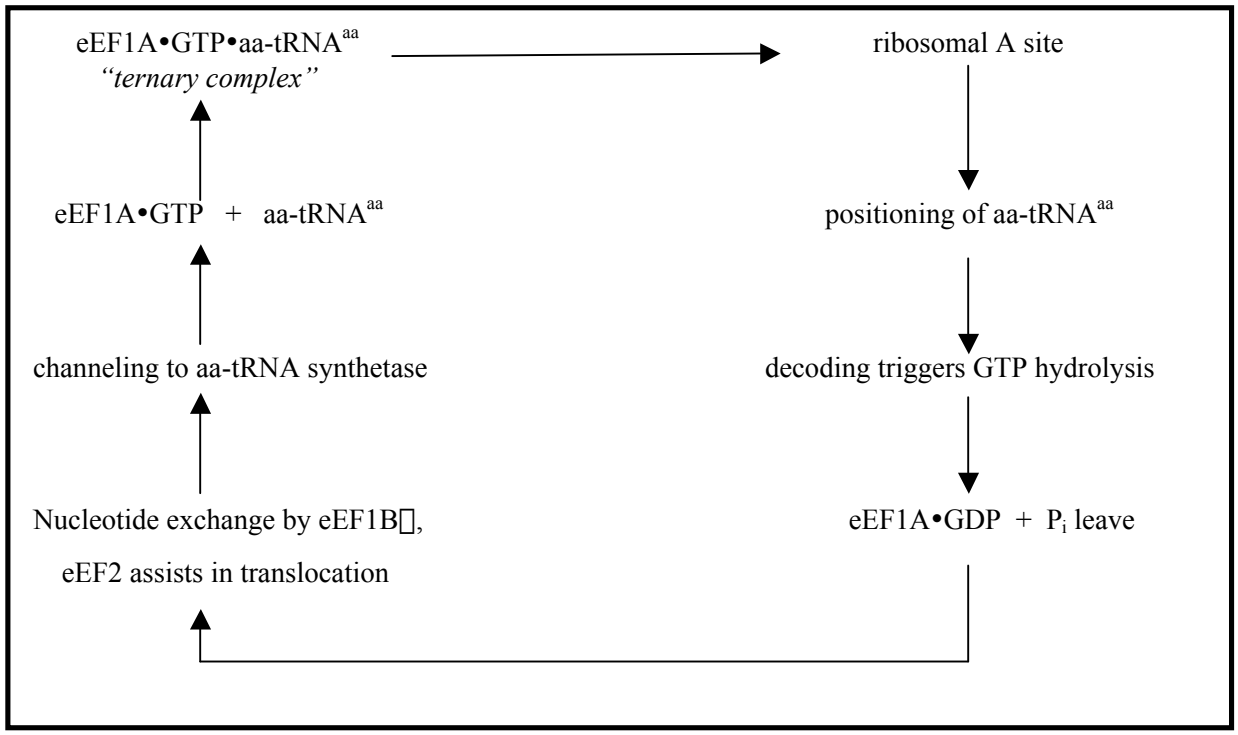

Figure 3.4: Canonical function of eEF1A in protein synthesis.
The cycle starts with the ternary complex approaching the ribosome, further details in main text.

Other G proteins have residues that stabilize the transitional state from within. Translation factors have to wait for a biological relevant signal, i. e. the establishment of the cognate codon anticodon interaction between mRNA and aa-tRNA^{aa} needs time. The ribosome then induces a high rate of biological meaningful hydrolysis after decoding of the right aa-tRNA^{aa}. As the GDP•eEF1A•P_i diffuse

away, the cognate aa-tRNA^{aa} accommodates into the peptidyl transferase site while a near-cognate aa-tRNA^{aa} would be rejected in a kinetic proofreading step (18,20,48,49).

The nucleotide exchange from GDP to GTP requires the interaction of the guanine nucleotide exchange factor eEF1Bα with eEF1A. Archaea and yeast have only eEF1Bα whereas metazoa have a heterodimeric complex of eEF1Bα/β. The homolog in bacteria is EF1B, formerly known as EF-Ts. eEF1Bα promotes nucleotide exchange by a theme common among GTPases: disruption of the binding site for the co-ordinated Mg^{2+} and the β-phosphate (50-54).

Insertion of a specific lysine into the Mg^{2+}-binding site disrupts the switch 2 region of eEF1A, which is part of the binding pocket for Mg^{2+} and the β-phosphate of GTP (see 3.3.2 and 3.3.3).

Formation of the binary eEF1A•GTP complex is driven by two features. Firstly, the 10-30 times higher cellular concentration of GTP over GDP – the K_d values for both complexes are very similar and in the 1 µM range (39,40). Secondly, this step is practically irreversible. The nucleotide exchange reaction is the rate limiting step in this life-cycle.

In a next step an aa-tRNA^{aa} triggers the release of eEF1Bα from eEF1A because the flexible loop of eEF1Bα and the terminal adenine base of the acceptor stem compete for binding to the same location on eEF1A. The aa-tRNA^{aa} has a higher affinity, although the dissolution was shown *in vitro* with eEF1A•eEF1Bα from *Artemia spec*. (55). However, aa-tRNA^{aa} is rarely found free in cells. It must be protected from both RNase degradation and amino ester bond hydrolysis. Aminoacyl-tRNA synthetases are associated with eEF1A through eEF1Bα and this constellation provides a direct channeling of the binary complex of eEF1A•GTP to the source for aa-tRNA^{aa} so that the ternary complex of can be formed and is ready for another round in the elongation cycle.

3.3.2 Structural description of the eukaryotic translation elongation factor 1A

In order to get insight into the function of eEF1A, it is helpful to look at its structure. Information about eEF1A was primarily gained through biochemical studies or cyrstal structure analysis of parts of the molecule, because eEF1A has been for long notoriously difficult to crystallize. The breakthrough came when the group of Nyborg published the model of eEF1A in complex with the active domain of its guanine nucleotide exchange factor eEF1Bα, both from the yeast *Saccharomyces cerevisiae* (53,54).

The overall structure and basic topology (Figures 3.5 and 3.8) is as described for the prokaryotic homolog EF1A (56-60). A three domain topology can be assigned to the molecule.

Domain I contains amino acids 1-243 and harbors the nucleotide binding pocket (Figure 3.5, red domain, yellow ellipse symbolizes a nucleotide) with all the elements of the P-loop fold typical for

NTPases (switch 1 and 2 regions, Walker A and B motif, NKxD motif). This domain contains the enzymatic activity of the molecule.

Domain II includes amino acids 244-333 (Figure 3.5, magenta/purple). This domain is essential for binding of both, aa-tRNA^{aa} and eEF1Bα, because it interacts with the aminoacyl group and the accepetor stem of aa-tRNA^{aa} and with Phe^{163} of eEF1Bα. Phe^{163} competes with the acceptor stem for a hydrophobic binding pocket whereas Pro^{160} competes with and the aminoacyl group of aa-tRNA^{aa} for His^{293}-His^{294} of eEF1A.

Domain III comprises amino acids 334-441. The amino acids 442-458 were not resolved in the crystal structure.

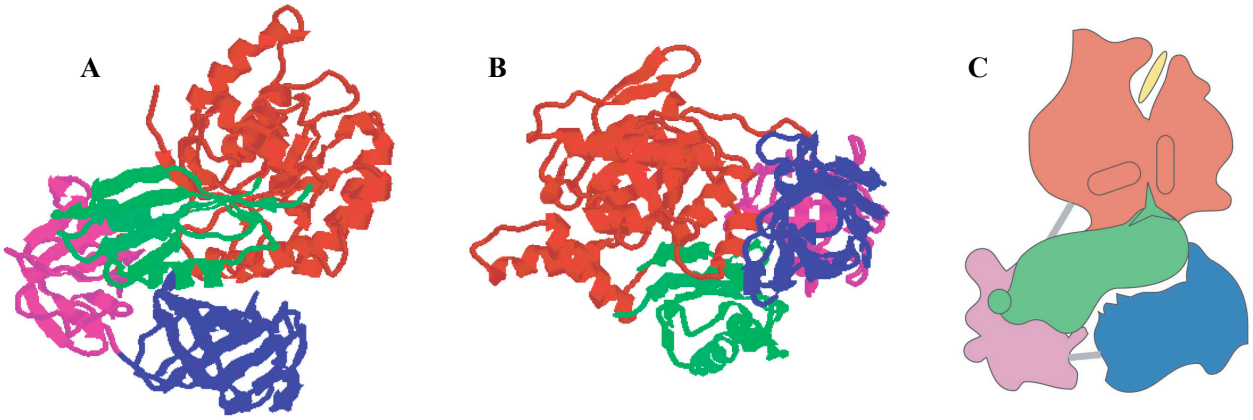

Figure 3.5: Cartoons of the eEF1A:eEF1Bα complex.
Domain I is given in red, domain II in magenta, domain III in blue, and eEF1Bα is in green. The structures in **A** and **B** were generated with RasMac PPC utilizing the PDB file with the accession number 1F60 (53,54) and **C** was drawn in Adobe Illustrator. B is rotated from A to emphasize the buried position of eEF1Bα between domain I and II of eEF1A. The green circle in C denotes the residue Phe^{163} and the star Lys^{205}, the yellow ellipse symbolizes a nucleotide (GTP/GDP) and the two rod-like structures depict the switch 1/2 region of the P-loop fold, see text for details.

The relative orientation of domain II and III is the same in pro- and eukaryotic translation elongation factor 1A. In both cases domain II and III seem to form a rigid single unit in crystal structures. However, the orientation of domain I with respect to domains II and III is slightly different between eukaryotic and prokaryotic elongation factor 1A. The C-terminal fragment (aa 117-205) of the 205 amino acid long nucleotide exchange factor eEF1Bα is deeply buried between domain I and II of eEF1A (Figure 3.5.B and 3.8) and has little contact with domain III.

However, a study applying scanning microcalorimetry and neutron scattering of rabbit eEF1A (61) suggests that eEF1A has no fixed rigid structure in solution and shows a significant amount of disorder. This study offers a reasoning that the possibility of large conformational changes of eEF1A upon interaction with a ligand is the actual cause for eEF1As ability to interact with many different

ligands. This is interesting information to be kept in mind with respect to the different functions in which eEF1A is involved (see 3.3), especially in light of the results of this work (see 5).

3.3.3 Mechanistic description of the eukaryotic translation elongation factor 1A

After delivering an aa-tRNA^{aa} to the ribosome, the decoding of the correct cognate anticodon triggers the hydrolysis of GTP by eEF1A to GDP, P_i and H^+. In contrast to other NTPases with a P-loop fold, where a conserved Glu acts as a general base, here the γ-phosphate group of GTP itself acts as general base by abstracting a proton H^+ from a water molecule (Figure 3.6). The resulting nucleophilic hydroxid ion attacks the γ-phosphate via an S_N2 mechanism (i. e. second-order nucleophilic substitution). In a concerted reaction a direct in-line transfer of the γ-phosphate to the hydroxid ion and inversion of the configuration around the pentavalent transition state induces the hydrolyzation of the bond between the β- and γ-phosphate by charge transfer to the β-phosphate group: a proton, an orthophosphate and GDP are generated.

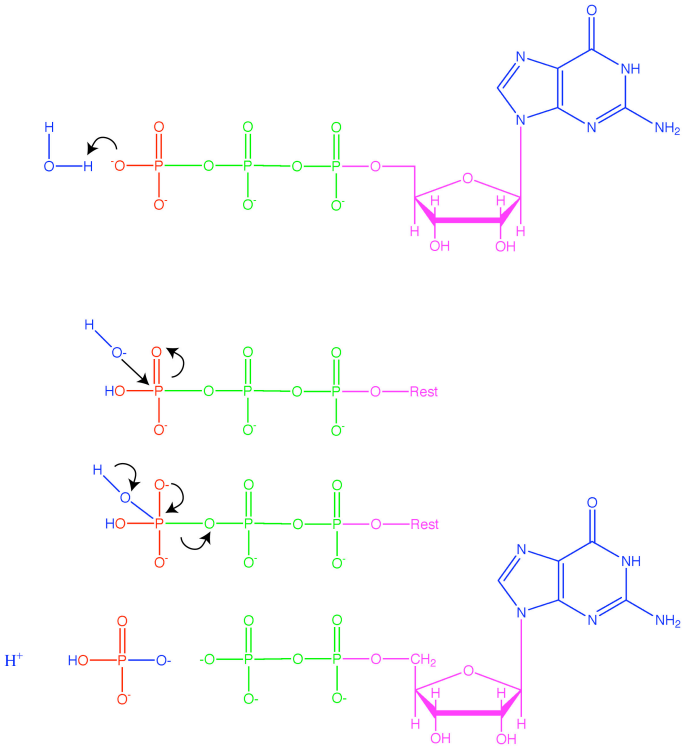

Figure 3.6: GTP hydrolysis via S_N2 mechanism.
The black arrows indicate the direction of attack or the transition of charges. See main text for details.

However, the presence of the co-ordinated hexavalent Mg^{2+} inhibits the spontaneous dissociation of the hydrolytic products from eEF1A. Figure 3.7 A depicts the spatial configuration of Mg^{2+} as a tetragonal bipyramid forming a regular octahedron. Figure 3.7 B shows which residues of eEF1A interact

with the nucleotide in its binding pocket. The first part of the switch 2 region is the Walker A motif with the consensus sequence GxxxxGKS (aa 14-21, x: any aa). It contains Lys^{20} which bridges the β- and γ-phosphate with its ε-amino group by two hydrogen bonds. The β- and γ-phosphate of GTP in turn provide two of the six co-ordination bonds to Mg^{2+}. Ser^{21} contributes another hydrogen bond to co-ordinate Mg^{2+}. The amino acid residues 21-31 form the important α-helix of the switch 2 region which gets displaced upon interaction with eEF1Bα (see below for reverse reaction).

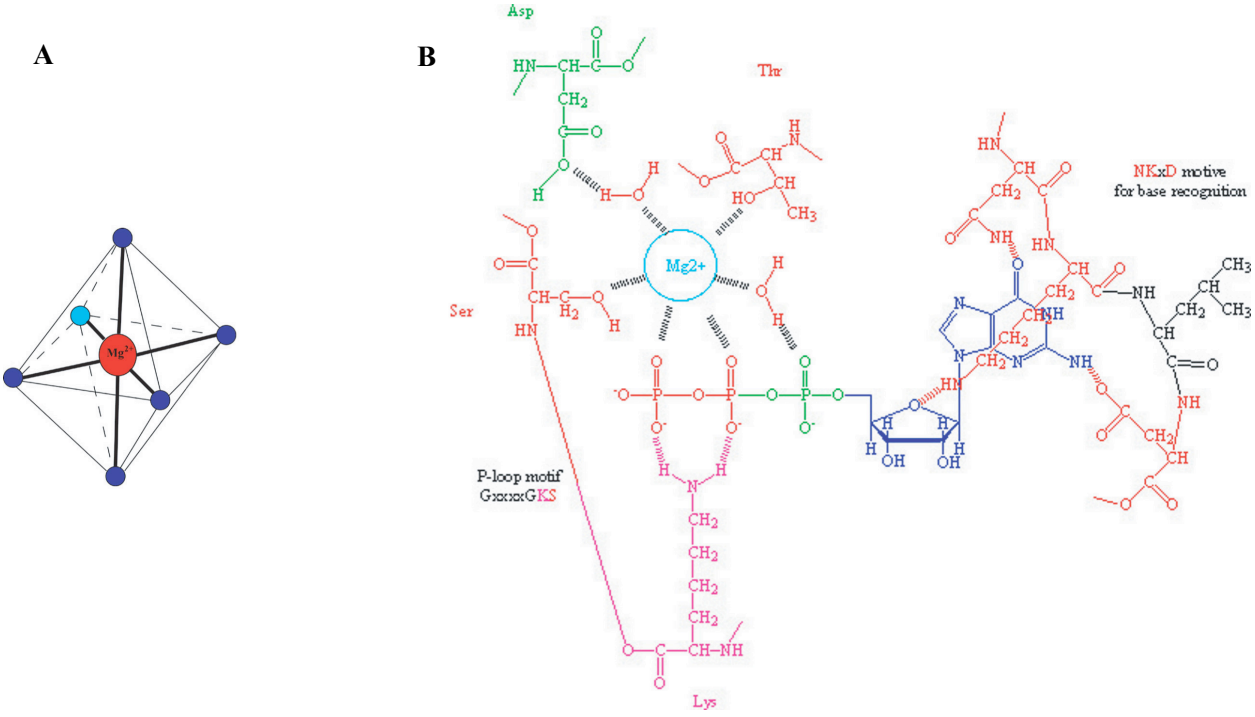

Figure 3.7: Co-ordination of Mg^{2+} and specificity for the guanine base.
A: General outline for the hexavalent co-ordination of Mg^{2+} via six oxygen atoms (blue). Cartoon drawn after a description from Wiberg (62). **B:** Residues and molecules involved in the co-ordination of the hexavalent Mg^{2+} and recognition of the proper base in eEF1A from *Saccharomyces cerevisiae*. From the Walker A consensus (GxxxxGKS) of the P-loop fold Lys^{20} (magenta) and Ser^{21} (red) are shown bottom and left, from the Walker B consensus (hhhhDxxG) of the P-loop fold Asp^{91} (green) is shown on top left. The NKxD motif which provides specificity for guanine over other bases is shown in red on the right side with Leu^{155} in black and Lys^{154} stretching over the base to the sugar of the nucleotide. Further co-ordination is facilitated by Thr^{72} of the switch 1 region and two water molecules. Cartoon drawn after Anderson (53,54) and Leipe (63,64).

From the Walker B consensus sequence hhhhDxxG (aa 87-94, h: hydrophobic aa, x: any aa) of the P-loop fold, Asp^{91} is co-ordinating Mg^{2+} via a hydrogen bonded water molecule. From the switch 1 region (aa 70-77) Thr^{72} facilitates a stabilizing effect on Mg^{2+} via another hydrogen bond. The last hydrogen bond is supplied by an ordered water molecule that itself is co-ordinated by the γ-phosphate group of the nucleotide.

Upon hydrolysis of GTP, there is a conformational change in eEF1A which results in its release from the ribosome (see below for details).

The guanine nucleotide exchange factor eEF1Bγ can bind now to eEF1A. As can be seen in Figure 3.5 A and B as well as in Figure 3.8, the C-terminal fragment of eEF1Bγ displays intricate interactions with eEF1A. The Phe^{163} of eEF1Bγ inserts into a hydrophobic pocket in domain II, where the 3' terminal adenine base of the acceptor stem of the aa-$tRNA^{aa}$ binds (see 3.3.2 for overlapping binding sites of eEF1Bγ and aa-$tRNA^{aa}$ on eEF1A).

Figure 3.8: Interaction of eEF1A with eEF1Bγ and P-loop motif.
Domain I of eEF1A (aa 1-235) is shown in blue and the C-terminal fragment of eEF1Bγ (117-205) in green. The P-loop motif consists of a Walker A and B motif, switch 1 and 2 region, the NKxD consensus sequence and the DxxG consensus sequence. The switch 1 region from amino acid 70-77 (GITIDIAL) is colored magenta. The switch 2 region consists of the Walker A loop (aa 14-21, GHVDSGKS) and an adjacent α-helix (aa 21-31) and is colored red. The NKMD sequence (aa 153-156) which provides specificity for guanine over other bases is shown in yellow. The last part of the P-loop fold, the Walker B motif (aa 91-94, DAPG) was left out for clarity. Model was generated utilizing the PDB file with the accession code 1F60 and the software RasMac.

Most importantly, eEF1Bγ is buried between the switch 1 and 2 region of eEF1A (Figure 3.8), two parts of the P-loop fold typical for a variety of NTPases. The switch 1 and 2 regions are elements of the "prototypical G-protein" (63,64) and are involved in both, Mg^{2+} stabilization and β-phosphate binding. This position enables eEF1Bγ to insert its Lys^{205} into the switch 2 region of eEF1A. This displaces the switch 2 region which is part of the binding pocket for Mg^{2+} and β-phosphate and hence disturbs the nucleotide binding site. Not only does Lys^{205} block the Mg^{2+} binding site but it prevents interaction of the P-loop fold with the β- and γ-phosphate which are disordered in the GDP state. As a result of the disruption of the Mg^{2+} binding site, P_i and Mg^{2+} leave eEF1A first, then followed by GDP.

The binding site for the sugar and base are open and remain undisturbed, so that base recognition is favourable. A new GTP molecule binds with the sugar and base moieties first, then positions the phosphates and Mg^{2+} correctly.

As it is the case with other G proteins, the binding energy is used to stabilize the switch regions enabling the G proteins in general to associate with an effector. In case of eEF1A, the effector is the translating ribosome and not a GTPase activating protein. The energy dissipates upon GTP hydrolysis and triggers domain re-arrangements. Correct binding of Mg^{2+} and GTP results in re-organization of the interface between switch 1 and 2 regions of domain I from eEF1A. The switch 2 region unwinds partially and re-orients its α-helix. This creates a binding site for domains II and III which rotate together by 90° as a rigid unit so that domain III sits with polar and charged residues against switch 2. The cavity between the three domains in the GDP state is closed and a negatively charged cleft between domain I and domain II is generated forming the binding site for the CCA acceptor stem with the aminoacyl group. The T-stem interacts with domain III.

eEF1Bα is easily replaced by an aa-tRNA^{aa} because both have overlapping binding sites on eEF1A, but eEF1Bα has a lower affinity to the binary complex eEF1A•GTP than aa-tRNA^{aa}. The stronger binding CCA acceptor stem of an aa-tRNA^{aa} substitutes the flexible loop of eEF1Bα. It has also been shown *in vitro* that the complex eEF1A•eEF1Bα from *Artemia spec.* is dissolved by aa-tRNA^{aa} (55). The aa-tRNA^{aa} is not free in solution but in complex with an aminoacyl-tRNA synthetase, which protects the aa-tRNA^{aa} from RNase degradation and the aminoacyl ester bond from hydrolysis.

The driving force towards ternary complex formation is the 10-30 times higher cellular concentration of GTP over GDP and the fast and stable association of the ternary complex. The nucleotide exchange reaction is the rate limiting step in the protein translation elongation process. The eEF1A•eEF1Bα complex exhibits a common theme among GTPases and their respective guanine nucleotide exchange factors: the disruption of the β-phosphate and Mg^{2+} binding site. Some examples are given in Table 3.1.

Complex	Function	Literature
Arf 1•Sec 7	Regulator of coatomer-coated vesicle transport between Golgi cisternae	(65)
Ras•Sos	Regulator of growth and differentiation	(66)
Rac 1•Tiam	Relaying signals from the cell-surface receptors to the actin cytoskeleton	(67)
EF1A•EF1B	Translation elongation factors in protein synthesis	(68,69)
eEF1A•eEF1Bα	Translation elongation factors in protein synthesis	(53,54)

Table 3.1: GTPases and their respective guanine nucleotide exchange factors.
The GTPase is written on the left site in the complex, the guanine nucleotide exchange factor is on the right site.

4 Aim of this work

The aim of this work was to elucidate in detail certain aspects of the complex interactions happening at the actively translating ribosome. The laboratory has an extensive practical and intellectual knowledge with respect to the investigation of ribosome associated factors. It has worked on the signal recognition particle (SRP), the Sec 61 complex (translocon), on molecular chaperones (Hsp 70/40), an N-acetyltransferase (p120), and in particular, it discovered the nascent polypeptide-associated complex (NAC).

An unidentified crosslinked protein of ~50 kDa was found in some experiments to crosslink efficiently to nascent polypeptide chains. It was identified by mass spectroscopy to be the eukaryotic translation elongation factor 1A, eEF1A. This led to the suggestion that the direct interaction of eEF1A with a nascent polypeptide chain may be biologically relevant.

The current understanding of the canonical eEF1A function is to deliver aa-tRNA^{aa} to the A site of the ribosome. From this explanation no meaningful function can be deduced as to why eEF1A should interact with a nascent polypeptide chain emerging from the ribosome. This work tries to gain a greater insight into the interactions of eEF1A with nascent polypeptide chains and the actively translating ribosome.

5 Results

5.1 General outline

Ribosome associated factors (RAFs) can be identified by their ability to co-fractionate with ribosomes under physiological salt conditions. Table 5.1 below provides a list of some of these ribosome associated factors. The interest lies specifically in a subset of these RAFs, which physically interact with nascent polypeptide chains emerging from the ribosome. Previously, several proteins have been identified to be in contact with nascent polypeptide chains, including signal recognition particle, DnaJ, nascent-polypeptide associated complex, Sec 61, and Ssb.

involved in translation	
Initiation factors	13 eukaryotic IFs known
Elongation factors	four eukaryotic EFs known
Release factors	three eukaryotic RFs known

involved in protein folding and transport/translocation across membranes	
Signal recognition particle	SRP
Translocon	Sec 61 complex
Nascent-polypeptide-associated complex	NAC
Molecular chaperones	Hsp 70/40, Ssb

involved in modifications	
N-acetyltransferases	p120
Methionine aminopeptidases	

involved in the RNAi machinery	
RISC	Argonaut-like proteins and others

Table 5.1: A list of some ribosome associated factors.

An approach towards elucidating those interactions is to combine the co-purification of RAFs (see Figure 5.1) with a site-specific photo-crosslinking technology, where the crosslinker is located in a known position of the growing polypeptide chain (70). This technique to probe the environment of the nascent polypeptide chains for RAFs requires formation of a stable ribosome nascent chain complex with photoactivatable crosslinker in the nascent polypeptide chains, followed by UV irradiation to activate the

crosslinking reagent. To accomplish this, a truncated mRNA is generated *in vitro* using restriction enzyme cut DNA as template (71) and then translated in the presence of ^{35}S-Methionine and the photoactivatable TDBA-Lys-tRNA^{Lys*}. To generate the photoactivatable TDBA-Lys-tRNA^{Lys*} tRNA^{Lys} was charged with lysine and then derivatized at the epsilon amino group of the lysines with the N-hydroxy-succinimido ester of 4-(3-trifluoromethyldiazirino) benzoic acid (TDBA).

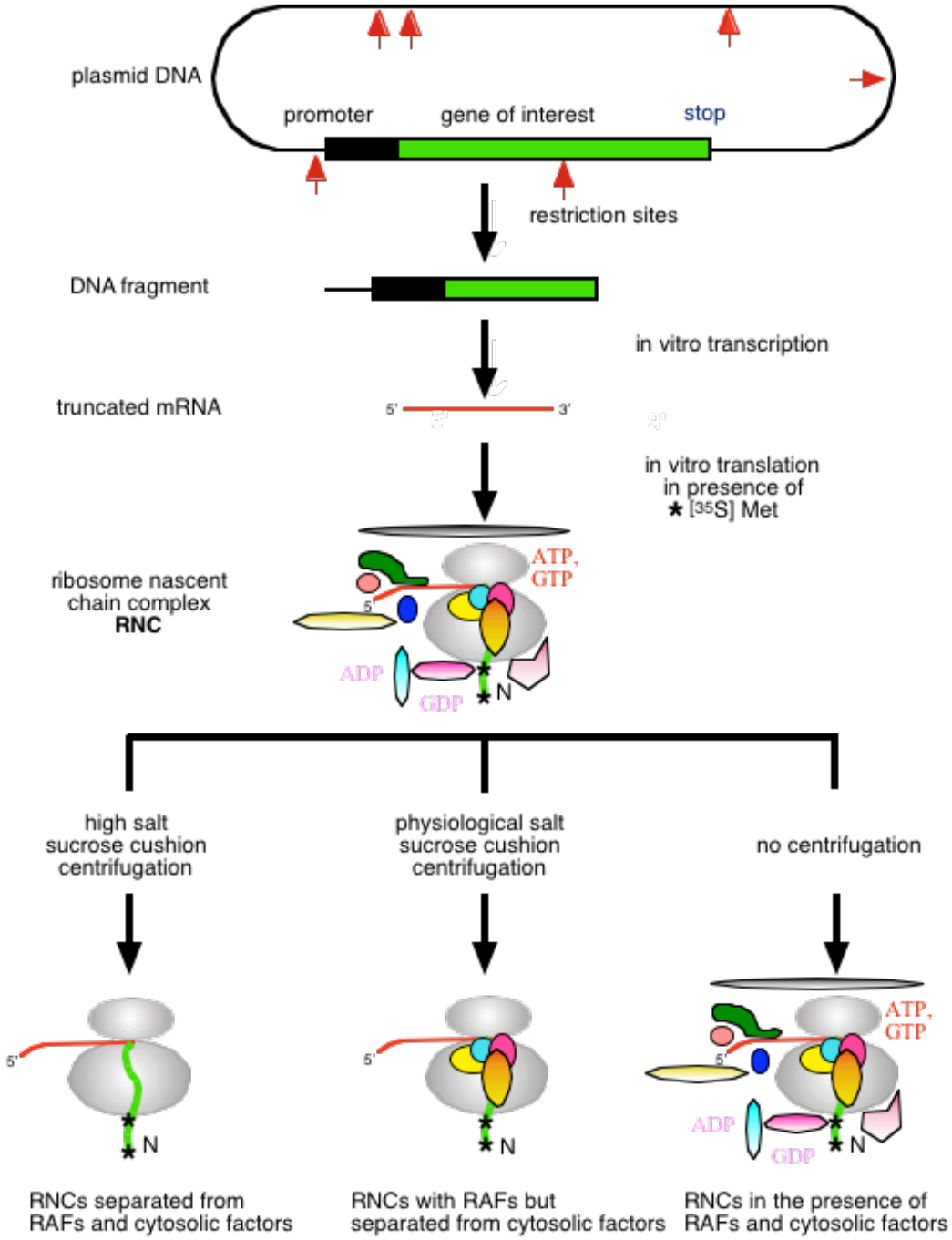

Figure 5.1: Truncated mRNA Technology. See main text for details.

In the absence of a stop codon on the mRNA, the nascent polypeptide chain remains stably associated with the ribosome. Under specifically chosen conditions (high or physiological salt sucrose cushion centrifugation) ribosome nascent chain complexes (RNCs) can be isolated. Subsequent photoactivation by UV irradiation (λ_{range} = 315 – 400 nm, λ_{max} = 365 nm) within given assay conditions results in formation of a highly reactive carbene on the derivatized lysines (see Figure 5.2). The highly reactive carbene has little if any selectivity for the reaction partner. This ensures that only molecules closely associated with the nascent polypeptide chains will be crosslinked.

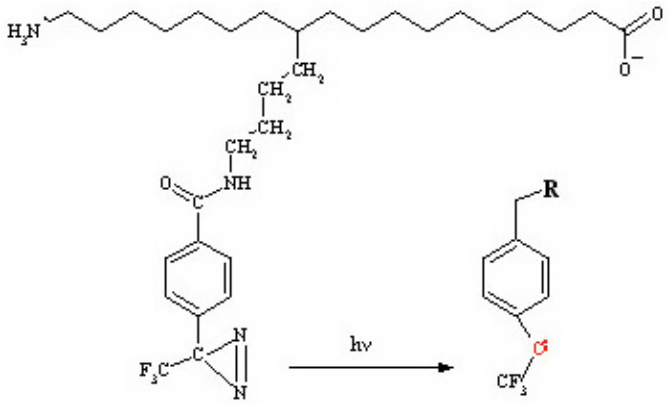

Figure 5.2: Photoactivation of TDBA-Lys-tRNA^{Lys*}. See main text for details.

The high specificity of this photo-crosslinking approach comes with the disadvantage that this reagent also rapidly reacts with water molecules, generally resulting in a low efficiency of crosslinking (72), especially for ribosome associated molecules with fast on and off rates of binding.

5.2 Interaction of the eukaryotic translation elongation factor 1A with nascent polypeptide chains

5.2.1 Interaction of an unidentified 50 Da protein with nascent polypeptide chains

The experiment illustrated in Figure 5.3 used a truncated mRNA encoding 169aa pPL-MN, which carries only two lysines at positions 4 and 9 (see Table 7.1). At this distance from the peptidyl transferase center the nascent polypeptide-associated complex is not efficiently crosslinked to nascent chains. Instead, two major crosslinked products of about 70 kDa and 140 kDa were observed, representing crosslinking partners of about 50 and 120 kDa, respectively. The focus of the following part is the identification and characterization of the 50 kDa protein.

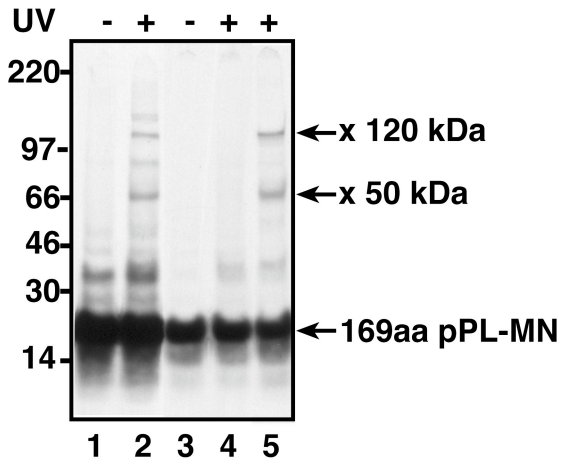

Figure 5.3: A 50 kDa protein associates with 169aa pPL-MN nascent chains.
169aa pPL-MN RNCs were irradiated with UV (lanes 2, 4 and 5) or not irradiated (lanes 1 and 3). RNCs were stripped of RAFs with high salt, then incubated with buffer A (lanes 3 and 4) or 2 ml rabbit reticulocyte lysate in a total volume of 12 ml (lane 5) prior to irradiation. Molecular masses in kDa are indicated on the left.

By definition, RAFs but not components of the ribosome itself are removed by treatment with high salt. Separation of the RNCs from released factors is accomplished by incubation of the translation mixture with high salt followed by centrifugation over a high salt sucrose cushion (see Figure 5.1 for a scheme and 7.2.2). Such high salt stripping of 169aa pPL-MN RNCs greatly reduced the intensity of both crosslinking products to the level of the non irradiated control (Figure 5.3, compare lanes 1 and 4). Addition of rabbit reticulocyte lysate to the high salt-stripped RNCs before irradiation restored the crosslink to the 50 and 120 kDa proteins (Figure 5.3, compare lanes 2 and 5). Collectively, these results indicate that the 50 and 120 kDa proteins are salt-extractable proteins and can rebind to the 169aa pPL-MN nascent chains after extraction. Rebinding of the 50 kDa protein provided an assay that was utilized for its purification.

5.2.2 Purification and identification of a 50 kDa nascent polypeptide associated protein

The 50 kDa protein that crosslinked to 169aa pPL-MN nascent chains was purified from rabbit reticulocyte lysate as follows. The supernatant from a high-speed centrifugation to sediment the ribosomes was precipitated with 66 % ammonium sulfate, dialyzed and applied to a Q-Sepharose column. The flow through, which contained the 50 kDa crosslinking partner, was applied to an S-Sepharose column and eluted with a gradient of potassium acetate from 10 mM to 1000 mM (see 7.2.4 for details). Figure 5.4 A shows in lanes 1 – 4 a silver stain of the protein pattern after SDS-PAGE for the different purification steps. The active fraction from the S-Sepharose chromatography corresponds to 390 – 450 mM potassium acetate and revealed a single band of 50 kDa (Figure 5.4 A, lane 4). The samples were assayed for crosslinking to 169aa pPL-MN nascent chains as shown in Figure 5.4 A, lanes 5 – 10. High

salt stripped RNCs, irradiated in buffer alone (Figure 5.4 A, lane 6) show that removal of the 50 kDa crosslinking partner was efficient. Figure 5.4 A, lane 10 shows the crosslinking products obtained with the active fractions from the S-Sepharose columns (390 – 450 mM potassium acetate). The only major crosslink observed is at ~70 kDa, indicating a ca. 50 kDa crosslinking partner, since 169aa pPL-MN is 19 kDa. There is a faint band visible at about 120 kDa, which is most likely a double crosslink to this protein.

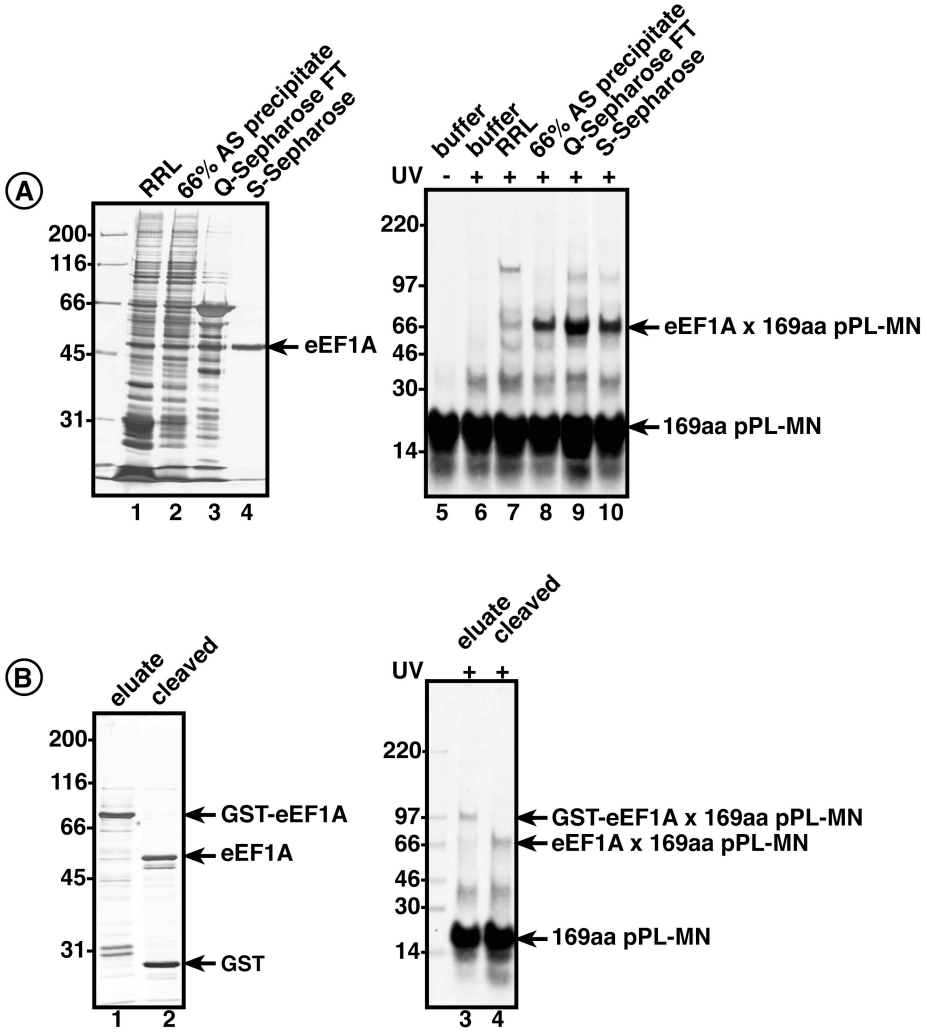

Figure 5.4: The 50 kDa protein that associates with 169aa pPL-MN NCs is eEF1A.
A: Protein fractions from the purification of eEF1A from rabbit reticulocyte lysate were analysed in parallel by separation on a 10 % SDS-PAGE (73), visualized by silver staining according to Blum (74) (lanes1-4) or by the standard crosslinking assay (lanes 5-10). The crosslinking assay employed high-salt stripped 169aa pPL-MN RNCs (lanes 5-10) incubated with buffer A (lanes 5 and 6) or protein fractions (lanes 7-10) prior to irradiation or, as a negative control, without irradiation (lane 5). Protein fractions are rabbit reticulocyte lysate (RRL) depleted of ribosomes by sedimentation (lanes 1 and 7), 66 % w/v ammonium sulfate fraction (lanes 2 and 8), Q-Sepharose flow through (lanes 3 and 9), and the active fraction eluted from S-Sepharose (lanes 4 and 10). **B:** Recombinant GST-eEF1A fusion protein was analysed after elution from glutathione-Sepharose (lanes 1 and 3) or after limited thrombin cleavage (lanes 2 and 4) by 10 % SDS-PAGE and silver staining of the gel (lanes 1 and 2) or by crosslinking (lanes 3 and 4) and autoradiography as described above. Molecular masses in kDa are indicated on the left.

Mass spectrometry (Targeted Proteomics Group of MSKCCs Molecular Biology Program) of seven peptides obtained from the excised protein from the SDS gel identified the purified protein as the eukaryotic translation elongation factor 1A (eEF1A). The experimental data found are in good agreement with the predicted sizes.

Experimental data	Predicted size
466.2 Da	466.25 Da
537.2 Da	537.29 Da
652.3 Da	652.32 Da
765.4 Da	765.40 Da
878.4 Da	878.48 Da
979.5 Da	979.53 Da
1078.6 Da	1078.60 Da

Table 5.2: Mass spectrometric data.

However, the possibility remained, that eEF1A, an abundant cytosolic protein, is contaminated by another protein that is the actual crosslinking partner. To rule this out, recombinant eEF1A expressed as a GST-fusion protein in *E. coli* (see 7.2.5) was purified and assayed for crosslinking to 169aa pPL-MN nascent chains. Both GST-eEF1A fusion protein and eEF1A produced by limited thrombin digestion of the fusion protein were able to crosslink to the 169aa pPL-MN nascent chain (Figure 5.4 B lane 3 and 4). These data prove that it is indeed eEF1A that interacts with the RNCs.

5.2.3 The eukaryotic translation elongation factor 1A associates with a wide range of nascent chains

An obvious question to answer is whether eEF1A can interact with other nascent chains of varying lengths and amino acid sequences. Both purified eEF1A and rabbit reticulocyte lysate were assayed for the production of crosslinks to the following nascent chains: 85aa and 221aa β-actin (Figure 5.5 A), 86aa and 169aa pPL-MN (Figure 5.5 B), and 77aa and 197aa ffLuc (Figure 5.5 C).

Purified eEF1A crosslinked to all nascent chains tested (Figure 5.5, lanes 2 and 5, arrow). In general, incubation of RNCs with rabbit reticulocyte lysate also produced the crosslinking product expected of eEF1A (Figure 5.5, lanes 6 and Figure 5.5 C, lane 3, arrow). In two cases, though, the expected band was faint: 85aa β-actin (Figure 5.5 A, lane 3) and 86aa pPL-MN (Figure 5.5 B, lane 3). The longer versions of the same nascent chains, however, 169aa pPL-MN and 221aa β-actin, did crosslink efficiently with eEF1A in the reticulocyte lysate.

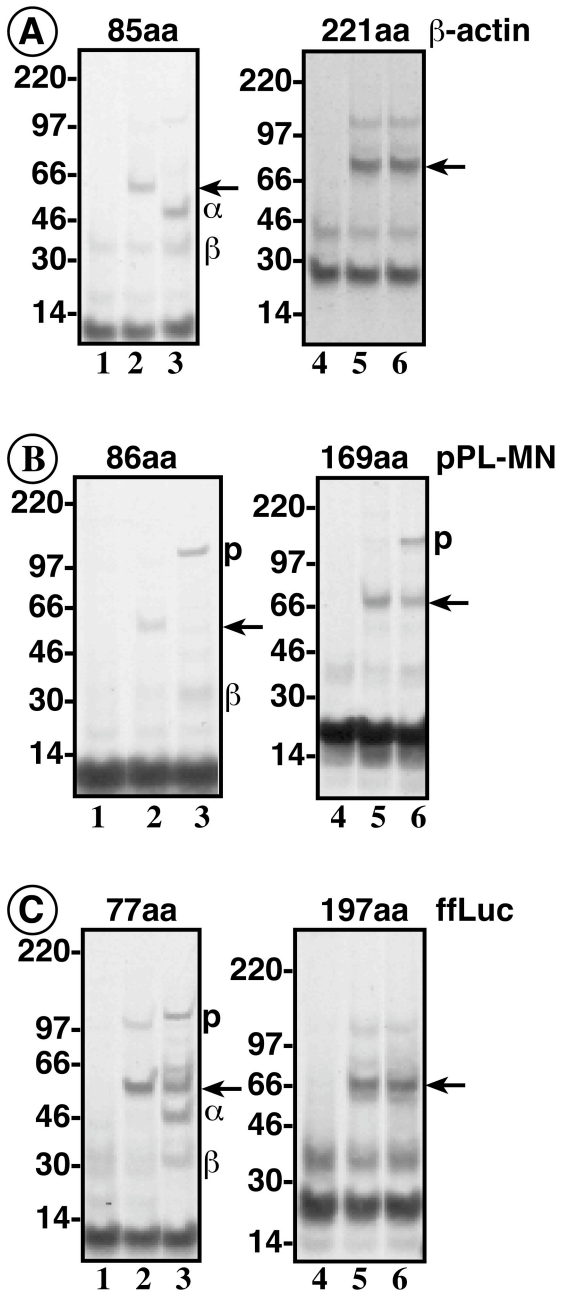

Figure 5.5: Association of purified eEF1A with nascent chains.
A: 85aa or 221aa β-actin RNCs were high salt-stripped then incubated with either buffer A (lanes 1 and 4), or purified eEF1A at a concentration of 160 nM (lane 2 and 5) or 2 ml rabbit reticulocyte lysate in 18 ml total assay (lanes 3 and 6) prior to UV irradiation. **B:** 86aa and 169aa pPL-MN RNCs were analysed as above. **C:** 77aa and 197aa ffLuc RNCs were analysed as above. Arrows indicate the position of eEF1A crosslinked to NC, while "β" and "α" mark crosslinks to both subunits of NAC and "p" the chrosslinks to p120. Molecular masses in kDa are indicated on the left.

Given that the shorter nascent chains crosslinked to purified eEF1A, this suggests that other components in the reticulocyte lysate may compete for binding to the nascent chains and that eEF1A competes better for binding to the longer nascent chains. In agreement with this, RRL incubated with

nascent chains clearly yields other crosslinked products, such as, β-NAC for 85aa β-actin (Figure 5.5.A, lane 3), p120 for 86aa pPL-MN (Figure 5.5 B, lane 3), and both NAC subunits and p120 for ffLuc (Figure 5.5 C, lane 3). In some cases, the decreased intensity of the crosslink to eEF1A for the shorter nascent chain may be due to fewer lysines available for crosslinking. For example, 86aa β-actin has only 5 lysines compared to 10 in 221aa β-actin (see Table 7.1). This is not the case, however, for pPL-MN, which has only two lysines, at positions 4 and 9, the same for 86aa pPL-MN as for 169aa pPL-MN. This suggests that eEF1A may be more effective than other factors at binding to the distal end of the nascent chain, where it is no longer associated with the ribosome. An extension of this reasoning is to ask whether eEF1A can bind to newly synthesized polypeptides even after their release from the ribosome.

5.2.4 The eukaryotic translation elongation factor 1A associates with unfolded polypeptide chains released from the ribosome

To test this idea, high salt-stripped 133aa β-actin RNCs were incubated with purified eEF1A or rabbit reticulocyte lysate depleted of ribosomes. Puromycin and RNase A were then added in order to release the nascent chains from the ribosome. After centrifugation through a high salt sucrose cushion the ribosomes with bound nascent chains were obtained in the pellet and the released nascent chains together with the RAFs were recovered from the supernatant. Both fractions were collected and then irradiated in parallel. Without puromycin or RNase A, very few nascent chains were released from the ribosome and, consequently, neither β-actin nor a crosslinked band was detected in the supernatant fraction (Figure 5.6, lanes 4 and 8).

In the presence of puromycin and RNase A, a larger fraction of nascent chains were released from the ribosome, and a band of puromycin-released 133aa β-actin crosslinked to eEF1A was detected in the supernatant fraction (Figure 5.6, lanes 5 and 9). Note that more than half of the released 133aa β-actin polypeptide crosslinks to eEF1A, regardless of whether purified protein (Figure 5.6, lane 5) or reticulocyte lysate (Figure 5.6, lane 9) was used. These results indicate that eEF1A still associates with polypeptide chains even after their release from the ribosome. Similar results were obtained when the nascent polypeptide chains were first released and that the eEF1A was added (data not shown).

It has been shown previously that most RAFs interacting with nascent chains do so only in the context of the ribosome. The experiments described above for Figure 5.6 indicate that eEF1A is, in this way, different and confirm that other RAFs do not crosslink to released polypeptides. Nascent chains crosslink to a variety of RAFs including but not restricted to eEF1A, α- and β-NAC and p120 (Figure 5.6, compare lanes 1 and 6). As expected, the other RAFs such as NAC and p120 are not seen to crosslink to puromycin-released 133aa β-actin (Figure 5.6, Lane 9). This is in agreement with published literature (15).

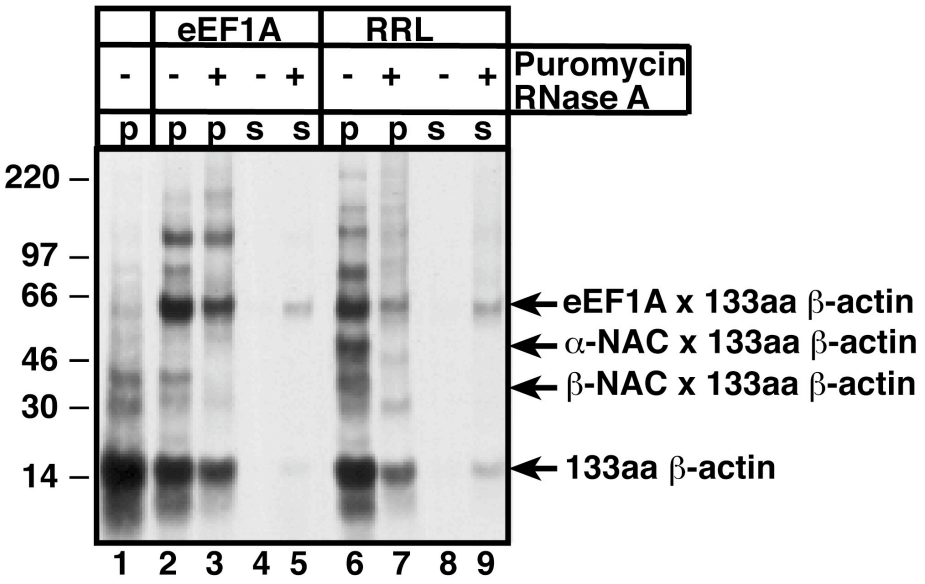

Figure 5.6: Association of purified eEF1A to polypeptide chains released from the ribosome.
133aa β-actin RNCs were high salt-stripped then incubated with buffer A (lane 1), 160 nM purified eEF1A (lanes 2 to 5) or 3 ml rabbit reticulocyte lysate in 18 ml total assay (RRL, lanes 6 to 9) for 5 min at 26 °C. Puromycin and RNase A were added as indicated, then ribosomes and released polypeptide chains were obtained as pellet (p) and supernatant (s), respectively, after centrifugation and subjected to UV irradiation. Molecular masses in kDa are indicated on the left.

The experiments described above establish that eEF1A can bind both to nascent chains and to released polypeptides but shed no light on the possible function of eEF1A in this context. Therefore the time dependence of the interaction was tested using full-length transcripts encoding two different proteins, ffLuc and pPL-M (Figure 5.7, Table 7.1), to further explore the interaction of eEF1A with polypeptides. pPL-M harbors three point mutations in the signal peptide of preprolactin, which prevents the protein from interacting with SRP and consequently blocks its secretion from cells. During its folding in the lumen of the ER, prolactin forms three disulfide bridges, which cannot be formed in the cytosolic environment. This is one reason why pPL-M cannot fold correctly under the conditions provided by the reticulocyte translation system. In contrast, ffLuc, a peroxisomal protein, is able to fold in reticulocyte lysate as demonstrated by its acquisition of enzymatic activity (75).

Synchronized translations were sampled at intervals up to 44 minutes (including a three minute initiation time, see 7.2.1) and assayed for crosslinks to translated proteins released by normal termination from the ribosome. Figure 5.7 A shows that full-length ffLuc, readily apparent in the supernatant starting from the 14 minute time point, shows no major crosslinking product. This is also the time when enzymatic activity is first observed (75). In contrast, full-length pPL-M, first detected in the supernatant at the 7 minute time point, displays a major crosslinking band of about 70 kDa, indicating association of pPL-M with eEF1A (Figure 5.7 B, asterisk). This experiment demonstrates that eEF1A interacts with the unfolded pPL-M protein, but not with the correctly folded ffLuc.

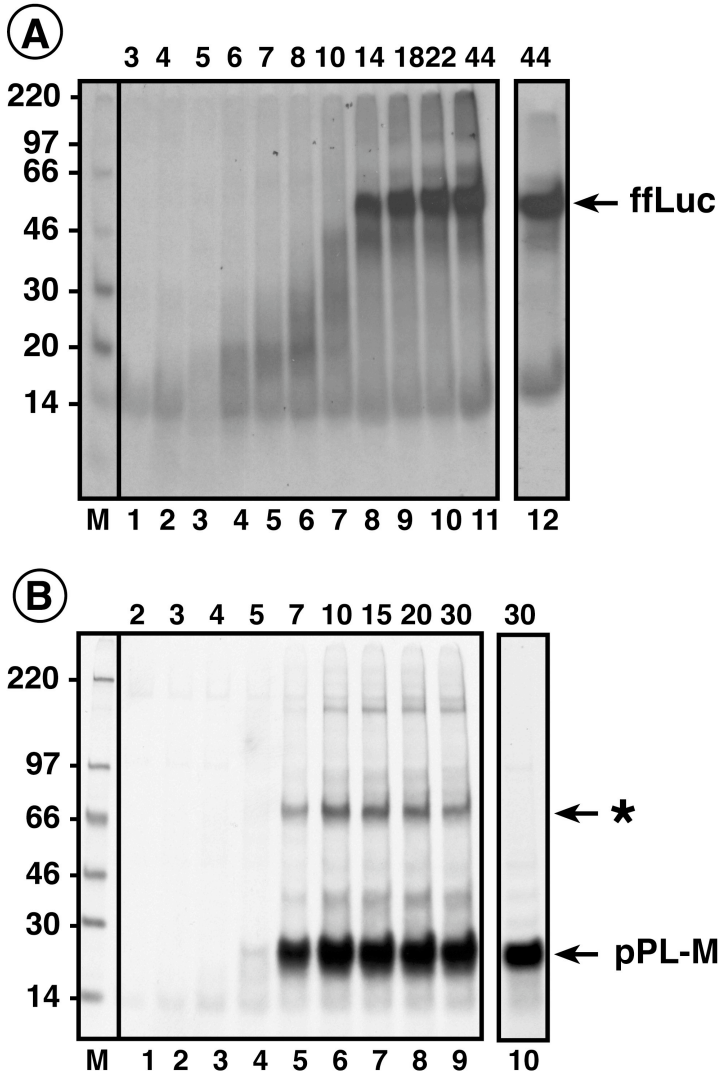

Figure 5.7: eEF1A binds to pPL-M but not to ffLuc after their release from the ribosome.
Synchronized translations of ffLuc (**A**) or pPL-M (**B**) were stopped by addition of cycloheximide to a final concentration of 5 mM at time points indicated on top of the gels. After UV irradiation RNCs were removed by sedimentation (see 7.2.2) and the supernatants analysed by 10 % SDS-PAGE and autoradiography. An asterisk indicates the position of eEF1A crosslinked to pPL-M. Lanes 12 in **A** and 10 in **B** show the non-irradiated controls at the indicated time point. Molecular masses in kDa are indicated on the left.

5.3 A novel peptide binding site on the eukaryotic translation elongation factor 1A with limited specificity

5.3.1 Rationale

In the context of its canonical function, eEF1A is known to have at least one protein binding site, i. e. the binding site for the guanine nucleotide exchange factor eEF1B. This was shown by solving the crystal structure of eEF1A in complex with a fragment of eEF1B (53,54). However, it is reasonable to assume the presence of more than only one protein or peptide binding site: not only has eEF1A to interact with eEF1B for nucleotide exchange, but also with an array of individual aminoacyl-tRNA synthetases for loading of aa-tRNA^{aa} and the ribosome for delivery of aa-tRNA^{aa}. Furthermore, as was shown above, eEF1A is readily crosslinked to several nascent polypeptide chains in rabbit reticulocyte lysate even in the presence and therefore in competition of the aforementioned proteins. To accommodate for these interacting proteins, it is well-grounded to propose more than one binding site. It has not escaped my notice that the specifics of these interactions suggest a possible overlapping of binding sites for the different proteins involved.

The fact that several nascent polypeptide chains of different origin and of different length can be crosslinked to eEF1A indicates a potential lack of requirement for a specific amino acid sequence or pattern. If this is the case, it should be possible to compete out the crosslinking of nascent polypeptide chains to eEF1A with –short– peptides of various origin.

5.3.2 Nascent chains and peptides compete for binding to rabbit elongation factor 1A

The ability of eEF1A to bind unfolded proteins (see 5.2.2 and 5.2.3) suggests that eEF1A may also bind relatively short peptides. In order to test the ability of eEF1A to bind to peptides, competition experiments were performed, assaying whether an excess of peptide could reduce crosslinking of eEF1A to a nascent chains. In short, the truncated mRNA encoding 77aa ffLuc was *in vitro* translated for 10 min at 27 ˚C in a rabbit reticulocyte lysate system supplemented with TDBA-Lys-tRNA^{Lys*} and ^{35}S-Met. Ribosome nascent chain complexes were prepared by high salt extraction: RNCs were loaded on a high salt sucrose cushion (500 mM sucrose, 20 mM Hepes/KOH pH 7.5, 700 mM KAc, 5 mM MgAc, 1 mM DTT) and centrifuged at 100000 rpm and 4 ˚C for 20 min in a TLA 100 rotor (Beckman). This procedure purifies RNCs free of contaminating cytosolic proteins and, more importantly, free of the majority of RAFs. eEF1A, purified from rabbit reticulocyte lysate, was preincubated with buffer or different concentrations of peptide for 5 min at room temperature. After addition of purified RNCs, the samples were incubated for an additional 10 min at 27 ˚C. Samples were UV irradiated or not as indicated and analyzed by SDS-PAGE. The dried SDS-PAGs were exposed to autoradiographic films.

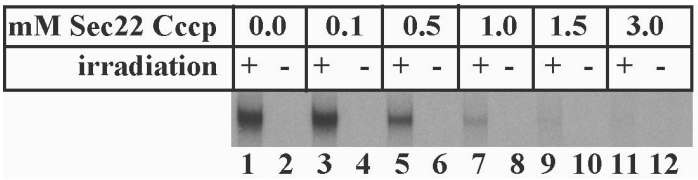

Figure 5.8: Competition of a peptide with nascent chains for binding to rabbit eEF1A.
This experiment used a 77 aa long nascent chain from the firefly *Photinus pyralis* (77aa ffLuc) with 7 lysines scattered over the length of the nascent chain to allow for crosslinking at different positions. Irradiated samples "+" are next to non-irradiated samples "-" of the same peptide concentration. Each assay contained the indicated amount of Sec 22 Cccp, 3.5 µM eEF1A from rabbit and RNCs corresponding to the equivalent of 6 µl original translation.

A crosslinking product is clearly visible after incubation with purified rabbit eEF1A (Figure 5.8 lane 1). A concentration of 0.1 mM of Sec 22 Cccp (36 aa of the C-terminal coiled coil part of the SNARE protein Sec 22, see Tables 5.3 and 7.4) had nearly no effect on the intensity of the crosslinking product with eEF1A. The crosslink to eEF1A was diminished by ca. 50 % with a peptide concentration of 0.5 mM and virtually eradicated at a peptide concentration of 1.5 mM or higher. Similar experiments are illustrated in Figures 5.10, 5.11 and 5.12.

5.3.3 Nascent chains and peptides compete for binding to yeast elongation factor 1A

At this point structural considerations let to an attempt to substitute eEF1A from rabbit with the eEF1A from yeast, since the crystal structure of yeast eEF1A in complex with a fragment of eEF1B is solved. The known structure could potentially provide crucial information for identifying the peptide binding site on eEF1A. In order to take advantage of the structure, it is prerequisite to show that the fungal eEF1A can functionally substitute its leporidaen homolog. The purification of eEF1A from yeast followed a modified method by Thiele (76).

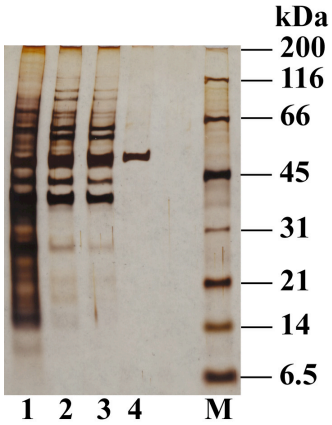

Figure 5.9: Purification of eEF1A from *Saccharomyces cerevisiae.*
Lane 1 represents the total yeast lysate, lane 2 is the supernatant of a 100000 rpm centrifugation step, lane 3 depicts the elution from the cation exchanger P11, and lane 4 illustrates the purified eEF1A after the cation exchanger S-Sepharose. M indicates the lane with the molecular weigth markers, and the molecular masses in kDa are indicated on the right. The SDS-PAG was stained with silver according to the procedure of Blum (74). See 7.2.4 for details.

In short, homogenization of the yeast cells is followed by two centrifugation steps, a batch process with the cation exchanger P11 and an S-Sepharose column. It is described in detail in section 7.2.4, and Figure 5.9 shows critical steps during the purification.

The following experiments were essentially performed as described in 5.3.2. Titration of peptide was not limited to Sec 22 Cccp, but also included the T4 bacteriophage derived Gol (see Tables 5.3 and 7.4 for details). The T4 bacteriophage derived coat protein peptide Gol has been shown previously (77) to bind to the prokaryotic homolog EF1A of the eukaryotic eEF1A in a specific manner. It was proposed that the association of Gol peptide with EF1A plays a role in T4 bacteriophage head assembly but that this association marks infected cells for "suicide" (see 5.3.5).

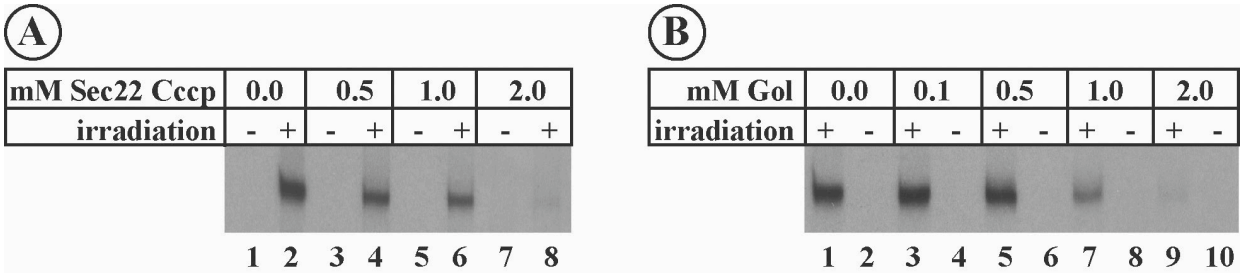

Figure 5.10: Competition of peptides with nascent chains for binding to yeast eEF1A.
This experiment used RNCs bearing the same nascent chain constructs as described in Figure 5.8. Irradiated samples "+" are next to non-irradiated samples "-" of the same peptide concentration. Each assay contained the indicated amount of peptide, 3.5 µM eEF1A from yeast and RNCs corresponding to the equivalent of 6 µl original translation.
A: Titration of Sec 22 Cccp, **B:** Titration of Gol

Figure 5.10 A demonstrates that the Sec 22 Cccp peptide, which bound to rabbit eEF1A (Figure 5.8), also binds to yeast eEF1A as shown by inhibition of the eEF1A crosslink to nascent polypeptide chains. Purified yeast eEF1A preincubated with different concentrations of Sec 22 Cccp or Gol (for details on peptides see Tables 5.3 and 7.4) was then crosslinked to high salt stripped 77aa ffLuc RNCs, as described above for experiments with rabbit eEF1A (see Figure 5.8). A prominent crosslink to eEF1A is seen in the absence of peptide (Figure 5.10 A lane 2 and Figure 5.10 B lane 1), and at concentrations of Gol up to 0.5 mM (Figure 5.10 B, lanes 3 and 5). The intensity of the crosslinking band is greatly reduced after preincubation of yeast eEF1A with 1.0 mM Sec 22 Cccp or Gol and eradicated with 2.0 mM of either peptide.

This shows clearly that the competition of nascent polypeptide chains and peptides for binding to eEF1A is reproducable and that eEF1A from rabbit can be functionally substituted by the yeast factor. It is important to point out that yeast eEF1A apparently interacts properly with the rabbit ribosomes in the same way as the rabbit eEF1A does (RNCs are still prepared from rabbit reticulocyte lysate!).

5.3.4 Various peptides compete with nascent chains for binding to the eukaryotic translation elongation factor 1A

The ability of eEF1A to bind unfolded proteins (see 5.2.2 and 5.2.3) suggested that an unfolded protein might compete with RNCs for binding to eEF1A, as shown by an inhibition of eEF1A crosslinking to nascent polypeptide chains. The ability of peptides to compete with nascent polypeptide chains for binding to eEF1A suggests that there is a specific site on eEF1A for binding to unfolded protein or peptides. An important question to ask is whether unfolded proteins or peptides need to fullfill specific requirements or whether any peptide can bind.

#	Peptide		length	M_W	pI	z	Competition
1	Bet 1	C	35	3985.5	9.98	+2	+
2	Gos 1	C	32	3648.2	12.32	+5	+
3	Nyv 1	N	28	3236.5	3.98	-5	+
4	Sec 22 Cccp	C	36	4108.6	9.31	+2	+
5	Sft 1	C	36	3933.4	9.98	+2	**weak**
6	Snc 1	N	36	4016.3	4.84	-3	**weak**
7	Snc 1	C	36	4082.6	9.82	+3	**weak**
8	Snc 2	N	36	3932.2	4.30	-3	+
9	Syntaxin 1A	N	38	4504.1	4.82	-4	**weak**
10	Syntaxin 1A	C	39	4612.2	9.46	+3	+
11	Tlg 1	C	36	4283.8	6.35	0	+
12	Vamp 2	N	35	4139.6	6.27	0	+
13	Vamp 2	C	35	4039.5	9.31	+2	**weak**
14	Vam 7	C	32	3624.9	6.77	0	**weak**
15	Vti 1	C	34	3984.5	9.98	+3	+
16	□-crystallin		24	3005.5	11.7	+5	—
17	DLG 4		16	1786.8	4.35	-1	—
18	FLAG		8	1012.9	3.97	-3	—
19	Gol		29	3059.6	8.29	+1	+
20	Gonc		31	3375.8	3.90	-4	+
21	Lysozyme		13	1661.9	8.38	+1	**enhances**
22	Mtj 1		17	2042.4	11.17	+7	+
23	Prol		31	3340.7	4.04	-3	**enhances**
24	Rim		25	3082.4	4.36	-6	+
25	Sec 61 □		10	930.0	5.91	0	—
26	Senc		32	3695.2	7.90	+1	**enhance**
27	SRP 14		15	1818.2	10.39	+6	**weak**
28	SRP R □		15	1793.1	9.52	+3	—
29	Tom 40		18	1862.1	4.37	-1	—
30	Tomosyn		15	1916.1	11.44	+5	—

Table 5.3: Initial set of peptides tested for competition in crosslinking assays.
N or C for the first 15 peptides denotes the N- or C-terminal half of a coiled coil region of the peptide derived from the corresponding SNARE protein. The peptide length is given by the number of amino acids. The molecular weight M_W was calculated from the amino acid sequence and is given in Daltons using the sequence analysis tool "ProtParam" from the ExPASy Molecular Biology Server at *http://us.expasy.org/tools/protparam.html*. The same source was used to determine the charge z of the peptides. The strength of the competition is based on visual comparisons between titrations for each peptide and therefore only of qualitative nature. For a complete list of all peptides used and further information on these peptides see Table 7.4.

In order to exclude the influence of an unidentified sequence bias as the hidden reason for the competition, a rigorous approach was attempted. Using basically the same experimental set-up as described before, a variety of short peptides were tested (kind gifts of members of the Wiedmann-, Rothman-, and Söllner-labs). Table 5.3 summarizes the lengths, the apparent molecular weights, the pI values, and charges of the peptides tested for binding to eEF1A in this set of experiments. A complete list of all tested peptides can be found in Table 7.4. Based on this limited sample of peptides, the only predictor of successful competition for binding to eEF1A is peptide length: a minimum length of ca. 20 amino acids is necessary for binding to eEF1A. There does not appear to be any clear sequence requirement for binding to eEF1A. Competition for binding to eEF1A is observed with a wide range of peptide sequence compositions including acidic and/or basic residues, bulky hydrophobic residues and helix-breaking residues such as prolines. It is interesting to note that the overall charge z of a peptide does not seem to be relevant because Gonc (pI = 3.90) inhibits as well as Gos 1 (pI = 12.32) does.

The large size of the peptides and the relative lack of sequence requirements suggest that binding requires many low energy interactions between peptide and eEF1A. Presumably, neutral or unfavorable interactions at a few specific residues would be outweighed by favorable interactions over the remainder of the peptide. Since it was shown in 5.2.3 that eEF1A binds to unfolded protein, it is noteworthy to mention that the found minimum length is significantly longer than typical binding sites in molecular chaperones or MHCs, which are about seven to nine amino acids in length (78).

In Figure 5.11 five peptides that failed to inhibit the crosslink to eEF1A at any concentration are shown at the highest concentration used (2.0 mM). They range in length from eigth aa (FLAG) to 18 aa (Tom 40).

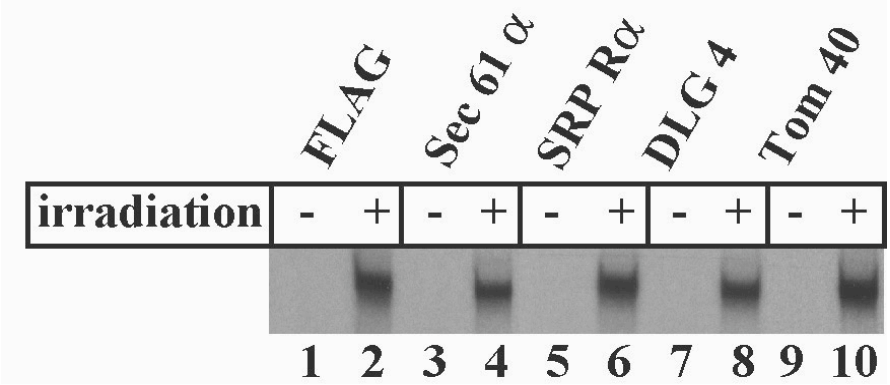

Figure 5.11: A variety of different peptides that do not bind to eEF1A.
This experiment used a 77 aa long nascent chain from the firefly *Photinus pyralis* (77aa ffLuc) with seven lysines scattered over the length of the nascent chain to allow for crosslinking at different positions. Irradiated samples "+" are next to non-irradiated samples "-" of the same peptide concentration. Each assay contained 2.0 mM of the indicated peptide, 3.5 µM eEF1A and RNCs corresponding to the equivalent of 6 µl original translation.

5.3.5 Systematic investigation of the effect of peptide length on competition

In earlier experiments it was already shown (see Tables 5.3 and 7.4), that the artificial created Gonc peptide was as efficient in competition experiments as Gol or Sec 22 Cccp. The Gonc peptide of has the following sequence:

1 5 6 19 20 31

MDIAIFDICGVQPMNSPTGEDQVDPRLIDGK

The N-terminal five amino acids 1 through 5 (green) consist of a common recognition sequence for N-acetylation derived from the human eye lens protein □-crystallin. At its core from amino acid 6 through 19 (blue) Gonc comprises the 14 C-terminal amino acids of the naturally occuring Gol peptide. The Gol peptide corresponds to amino acids 94 through 122 of the major capsid protein (MCP or gp23) of T-even and T-even like bacteriophages. The Gol region was defined by T4-mutants that allowed growth on Lit-producing bacteria. Lit is a metalloprotease from the probacteriophage e14 that cleaves EF-Tu, if the 29 amino acid long Gol is bound to domain II and III of EF-Tu. Eventually, this leads to a competition of two parasitic bacteriophages for one host resulting in a "suicide" of the bacterium by ceasing protein translation upon secondary infection by T-even or T-even like bacteriophages. This ensures that the DNA of the probacteriophage e14 can propagate through the bacterial culture.

The C-terminal twelfe amino acids 20 through 31 (red) encode the residues 6 through 17 of the heavy chain of Protein C, a vitamin K-dependent plasma zymogen. This Protein C-tag can be efficiently used for purification purposes via an anti-Protein C affinity matrix (Roche, Indianapolis IN). A monoclonal antibody binds to the Protein C-tag only in the presence of Ca^{2+}, but then with high affinity and specificity.

Name	Sequence	length [aa]	pI	Z	M_W [Da]
Gonc 31mer	MDIAIFDICGVQPMNSPTGEDQVDPRLIDGK	31	3.90	-4	3375.85
Gonc 29mer	IAIFDICGVQPMNSPTGEDQVDPRLIDGK	29	4.04	-3	3129.56
Gonc 27mer	IFDICGVQPMNSPTGEDQVDPRLIDGK	27	4.04	-3	2945.33
Gonc 25mer	DICGVQPMNSPTGEDQVDPRLIDGK	25	4.04	-3	2684.99
Gonc 23mer	CGVQPMNSPTGEDQVDPRLIDGK	23	4.23	-2	2456.74
Gonc 21mer	VQPMNSPTGEDQVDPRLIDGK	21	4.23	-2	2296.54
Gonc 19mer	PMNSPTGEDQVDPRLIDGK	19	4.23	-2	2069.28
Gonc 17mer	NSPTGEDQVDPRLIDGK	17	4.23	-2	1840.97
Gonc 15mer	PTGEDQVDPRLIDGK	15	4.23	-2	1639.78
Gonc 13mer	GEDQVDPRLIDGK	13	4.23	-2	1441.56

Table 5.4: Gonc and its truncated versions.
The amino acids are colored as charged, polar and hydrophobic. The M_W is listed as the theoretical average mass as provided by the manufacturer (Emory University Microchemical Facility, Atlanta GA). Peptide stock solutions were generally created by dissolving a corresponding amount of peptide in 1/10 vol. of 100 % DMSO, then adding 9/10 vol. of 50 mM Hepes pH 7.5 to reach a concentration of 5 mM. A solution of 10 % DMSO in buffer did not affect crosslinking efficiencies or intensities.

The strategy to investigate the length dependency includes utilizing the Gonc peptide and subsequently increasingly truncated derivatives of Gonc in the established crosslinking assay. The sequences and terminology for Gonc and the derived peptides can be found in Tables 5.4 and 7.4.

The crosslinking experiment was essentially performed as described in 5.3.2 with 77aa ffLuc mRNA as the source for RNCs. Details are given in the legend to Figure 5.12.

Gonc and its derivatives have a mixed effect on the crosslinking efficiency of the employed RNCs with respect to eEF1A. The negative control in Figure 5.12 (lane 1) shows clearly the absence of a crosslink to eEF1A. The positive control (lane 2) shows the expected crosslink of 77aa ffLuc to eEF1A, which has an apparent molecular weight of ~58 kDa. The intensity of this crosslinking product was quantified by exposing the dried gel to a Phosphor screen and analyzed as described elsewhere (7.3), and was arbitrarily set to 100 %.

For the Gonc derivatives with a chain length from 13 to 29 amino acids the intensity of the crosslinked product seems to increase overall with increasing chain length. Displaying the data gained from the Phosphor Imager analysis as data points and applying a curve fit yields a linear curve with a correlation coefficient of R = 0.94, indicative of a very good positive linear dependency of the intensity from the chain length (data not shown, but see Figure 5.13).

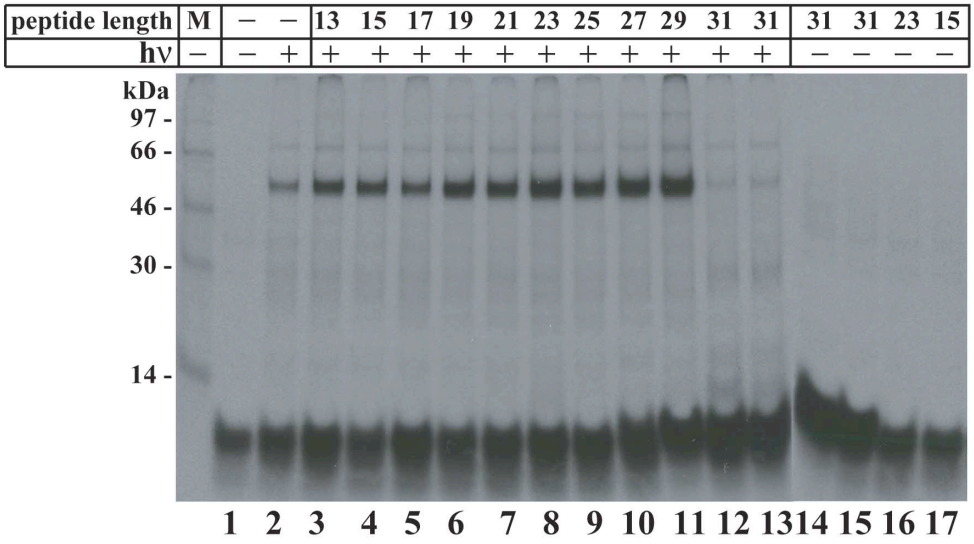

Figure 5.12: Influence of Gonc and its derivatives on crosslinks of eEF1A to nascent polypeptide chains.
77aa ffLuc mRNA was translated for 10 min at 26 ˚C and RNCs were isolated twice over high salt sucrose cushion. Irradiation is referred to as "h□", irradiated samples are marked "+", non-irradiated samples "-". Each 20 µl assay contained 2.5 mM of the indicated peptide, 2.5 µM eEF1A and RNCs corresponding to the equivalent of 12 µl original translation. The peptides used in lanes 3 to 12 and 15 to 17 were purchased from the Microchemical Facility of the Emory University (Atlanta, GA), the 31mer used in lanes 13 and 14 was from SynPep (Dublin, CA). Molecular masses in kDa are indicated on the left, the marker "M" is found in the unnumbered lane.

The presence of the 31mer Gonc changes the picture drastically, because the intensity of the crosslinking band is reduced by ~50 % compared to the positive control in lane 2. The intensities found in lanes 12 and 13 are strikingly similar, although the peptides came from two different suppliers.

A different representation of these data is illustrated in Figure 5.13, where the intensity of the crosslinking product is shown as the percentage of the total intensity of crosslinking product and the band generated by the nascent polypeptide chain.

Three features can be deduced from Figure 5.13. Firstly, the crosslinking efficiency in this type of experiments is per se exceptionally good, which can be confirmed visually by looking at Figure 5.12.

Secondly, with the exception of the 17mer Gonc, the crosslinking efficiency seems to reach a saturating level of about 20 %. This is surprising, given the visual impression from Figure 5.12, where the crosslinking efficiency seems to increase with chain length. Apparently, the increase of the intensity of RNCs is not so easy to detect visually.

Thirdly, in this representation the effect of the 31mer Gonc is even more pronounced dropping the percentage from ~11 % for the crosslink of 77aa ffLuc to eEF1A down to ~3 %.

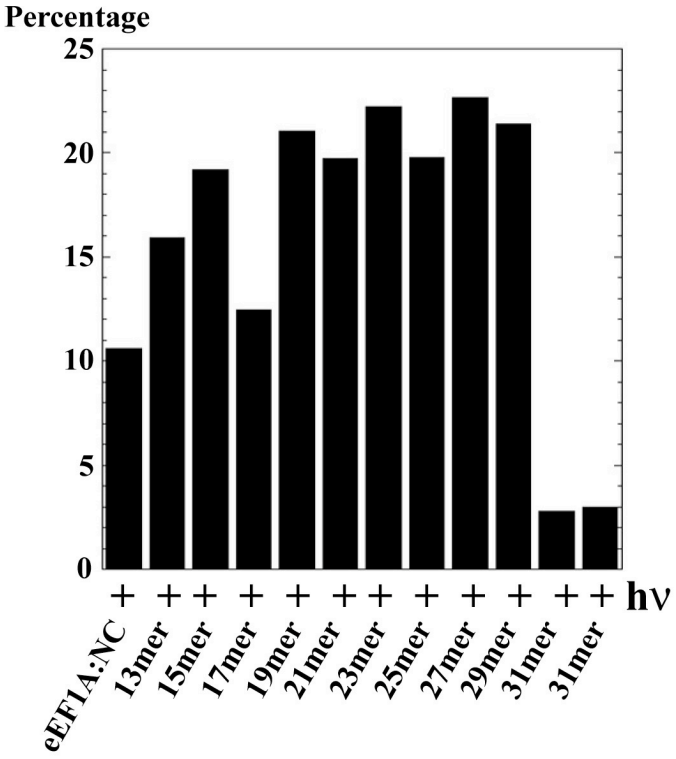

Figure 5.13: Intensity of crosslinks of eEF1A to nascent chains as percentage of the total intensity.

The calculus reads $Percentage = \frac{I_X}{I_X + I_{NC}} \bullet 100$ where I_X is the intensity of the crosslink and I_{NC} is the intensity of the nascent polypeptide chain. This is a first approximation only because the error due to ignoring minor other bands is not corrected for. eEF1A:NC corresponds to lane 2, followed by lanes 3-13 in Figure 5.12. For details on samples see Figure 5.12 and for details on the procedure see 7.3.

5.3.6 The conformational and oligomeric state of 29mer and 31mer Gonc peptides

The astonishing difference with respect to the effect caused by the 29mer and the 31mer of Gonc is not easily explainable. That the presence of two more amino acids on the N-terminus can have such a drastic effect led to speculations about the state of oligomerization of the two peptides. NMR spectroscopy and gel-filtration chromatography were applied to gain more knowledge about the peptides.

NMR

In order to gains some insight into the structural features of the two longest Gonc peptides, NMR spectra were kindly recorded by Dr. Ananya Majumdar from the Structural Biology Department of the MSKCC, Nucleic Acid and Protein Structure Program (Dr. Dinshaw Patel).

Figure 5.14 A and B represent the 1D ^{1}H spectra for the 29mer and 31mer of Gonc, respectively. Both spectra show particular features. A completely unstructured peptide or protein would give rise to a very broad peak for the chemical shift from the backbone amide protons between 7.0 and 9.0 ppm. Both peptides do exhibit a discrete spectrum with several distinguishable sharp peaks between 7.0 and 8.5 ppm. Therefore they are not completely unstructured. However, a peculiar feature in both cases is the clear cut off of the chemical shift at $\delta \approx 8.5$ ppm. Even small but well structured proteins usually generate chemical shifts up to $\delta \approx 9.5$ ppm.

At the higher end of the spectrum the 29mer exhibits just slightly broader peaks than the 31mer, but it is debatable whether this is a significant difference (personal communication Dr. A. Majumdar).

For the 29mer out of the 29 expected separate peaks 23 were identified in the range between 7.4 and 8.5 ppm of the spectrum (Figure 5.14 A). Four more could potentially be assigned to shoulders in the spectrum. Between 7.1 and 7.4 ppm signals from side chains are detectable and the strong signals between 6.8 and 6.9 ppm are most likely from Asp/Glu side chains.

For the 31mer 22 out of 31 expected separate peaks were identified in the range between 7.4 and 8.5 ppm of the spectrum (Figure 5.14 B). Seven more could potentially be assigned to shoulders in the spectrum. The signals for $\delta < 4.7$ are essentially the same as for the 29mer (Figure 5.14 A and B).

Since the 1D ^{1}H spectra did not demonstrate clear differences between the two peptides, a 2D NOESY was performed on the 31mer only. The obtained result was rather inconclusive, since a proton pattern emerged that either pointed to a very large protein or was indicative of problems with setting parameters like mixing times (personal communication Dr. A. Majumdar, data not shown).

In a third attempt both peptides were subjected to 2D HSQC measurements (Figure 5.14 C and D). In this type of spectroscopy the signals of two different nuclei (^{1}H and ^{15}N) are recorded. ^{1}H gives a strong signal around $\delta = 8.5$ ppm and ^{15}N around $\delta = 108$ ppm. The exploitation of a second nuclei provides an enhanced resolution and improves sensitivity, which turns HSQC into a less ambiguous

method than NOE-based assignments. However, the disadvantage in this particular set of experiments is that both peptides were not specifically labeled with ^{15}N so that the measurements had to rely on the naturally incorporated ^{15}N, which has a natural abundance of only 0.36 % among N isotopes. For this reason the spectra were recorded over 17 h and the peptide concentration was raised to 4.76 mM.

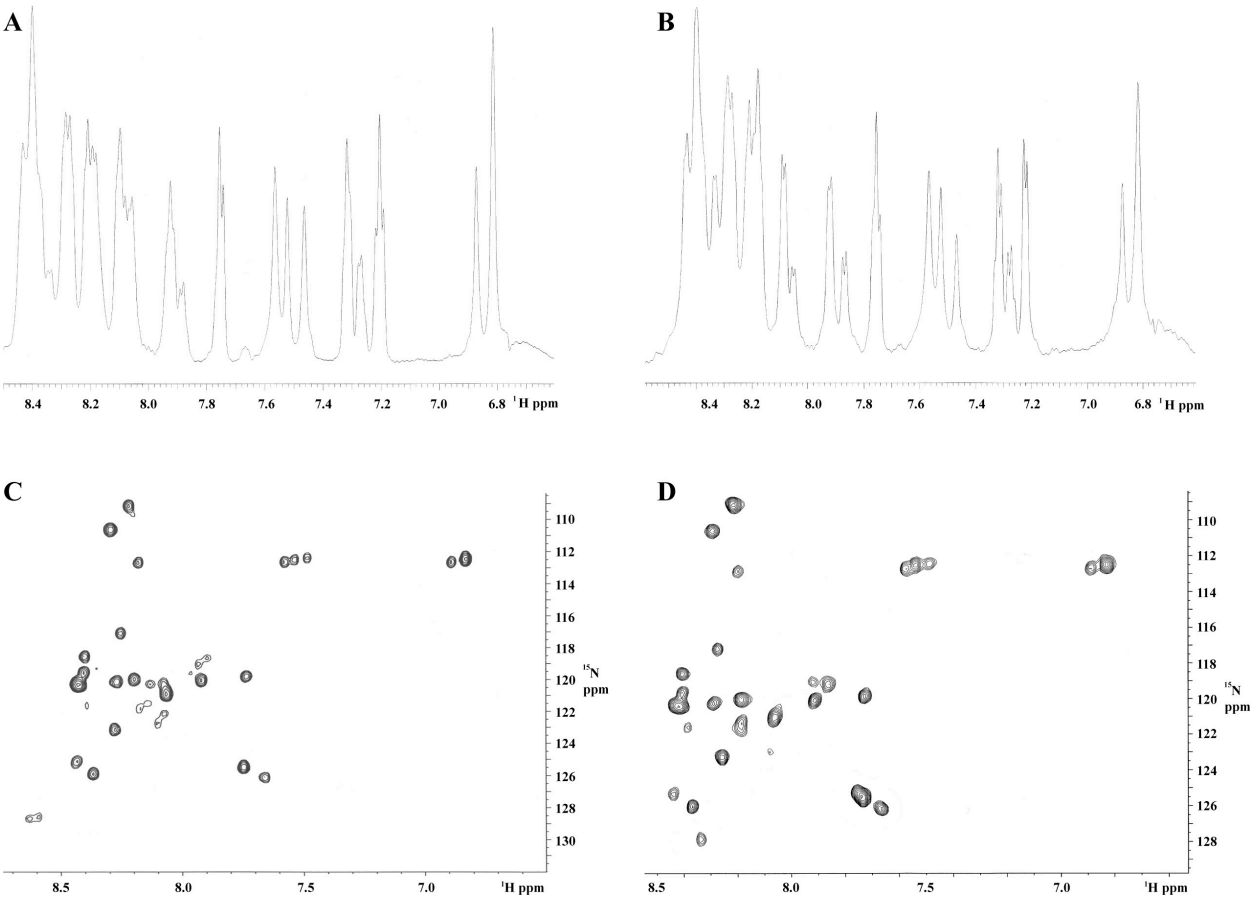

Figure 5.14: NMR spectroscopy of Gonc peptides.
A: 1D ^{1}H spectrum of 29mer Gonc. **B:** 1D ^{1}H spectrum of 31mer Gonc.
C: HSQC spectrum of 29mer Gonc. **D:** HSQC spectrum of 31mer Gonc.
For the 1D ^{1}H spectra 500 µl of a 1 mM peptide solution in 10 mM Hepes pH 7.8, 20 mM Tris/HCl pH 7.8, 150 mM KCl, 2 % DMSO, and 10 % v/v D_2O (99.9 atom % D) was measured. For the HSQC spectra peptide concentration was 4.76 mM in 50 mM Hepes pH 7.8, 10 % v/v DMSO, and 10 % v/v D_2O (99.9 atom % D). The peptide solutions were centrifuged for 10 min at 100000 rpm and 4 ˚C in a Beckman ultracentrifuge (TLA 120.1 rotor) and the supernatant was transferred into quarz tubes for spectroscopic analysis. Neither a visible pellet was obtained nor was peptide detected on silver stained PAGs.

Figures 5.14 C and D show that both peptides gave very similar spectra. Several features can be identified: the majority of the crosspeaks is rather identical in both peptides (personal communication Dr. A. Majumdar). The three peaks localized at δ_H = 8.2-8.3 ppm and δ_N = 109-113 ppm in both spectra are potentially caused by the three glycines. There are in both spectra signals typically generated by amide groups of the side chains of asparagin, glutamine, or arginine (but not lysine). They can be identified as a

triple peak at δ_H = 7.4-7.6 ppm and δ_N = 112-113 ppm and as a double peak at δ_H = 6.8-7.0 ppm and δ_N = 112-113 ppm. If the peptides were completely unstructured, i.e. all residues were in the same environment, these five signals would converge into one large single signal around δ_H = 7.2 ppm and δ_N = 112-113 ppm.

There is only one crosspeak that has a different location and shape in the two spectra. In the case of the 29mer it is localized at δ_H = 8.6 ppm and δ_N = 129 ppm and exhibits a split ^{1}H signal. In the case of the 31mer it can be found at at δ_H = 8.3 ppm and δ_N = 129 ppm and is not split. A split chemical shift can be produced by either terminus of a peptide. Since both peptides have the same C-terminus, the split could potentially be assigned to the N-terminus of the 29mer. There are four signals in Figure 5.14 C located at δ_H = 7.9-8.2 ppm and δ_N = 118-123 ppm that are less strong than in Figure 5.14 D. This can be indicative of a more flexible configuration in the 29mer compared to the 31mer.

Given the limitations of the presented NMR studies, these results clearly qualify as prelimnary results and require further investigations. Nevertheless, these prelimnary results already indicate that there may be a structural difference between the two peptides, however small this may be. Furthermore, the peptides are at least partially structured due to the unique signals obtained. This is not necessarily expected, since both sequences have three prolines and three glycines in their sequence, which accounts for ~20 % of the residues.

Gel-filtration chromatography

Another technique to characterize a molecule under investigation is the separation due to size differences by gel-filtration chromatography. Figure 5.15 A illustrates the result for the 29mer of Gonc. The peptide eluted in fractions 34-39, which corresponds to 13.04-14.84 ml eluate (first 0.8 ml not collected). The two main fractions of the 29mer Gonc elute at the same volume where the chymotrypsinogen A elutes (25 kDa), ribonuclease A (13.7 kDa) follows shortly thereafter.

This result would indicate an octameric state for the 29mer of Gonc or rather a tetramer of dimers, since the monomer has an apparent molecular weight of 3.13 kDa and both, the 29mer and 31mer, exhibit an apparent molecular weight of ~6 kDa on SDS-PAGs even under harsh conditions. Note the small range of only six fractions to cover the whole elution of 29mer Gonc and the two fractions that account for more than 80 % of the peptide.

Figure 5.15 B shows the same experiment for the 31mer of Gonc. According to the manufacturers instructions, the Superdex 75 column has a fractionation range for globular proteins from 3 to 70 kDa. Unexpectedly, the peptide eluted in fraction 21-23, which corresponds to an elution volume of 8.36-9.08 ml (first 0.8 ml not collected). This was prior to any protein used in the five protein standard (Table 7.3). Since bovine serum albumin is with 67 kDa at the limit of the exclusion size and 31mer Gonc elutes to

~90 % in one single fraction two fractions prior to this protein, it indicates that 31mer Gonc is in an oligomerization state that is beyond the fractionation range of the Superdex 75 column.

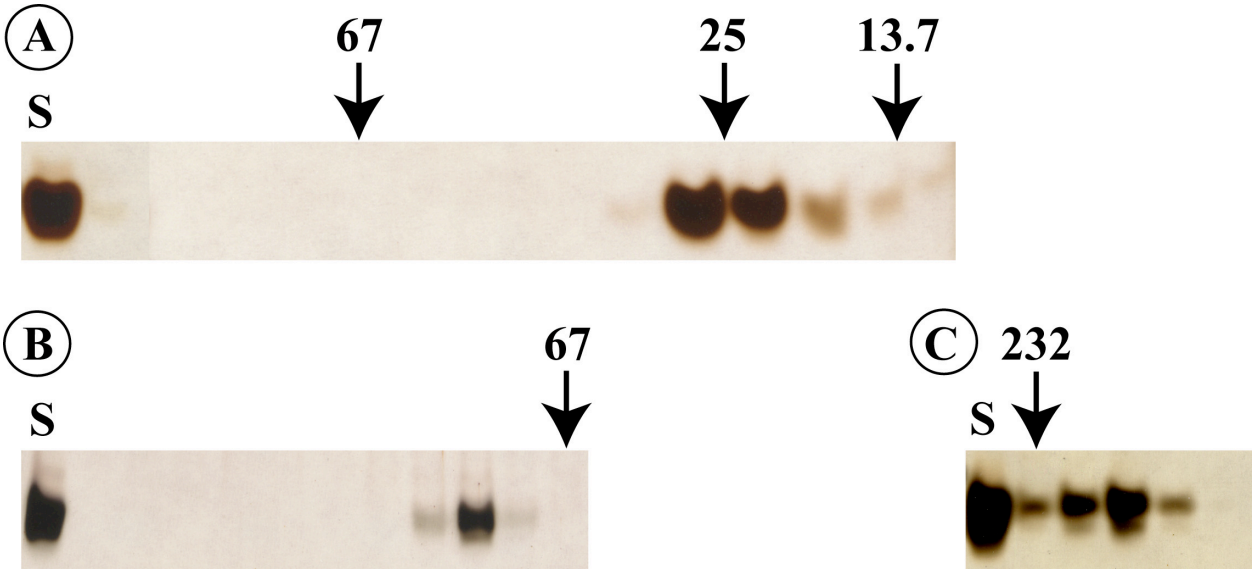

Figure 5.15: Gel-filtration chromatography of 29mer and 31mer Gonc peptide.
In each case 200 µl of a 1 mM peptide solution were loaded onto the corresponding Superdex column (24 ml bed volume, 0.4 ml/min flow rate). The void volume of the column is 8.0 ml. "S" refers to an aliquot of the starting material. Numbers above arrows indicate the apparent molecular weight in kDa of standard proteins as listed in Table 7.3. The arrows indicate the approximate location of maximum peak position of the standard proteins, except for Figure 5.15 C, where it indicates the first fraction where the tetrameric catalase appears. 15 µl of each fraction was analyzed on a silver stained 10 % NuPage gel (Invitrogen, Carlsbad CA). **A, B:** Superdex 75 column, 0.36 ml fractions were collected. **C:** Superdex 200 column, 1 ml fractions were collected. For details see 7.2.8 and main text.

Figure 5.15 C demonstrates the elution profile of 31mer Gonc peptide on a Superdex 200 column. According to the manufacturers instructions, this column offers a fractionation range for globular proteins from 10 kDa to 600 kDa. The column was calibrated with the seven protein standard (see 7.2.8, Table 7.3), which included the oligomeric proteins aldolase and catalase. Surprisingly, the 31mer peptide eluted in four 1 ml fractions at 9-12 ml. From the marker proteins, the tetrameric catalase (232 kDa) eluted in eight 1 ml fractions starting at the same 9 ml fraction. It is also of interest that, although the collected fractions were 1 ml compared to 0.36 ml on the Superdex 75 column (bed volume and flow rate were the same), the 31mer is now distributed over more eluted volume. This suggests that the peptide actually diffused into the gel matrix and got separated by its size. But the most astonishing conclusion is that the 31mer Gonc peptide (3.4 kDa) must be present in a huge complex of 60 or more molecules. This is clearly a difference to the oligomerization state of the 29mer Gonc.

It was described in a previous section (5.3.5) that the 31mer but not the 29mer of the Gonc peptide exerted a strong influence on the crosslinking capability of a nascent chain towards eEF1A. Thus,

the question arose, as to whether or not this interaction would result in a different diffusion behaviour of the 31mer Gonc peptide on the Superdex 200 gel-filtration column. Figure 5.16 gives an example of such an experiment. The assay contained 2.5 µM eEF1A, 2.5 mM 31mer Gonc and 250 µM aa-tRNA^{aa}. It was loaded onto a Superdex 200 column after a high speed centrifugation (see 7.2.8).

Very surprisingly, the 31mer Gonc peptide exhibits now an entirely different elution behaviour. Its elution covers the complete range starting from the size it displays when loaded alone (5.15 C) down to its monomeric size. It appears first in fraction 5 (10 ml), which is 1 ml later than where catalase starts eluting (9 ml, 232 kDa) and continues to elute even after fraction 17/18 where the peak of the monomeric aprotinin (~19.5 ml, 6.5 kDa) is localized. Apparently, the huge complex of 31mer Gonc as seen in 5.15 C is dissolved in presence of eEF1A and aa-tRNA^{aa}.

The elution profile of eEF1A changed as well: eEF1A co-elutes with the 31mer Gonc peptide over the whole range (Figure 5.16), although to a much less extend on the low molecular weight side. However, if gel-filtrated by itself, eEF1A elutes around the peak of bovine serum albumin (fraction 12, 15.3 ml, 67 kDa), i. e. in fraction 11-13 (14.6-16.1 ml); eEF1A exhibited the same elution behaviour in presence of aa-tRNA^{aa} (data not shown).

The elution profile of 31mer Gonc in presence of eEF1A without charged tRNA under otherwise the same conditions restricts the elution range to fractions 5-12 (10-15.3 ml; data not shown).

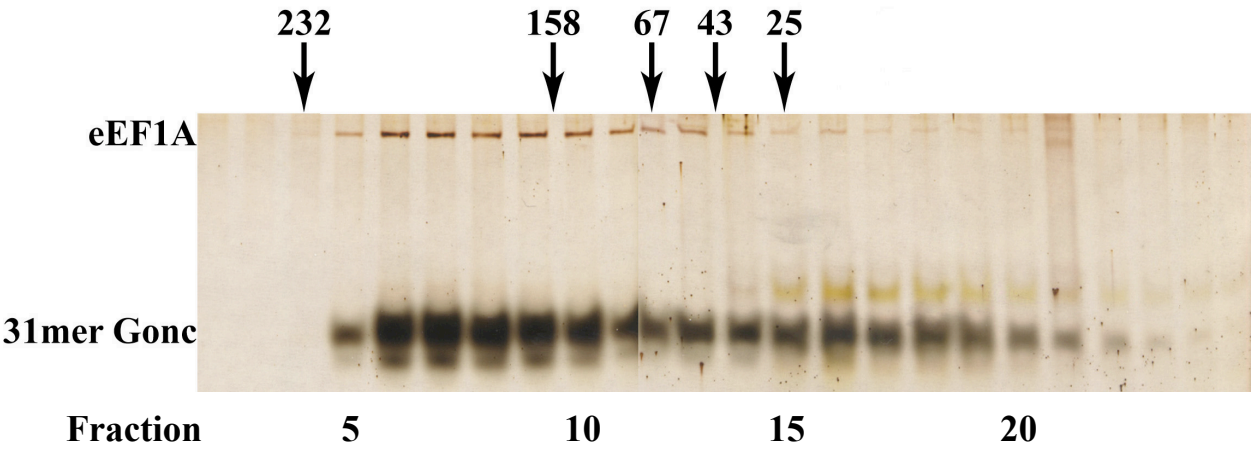

Figure 5.16: Superdex 200 gel-filtration of 31mer Gonc in presence of eEF1A and aa-tRNA^{aa}.
A 200 µl assay contained 2.5 mM 31mer Gonc, 2.5 µM eEF1A, 250 µM aa-tRNA^{aa} in 50 mM Hepes pH 7.5, 150 mM KAc, 5 mM MgAc, 1 mM DTT, 2 % v/v DMSO, and 10 % v/v glycerol and was centrifuged before loading onto the column. Numbers above arrows indicate the apparent molecular weight in kDa of standard proteins. The arrows indicate the approximate location of maximum peak position of the standard proteins, except for 232, where it indicates the first fraction where the tetrameric catalase appears. The first 6.2 ml were not collected, subsequent fractions were 0.8 ml each. 15 µl of each fraction was loaded onto a 10 % NuPage gel (Invitrogen, Carlsbad CA) and silver stained. For details see 7.2.8 and main text.

5.3.7 Influence of charged aa-tRNA^{aa} and uncharged tRNA^{aa} on crosslinking of nascent polypeptide chains to the eukaryotic translation elongation factor 1A

The following experiments were conducted after the effect of charged aa-tRNA^{aa} on the GTPase activity of eEF1A became clear (section 5.5.1).

Charged aa-tRNA^{aa} is as a component of the ternary complex naturally associated with eEF1A. Therefore, it is interesting to ask whether charged aa-tRNA^{aa} –or even uncharged tRNA^{aa}– has the ability to compete with a nascent polypeptide chain for binding to eEF1A. Figure 5.17 illustrates the outcome of such a competition assay. 77aa fflLuc mRNA was translated for 10 min *in vitro*, and RNCs were subsequently isolated as described elsewhere (7.2.1 and 7.2.2). A 10 µl assay contained the RNC-equivalent of 6 µl original translation lysate, 2.5 µM eEF1A, and 25 or 250 µM of the charged aa-tRNA^{aa} or uncharged tRNA^{aa} as noted. After 10 min at 26 ˚C, aliquots were irradiated for 10 min as specified. Samples were treated with RNase A and EDTA prior to SDS-PAGE and analyzed by autoradiography. The intensities of the crosslinking products were quantified by exposing the dried gels to a Phosphor screen and analyzed as described elsewhere (7.3).

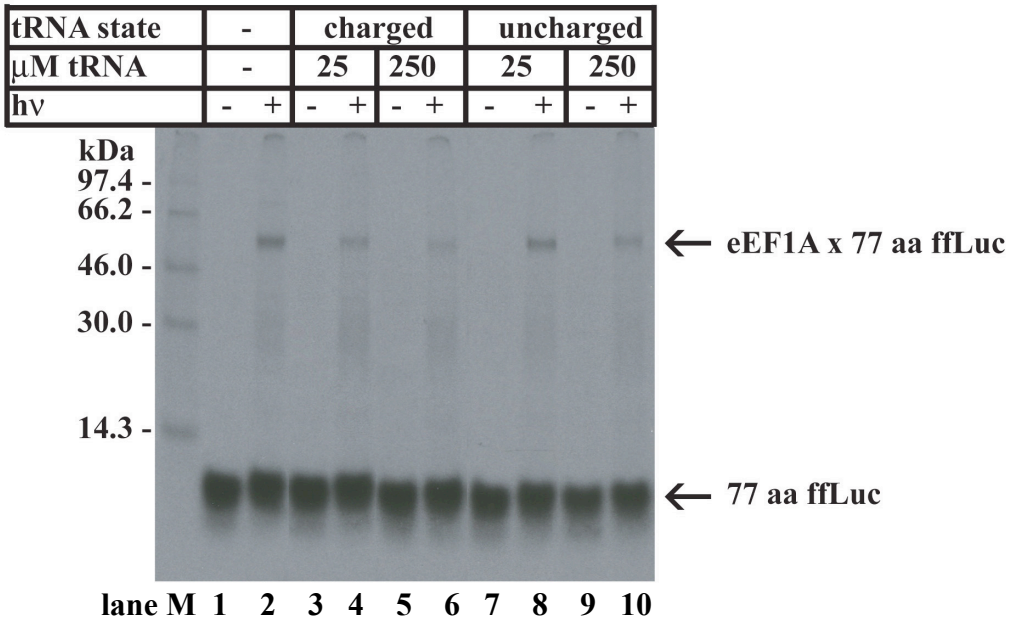

Figure 5.17: Competition of aa-tRNA^{aa} and tRNA^{aa} for crosslinking of 77 aa Luciferase to eEF1A.
M designates the lane with the molecular weigth marker and molecular masses are indicated on the left in kDa.

Compared to the positive control (Figure 5.17, lane 2), the intensities of the crosslinking products are in all cases markedly reduced. However, at a given tRNA concentration aa-tRNA^{aa} interferes stronger than tRNA^{aa} (compare lane 4 with 8 and lane 6 with 10, respectively). Furthermore, higher concentrations of aa-tRNA^{aa} or tRNA^{aa} provoke a stronger effect than lower concentrations (compare lane 4 with 6 and

lane 8 with 10). Note that the concentration of eEF1A resembles the cellular concentration and that the chosen concentrations for tRNA are 10 and 100 times higher than the concentration of eEF1A. In the cellular environment tRNA would be about 20 times higher than eEF1A (39-41).

5.4 Localization of the novel peptide binding site on the eukaryotic translation elongation factor 1A

5.4.1 Rationale

It was shown in previous sections of this chapter that eEF1A can be crosslinked to nascent polypeptide chains. Moreover, this crosslinking can be competed out with short peptides. Furthermore, it is known that eEF1A is able to interact with other proteins (3.3). It is therefore reasonable to assume that eEF1A has at least one peptide or protein binding site.

Given the recent publication of the yeast eEF1A X-ray crystal structure (53,54), the identification of the peptide binding site would provide valuable information about the elucidation of the particular function of eEF1A in the context of its interacting with nascent polypeptide chains or short peptides.

5.4.2 Strategy to identify the the peptide binding site on the eukaryotic translation elongation factor 1A

The general method described in earlier parts of this chapter takes advantage of both, radioactive ^{35}S-Met and a site-specific photoactivatable crosslinker. However, this approach is not feasable due to the dependency on *in vitro* translated nascent polypeptide chains, which limits the material for subsequent analysis drastically. Hence, a strategy was developed that benefits from the rather non-limiting amount of purified eEF1A and commercially available bifunctional crosslinker as well as short peptide. This not only provided enough material but also eliminated the presence of radioactive ^{35}S-Met.

The general outline of the crosslinking procedure can be described as a four-step method. A short peptide is completely reduced and then modified with a heterobifunctional chemical crosslinker. The modified peptide is subsequently incubated with eEF1A to facilitate binding to the peptide binding site. In a last step the conjugate between the peptide and eEF1A is irreversibly created by irradiation. By performing an SDS-PAGE, the crosslinking product is supposed to have a higher apparent molecular weigth than eEF1A alone: ~50 kDa for eEF1A, ~3.4 kDa for Gonc and ~308 Da for the remains of the crosslinker. The band can be excised from the gel and analyzed by mass spectroscopy after trypsin digestion.

After performing this procedure under a great variety of conditions with respect to incubation times, buffer and salt conditions, peptide to crosslinker ratio, the outcome of these crosslinking experiments can be summarized as illustrated in the diagram of Figure 5.18.

The most astounding result was that eEF1A was completely crosslinked away under several conditions. (Figure 5.18, lane 6). Although no discrete band of a crosslinked product could be detected, a smear with an apparent molecular weight of 300 kDa and more was visible. In many cases the smear did not enter the 8 % resolution gels completely but stayed partially in the stacking gel. With the lack of a distinctive band it was not possible to analyze these samples by mass spectroscopy. However, since the crosslinked product still could enter the resolution gel in most cases, it indicates that eEF1A does not form extended aggregates upon being crosslinked.

One possible explanation for this result is that APDP targets not only sulfhydryl-groups but also amine-groups of Gonc, although this should not happen according to the manufacturers instructions. Multiple crosslinkers per Gonc peptide could give rise to the kind of observed smear.

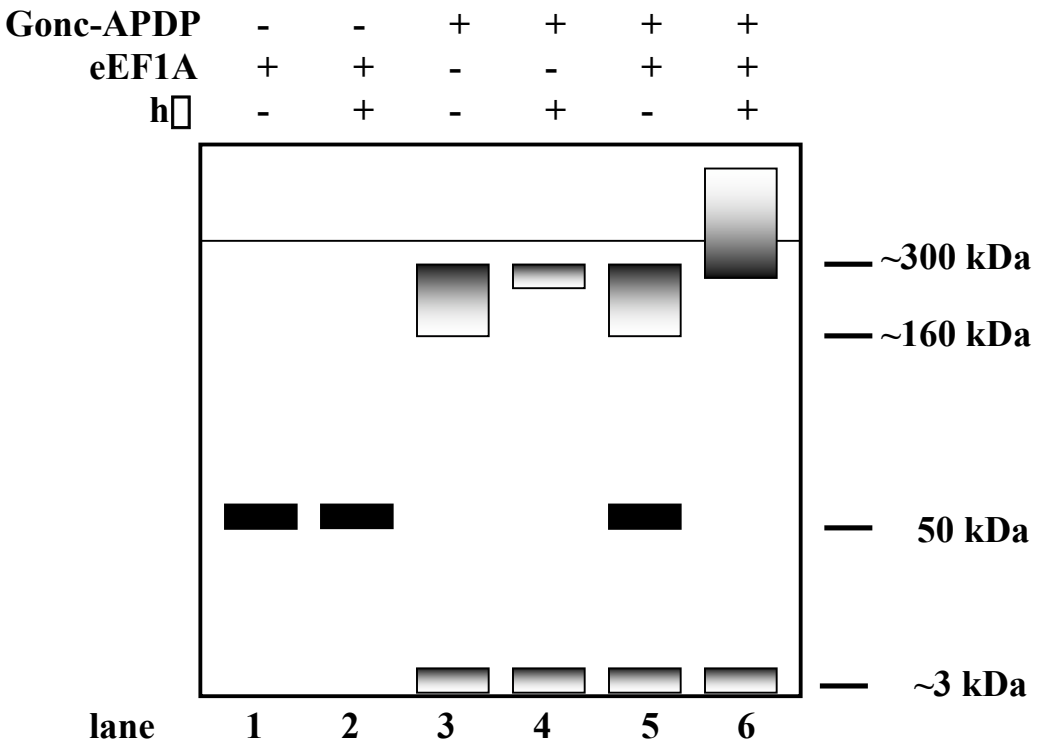

Figure 5.18: General outcome of APDP experiments under various conditions.
This diagram depicts an 8 % SDS-PAG. The ~3 kDa band illustrates the Gonc peptide, the ~50 kDa band eEF1A. The high molecular weight smear started to appear at ~300 kDa when eEF1A was present and continued into the stacking gel.

Eventually, a promising system was established by adding a reducing step after irradiation of the samples. The procedure is described in detail in 7.2.9. In order to identify the peptide binding site of eEF1A, the Gonc peptide is necessary only for the specific interaction with eEF1A but not for identifying the eEF1A fragment by mass spectroscopy. Therefore, treatment of the crosslinked product/smear with strong reducing agents like DTT or TCEP (Tris-(2-carboxyethyl)phosphine hydrochloride) should break

the disulfide bridge between crosslinker and Gonc peptide. The remaining part of the crosslinker, a phenylnitrene, is about 308 Da in size (Figure 7.3) and should be easily detected in a mass spectroscopic analysis. In analogy to a more famous radioactive technique the process could be termed "*label-transfer without a label*".

Figure 5.19 shows a Coomassie stained 8 % SDS-PAG. It can be seen that the irradiated and DTT treated samples (P_1 and P_2) run at slighly higher apparent molecular weigth than the untreated eEF1A (lane C). All three bands were excised, Trypsin digested and analyzed by mass spectroscopy by the Targeted Proteomics Group of MSKCCs Molecular Biology Program.

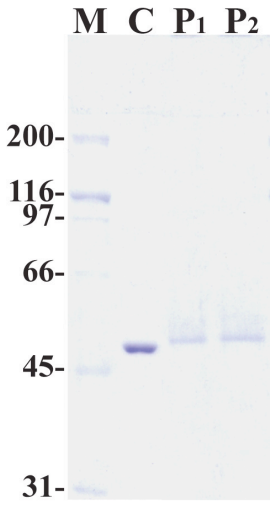

Figure 5.19 Sample preparation for mass spectroscopy.
This is a scan of a Coomassie stained 8 % SDS-PAG. M is the molecular weight marker, molecular masses in kDa are indicated on the left, C represents the lane with 2.7 µg purified and untreated eEF1A as control, the lanes with the two probes are designated P_1 and P_2 and contain 1.5 and 2.0 µg eEF1A respectively. The Gonc peptide has an apparent molecular weight of 3 kDa and ran off the gel. Probes were treated as outlined in this section and described in more detail in 7.2.9.

Unfortunately, the mass spectroscopic data did not provide the sought after sequence information. The data show that the major signals in all samples, control C and probes P_1 and P_2, map to the same region in the studied protein eEF1A. There are some unique peptide masses found in the crosslinked protein digest. However, when the crosslinking adduct (~308 Da for the arylnitrene) is substracted from these unique peptide masses, there is no sequence in the predicted peptides matching with the new mass (personal communication with Dr. Hediye Erdjument-Bromage).

As stated in 7.2.9, similar experiments were performed with the chemical crosslinkers EDC and SAND, but they were even less successful in that they did not show any effect on the migration of eEF1A and the peptide on SDS-PAGs.

5.5 The GTPase activity of the eukaryotic translation elongation factor 1A

Heterotrimeric G proteins (e.g. $G_i\alpha 1$) exhibit intrinsic GTP hydrolysis rates that are higher than those of members of the small GTPases (e.g. Ras p21) and much higher than those of translation elongation factors that are G proteins (52,79-81). As mentioned elsewhere (3.3.1) the very low intrinsic GTPase activity of eEF1A is an essential requirement in translation elongation because the establishment of the cognate codon anticodon interaction between aa-tRNA^{aa} and mRNA needs time. It is only under the biological relevant condition of correct decoding that the ribosome can induce a high rate of GTP hydrolysis in translation elongation factors.

5.5.1 Influence of charged and uncharged tRNA^{aa} on the GTPase activity of the eukaryotic translation elongation factor 1A

It was previously shown (section 5.3.7) that charged aa-tRNA^{aa} and uncharged tRNA^{aa} exhibited an influence on the ability of eEF1A to crosslink to a nascent polypeptide chains. It is obvious to ask whether or not charged aa-tRNA^{aa} and uncharged tRNA^{aa} initiate a change in the low intrinsic GTPase activity of eEF1A as well. In order to investigate the influence of both species of tRNA on the GTPase activity of eEF1A, GTPase assays were performed as outlined in detail in section 7.2.10.

One sample (Figure 5.20 "Buffer") contained only adjusting and incubation buffer in order to detect auto-hydrolysis of GTP and verify the quality of the purchased γ-^{32}P-GTP. The intrinsic GTPase activity of eEF1A was determined by a sample (Figure 5.20 "eEF1A") containing only eEF1A in adjusting and incubation buffer. Uncharged tRNA^{aa} was titrated from an equimolar ratio with respect to eEF1A up to a 200 fold excess as indicated. After 3 min pre-incubation to allow for complex formation the GTPase reaction was started by adding Mg^{2+} to a final concentration of 12.5 mM. Samples were taken at various time points. It has to be mentioned that each assay contained 100 µM unlabeled GTP, which equals cellular levels, but only 3.3 nM γ-^{32}P-GTP.

The developed chromatogram was exposed to a sensitive film. The nucleotide spots were easily detected with the help of a mobile UV light source, marked, cut out, and measured in a scintillation counter. From the acquired cpm values the percentage of produced GDP was calculated based on three assumptions: (i) eEF1A does not discriminate between labeled and unlabeled GTP, (ii) the distribution of labeled and unlabeled GTP is even and (iii) the sum of the measured cpm values from the spots for GTP and GDP accounts for 100 % of the radioactivity.

Figure 5.20 A illustrates a typical chromatogram after exposure to a sensitive film, whereas Figure 5.20 B represents the relative amounts of produced GTP as calculated from scintillation data.

No increasing auto-hydrolysis was detected over the time course in the "Buffer" sample, but a stable background of about 3 % of produced GDP was maintained.

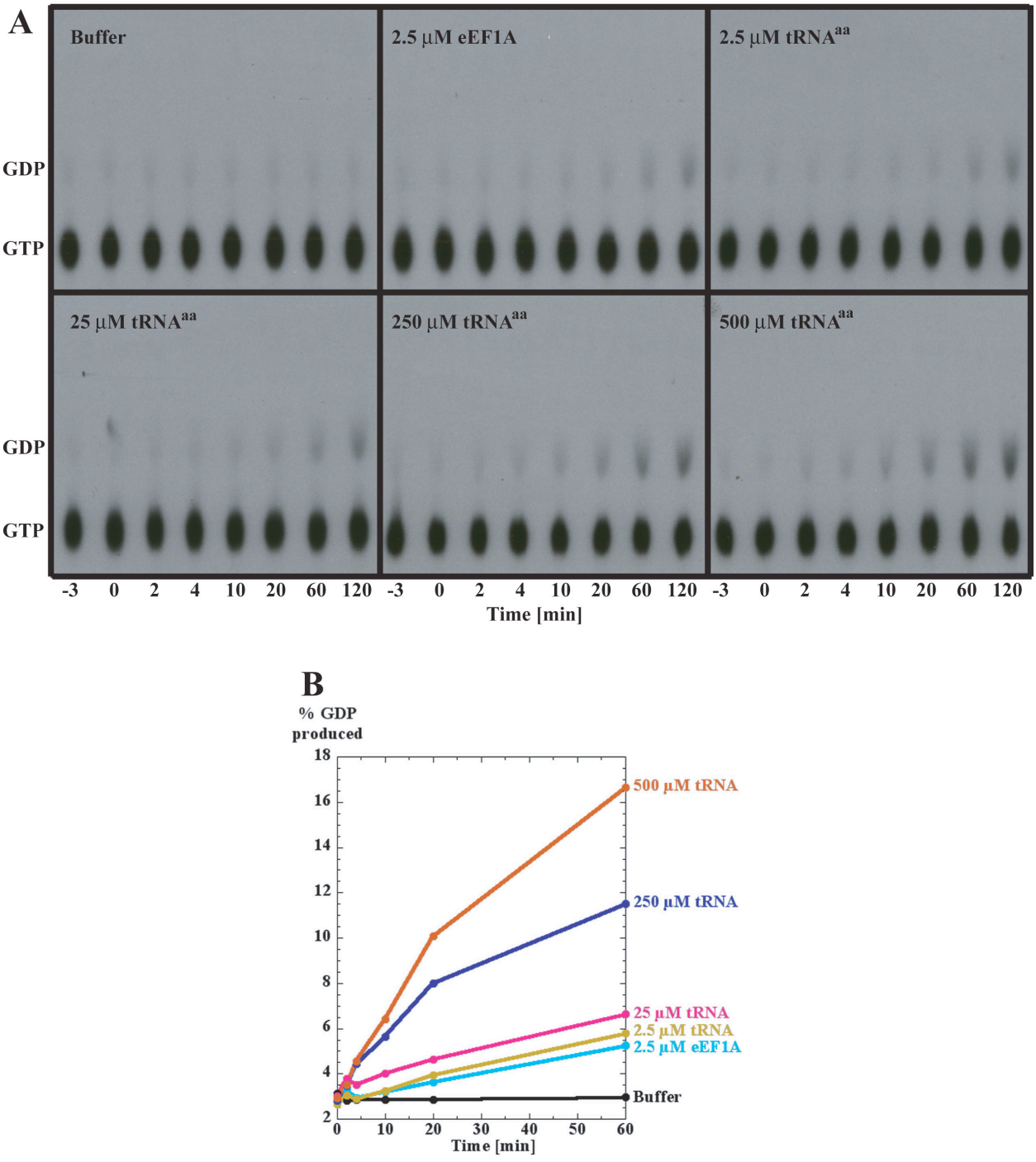

Figure 5.20: Titration of uncharged tRNA^{aa} in GTPase assays.
The assays for the different amounts of tRNA^{aa} contained 2.5 µM eEF1A. The experiment was performed as described in detail in 7.2.10. **A:** Scan of a chromatogram-exposed film. **B:** Amount of generated GDP calculated from data acquired by scintillation counting. See main text for details.

The asssay accounting for the intrinsic GTPase activity of eEF1A (Figure 5.20 A, B "eEF1A") indicates that eEF1A itself has a very low turnover rate (see also section 3.3.1).

The developed chromatogram shows clearly the increased production of GDP over time for the different concentrations of tRNA^{aa}. Typical dose-dependent curves were obtained from the scintillation data.

There seems to be a linear range for the turnover during the first 20 min, although this can be seen clearly only for the two highest concentrations. Another feature exhibited by this kind of experiments is the non-linear correlation between increase of tRNA^{aa} amount and increase of generated GDP: increasing the concentration of tRNA^{aa} tenfold does not increase the amount of produced GDP tenfold.

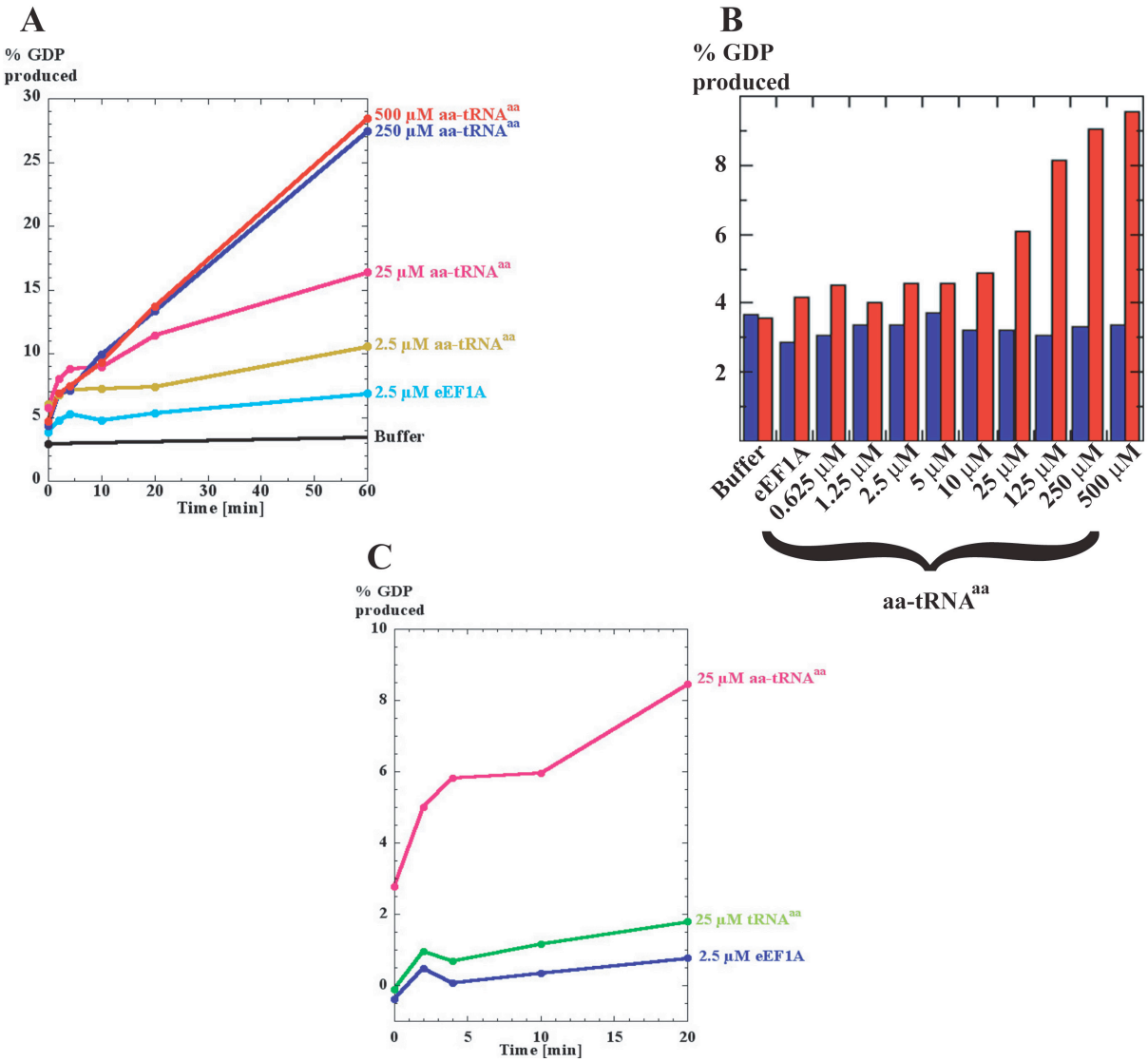

Figure 5.21: Titration of charged aa-tRNA^{aa} in GTPase assays.
The experiment was performed as described in detail in 7.2.10, see also Figure 5.20. The assays for the different amounts of aa-tRNA^{aa} contained 2.5 µM eEF1A. **A:** Amount of generated GDP calculated from data acquired by scintillation counting. **B:** Measurement at two time points in the linear range to gain a finer resolution with respect to the amount of aa-tRNA^{aa}. Blue bars 0 min, red bars after 15 min incubation. **C:** Direct comparison of the effect of background corrected 25 µM tRNA^{aa} (from Figure 5.20 B) and 25 µM aa-tRNA^{aa} (from Figure 5.21 A). See main text for details.

The experiments performed to obtain the graphs in Figure 5.21 A were essentially the same as described for Figure 5.20, only charged aa-tRNA^{aa} was used. For Figure 5.21 B a greater variety of concentrations of aa-tRNA^{aa} was employed in order to gain a finer resolution; samples were taken at 0 min and 15 min only. Figure 5.21 C compares directly the values from Figure 5.20 B and 5.21 A for one concentration of tRNA^{aa} and aa-tRNA^{aa} at early time points; 25 µM was chosen because it is tenfold higher than the 2.5 µM for eEF1A and this represents cellular levels.

The samples "Buffer" and "eEF1A" in Figure 5.21 A present principally the same result a in Figure 5.20 B. The graphs show clearly the increased production of GDP over time for the different concentrations of aa-tRNA^{aa}, and typical dose-dependent curves were obtained from the scintillation data. The difference to the data presented in Figure 5.20 B is evident: charged aa-tRNA^{aa} stimulates the GTPase activity of eEF1A much stronger than uncharged tRNA^{aa} does. About twice as much GDP is produced in presence of aa-tRNA^{aa} during the same time than in the presence of tRNA^{aa}.

Measuring the generated amount of GDP in the linear range (Figure 5.21 B) demonstrated clearly the dependency of the increased GTPase activity from the applied dose of aa-tRNA^{aa}.

The data in the linear range (Figures 5.20 B and 5.21 A) provided a way to calculate the rate of turnover. For example, in presence of 250 µM tRNA^{aa} 100 nM GTP was converted into GDP per min and per µM eEF1A, whereas in presence of 250 µM aa-tRNA^{aa} 150 nM GTP was converted into GDP per min and per µM eEF1A. Whereas doubling the amount of aa-tRNA^{aa} did not increase the rate significantly, doubling the amount of tRNA^{aa} increased the rate to about 140 nM GDP produced per min and per µM eEF1A. The overall conclusion of the titration experiments is that charged aa-tRNA^{aa} stimulates the GTPase activity of eEF1A to a greater extend than uncharged tRNA^{aa}.

Figure 5.21 C shows a close up of the first 20 min of the assays with the background, as defined by the buffer, subtracted. The chosen concentrations for eEF1A, tRNA^{aa} and aa-tRNA^{aa} correspond to cellular levels. It can clearly be seen that eEF1A shows little intrinsic activity, which is not much enhanced if tRNA^{aa} is present. However, the presence of charged aa-tRNA^{aa} changes the picture drastically, and a biphasic shape for the obtained curve becomes evident. There is a fast reaction within the first four minutes which slows into a more linear reaction over time (see Figure 5.21 A for later time points).

5.5.2 Influence of Gonc peptides on the GTPase activity of the eukaryotic translation elongation factor 1A

It was shown in section 5.3.5 that the 31mer of Gonc reduces the ability of eEF1A to crosslink to nascent polypeptide chains. In contrast, all other derivatives of the Gonc peptide from the 13mer to the

29mer were not able to reduce the crosslinking capacity, but rather enhanced it. Naturally, the question arose whether or not the Gonc peptides manifest any effect on the GTPase activity of eEF1A.

The GTPase assays were performed as described (see 5.5.1 and 7.2.10), with the slight modification that the incubation time at 37 ˚C was reduced to 20 min, and aa-tRNA^{aa} was present at 10 µM. One Gonc derivative (13mer to 31mer) was added at a concentration of 2.5 mM per assay.

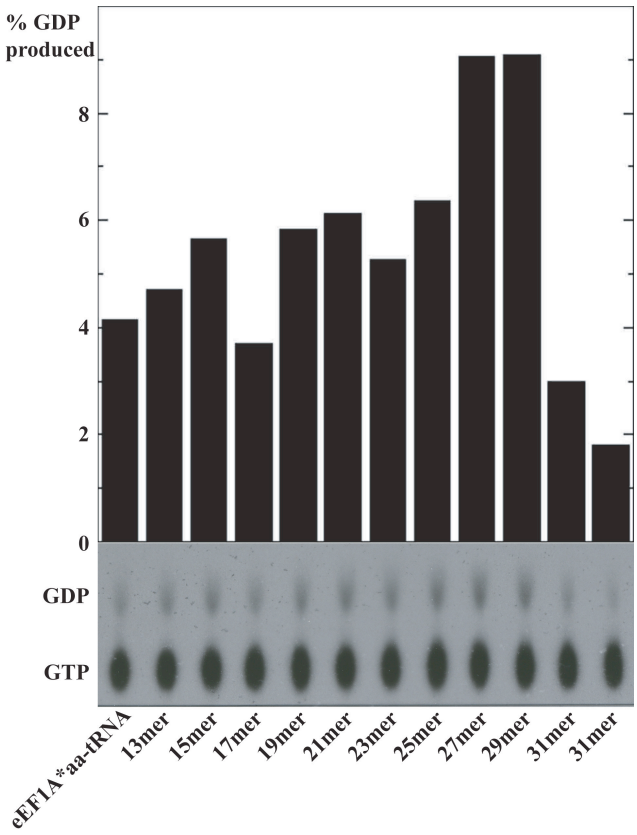

Figure 5.22 Influence of Gonc peptides on the GTPase activity of eEF1A.
The experiment followed the procedure described elsewhere (5.5.1 and 7.2.10) and contained 2.5 µM eEF1A, 10 µM aa-tRNA^{aa}, 2.5 mM of the indicated Gonc peptide, 100 µM unlabeled GTP, and 3.3 nM □-^{32}P-GTP. After 3 min preincubation on ice, the reaction was started by adding Mg^{2+} to a final concentration of 12.5 mM and incubation for 20 min at 37 ˚C. The histogram was derived from measuring the cpm of the separated spots in a scintillation counter. The shown data are buffer corrected. The two 31mer were from two different suppliers.

The buffer gave a background of about 4 % of the produced GDP, which is normal. The assay containing only eEF1A and aa-tRNA^{aa} turned over about 4 % of the radiolabeled GTP into GDP. The Gonc peptides from the 13mer to the 25mer increased the GTPase activity of eEF1A slightly. The 27mer and the 29mer stimulated the GTPase activity of eEF1A to more than twice the level of the ternary complex alone.

Surprisingly, the 31mer Gonc peptide effectively inhibited the GTPase activity of eEF1A by about 50 % compared to the ternary complex.

Appendix

5.6 Identification of γ-secretase as an example of site-specific protein-protein interaction

My first project in the laboratory of Dr. M. Wiedmann was to approach the identification of the components of the –at the time– still elusive γ-secretase activity. Partial characterization of presenilin, one of four components of the γ-secretase complex, was achieved.

5.6.1 Introduction

Alzheimer Disease is the most common neurodegenerative disease in humans. Diagnostic hallmarks of Alzheimer Disease are speech impediments and loss of both memory and learned skills. Pathologic hallmarks visible in brain sections include atrophic tissue in the cerebral cortex, extracellular plaques as well as intraneural depositions of fibrillar amyloid protein(s) (82,83).

The main component of the extracellular plaques is a short peptide termed Aβ. This peptide has an apparent molecular weight of about 4.5 kDa and is a cleavage product from the amyloid precursor protein (APP), a ~90 kDa transmembrane protein. APP is found in various tissues and exists in at least ten alternative splicing products (ExPASy database, Swiss-Prot accession number P05067 at *http://us.expasy.org/cgi-bin/niceprot.pl?P05067*). APP is processed by several different proteases originally termed as α-, β- and γ-secretases. Cleavage by either α- or β-secretase generates a large soluble extracellular peptide. The subsequent cleavage by γ-secretase occurs within the transmembrane domain of APP. The combined activities of β- and γ-secretases generate the insoluble Aβ peptide which is the dominant peptide found in the extracellular plaques in brains of Alzheimer patients.

The metalloproteases TACE and ADAM10 were discussed as potential candidates for the α-secretase (84,85). β-secretase was identified by at least five groups and is known as BACE, Asp2 or Memapsin 2 (86-90). The γ-secretase remained elusive at that time, although the presenilins (PS1 and PS2) were discussed as potentially being γ-secretase(s) or part of a larger γ-secretase complex (91).

The principal interest to investigate the particular intriguing nature of γ-secretase was its ability to cleave APP in its transmembrane domain, i.e. within the lipid bilayer (92,93). The unusual regulated intramembrane proteolysis is only known from four proteins: Notch, Ire1, ATF6 and SREBP (sterol regulatory element-binding protein). And only one protease, the Site-2 protease S2P, had been identified at that time to cleave SREBP (94).

The importance to elucidate the nature of γ-secretase is revealed by the fact that the cleavage is necessary to generate the pathogenic plaque forming Aβ peptide in combination with the β-secretase. Furthermore, the gene encoding for APP is expressed in various tissues and APP-cleavage by α- and γ-

secretase seems to be a normal event in the cellular context. In order to prevent "mis-cleavage" the process of cleaving APP has to be tightly regulated either by cofactors or by conformational mechanisms.

5.6.2 Strategy

In order to investigate the environment of the β-secretase cleavage site, a construct (Figure 5.23) coding for C-99 was used in combination with a crosslinking approach with a suppresor tRNA method. The construct contains the signal sequence of preprolactin. The cleavage of the signal sequence mimics the cleavage of APP by β-secretase – the first step to generate C-99. Also, the signal sequence ensures that the construct is inserted into the membrane of the ER. The construct also contains a His_6 tag that allows for a purification over Ni-NTA-Agarose (Qiagen, Valencia CA) beads or Co-Talon-Sepharose (Clontech, Palo Alto CA) beads. A c-myc tag for identification purposes was also attached.

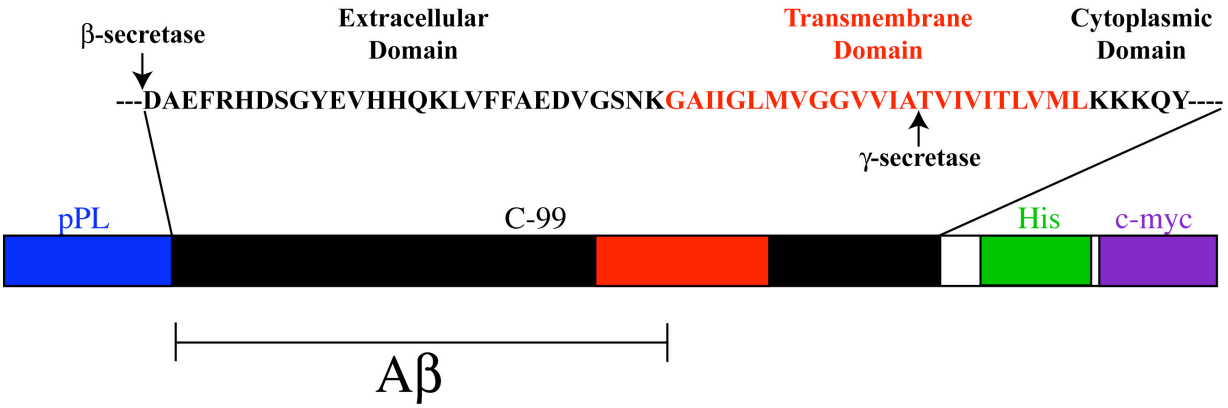

Figure 5.23: Features of APP sequence and C-99 construct.
Top: The partial sequence of APP is shown from Asp^{672} (β-secreatese cleaves N-terminal) until Tyr^{728}. The transmembrane domain is highlighted in red. The cleavage site of β-secretase is between Ala^{713} and Thr^{714}. **Bottom:** The signal sequence of preprolaction (pPL, amino acids 1-30) was placed N-terminal to C-99. Position 31-129 is occupied by C-99 which stretches from Asp^{672} to Asn^{770} of APP. The transmembrane domain ranges from amino acid 59-81 of the modified C-99. A His_6 tag was added and occupies amino acids 135-140. At the C-terminal end a c-myc tag stretches from amino acids 144-155. The complete sequence in the same color code as above and with the crosslinker indicated as **F*** is thus:
MDSKGSSQKGSRLLLLLVVSNLLLCQGVVSDAEFRHDSGYEVHHQKLVFFAEDVGSNKGAIIGLMVGGVVIA**F***VIVI
TLVMLKKKQYTSIHHGVVEVDAAVTPEERHLSKMQQNGYENPTYKFFEQMQNSMGASHHHHHHMRSEQKLISEEDLLQ

The original sequence was mutated from a threonine codon to the amber stop codon TAG (Figure 5.23, Thr^{714} of APP, which is Thr^{73} of C-99 or F* in the modified C-99). This amber stop codon is C-terminal to the peptide bond that is cleaved by β-secretase. The photoactivatable diazirino crosslinker Tmd-Phe*, or L-4'-[3-(Trifluoromethyl)-3H-diazirin-3-yl]phenylalanine, will be introduced during *in vitro* translation at this position via the modified Tmd-Phe-$tRNA^{Phe*}$. In order to recognize the amber stop codon as a phenylalanine codon, the anticodon UUU of the $tRNA^{Phe}$ was mutated to CUA to match the amber stop codon. Published procedures to generate the needed material were followed (95,96).

The major advantages of the suppressor tRNA method are its particular specificities. (i) crosslinks are **only** possible, if the modified Tmd-Phe-tRNA^{Phe*} suppresses the amber stop codon and incorporates the crosslinker Tmd-Phe during *in vitro* translation, (ii) there is only **one** location possible for the incorporation of the crosslinker, (iii) phenylalanine has an intrinsic bias towards a hydrophobic environment like the transmembrane domain, and (iv) it is not necessary to modify the remaining sequence – in contrast to many approaches using lysines as potential sites to introduce a crosslinker.

5.6.3 Results establishing the model system

It was first demonstrated that the material generated for the Tmd-Phe-tRNA^{Phe*} suppressor system functioned properly. This included sequencing the plasmid DNA of the construct and the plasmid encoding the modified tRNA^{Phe}, *in vitro* transcription of the construct, optimizing *in vitro* translation conditions in commercial and self-made rabbit reticulocyte lysate (97) and comparison to self-made wheat germ extract (98), *in vitro* translation of the corresponding mRNA in presence/absence of Tmd-Phe-tRNA^{Phe*} to verify the functionality of the system (full length construct of 17.2 kDa was achieved only in presence of Tmd-Phe-tRNA^{Phe*}, in absence a truncated form was generated), *in vitro* translation of the mRNA in presence/absence of ER membranes to verify proper localization (microsomal membranes were centrifuged through a physiological salt sucrose cushion) and processing of the construct (microsomal membranes provide the signal peptidase complex and C-99 showed an apparent molecular weight of 14.2 kDa after cleavage of the pPL signal sequence).

Furthermore, a buffer system was developed that ensured the solubilization of the ER membranes during purification of the crosslinked product and maintained the integrity of properties of the immobilized metal affinity chromatography (Ni-NTA-Agarose or Co-Talon-Sepharose). A suitable system is 50 mM Hepes/KOH pH 7.5, 400 mM KAc, 5 mM MgAc, 0.5 % (v/v) Triton X100, 0.1 % (v/v) Imidazole. Elution of the crosslinked product from the immobilized metal matrix was possible with 150 mM EDTA/100 mM Imidazole.

Besides the commercial antibodies 6E10 (anti-Aβ) and 9E10 (anti-c-myc) several antibodies against presenilin1 were created and all were tested in Western blottings and immunoprecipitation experiments.

5.6.4 Approaches towards the identification and characterization of the crosslinked product

In order to identify the components of the crosslink an immunoprecipitation was performed using the anti-Aβ antibody 6E10 and a selfmade anti-presenilin1 antibody. As shown in lane 2 and 3 of Figure 5.24, the crosslink was immunoprecipitated with the anti-C-99 antibody but not with the anti-presenilin1 antibody. However, the anti-presenilin1 antibody was able to pull down presenilin1. Using the relative

mobility of known molecular weight markers (lane 1), the crosslink recognized by anti-Aβ antibody 6E10 (lane 2), and a positive control for presenilin from a different membrane preparation (not shown), the visually determined molecular weight of the crosslink is ~70 kDa and the calculated one is 68.8 kDa. If the crosslink has an apparent molecular weight of ~70 kDa and the C-99 has one of ~14 kDa, the crosslinked protein can be expected to have an apparent molecular weight of ~56 kDa, which is roughly the size of presenilin1.

Unfortunately, the 50-60 kDa range also accounts for a vast amount of membrane proteins. Since C-99 has to be inserted into a membrane it has to be excluded that the band results from a crosslink to components of the translocation machinery. The preeminent suspect for this case would be Sec 61, with an apparent molecular weight of ~50 kDa the largest protein of the translocon. Other proteins are unlikely, because they are too small (e. g. TRAM, signal peptidase subunits, β-TRAP) or are excluded by the physiological salt sucrose cushion centrifugation.

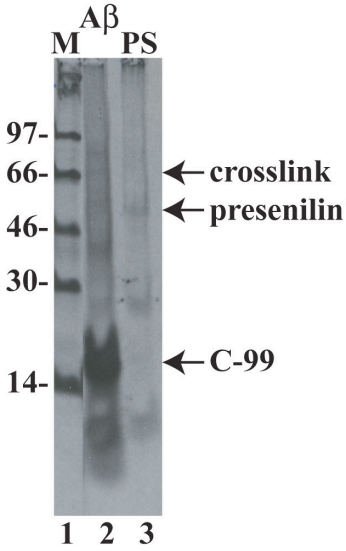

Figure 5.24: Attempted immunoprecipitation of a C-99 crosslink with anti-Aβ or anti-presenilin.
C-99 was translated *in vitro* for 30 min at 30 ˚C using a standard procedure essentially described in 7.2.1. Each assay contained 26 µl translation mix, 4.8 µl mRNA, 4.2 µl rough ER membranes (RM32) and 4 µl Tmd-Phe-tRNA^{Phe*}. After centrifugation through a physiological salt sucrose cushion (7.2.2 and 7.2.3) the pellets were resuspended in TBB and the majority was irradiated for 10 min at 365 nm. Immunoprecipitation followed as described (7.2.6). Antibodies used for immunoprecipitation are given on top, M is the molecular weight marker and molecular masses in kDa are indicated on the left.

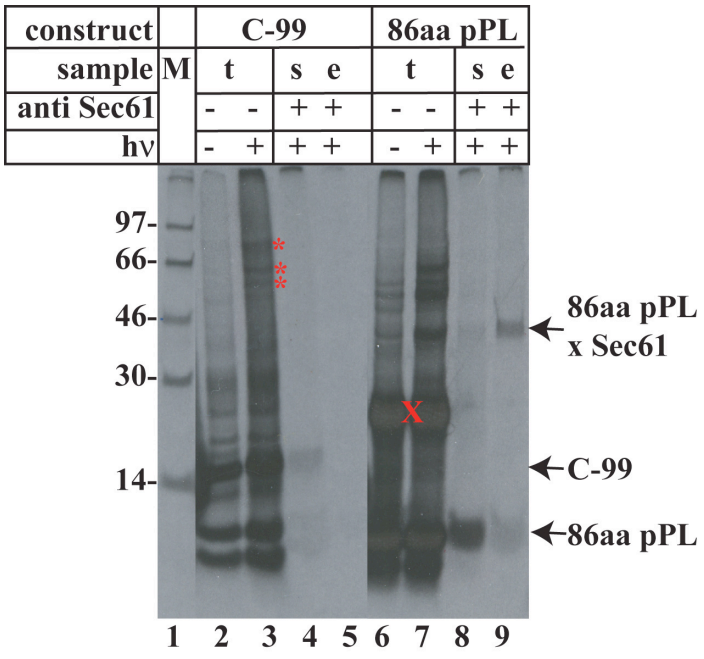

Figure 5.25: Immunoprecipitation of C-99 and 86aa pPL with anti-Sec61 antibody.
The procedure was as described in Figure 5.24 and references therein, except that 86aa pPL was translated for 15 min instead of 30 min and rough ER membranes were RM9. Lane 1 shows the molecular weight markers "M", lane 2 and 6 the non-irradiated samples after physiological salt sucrose centrifugation, lane 3 and 7 the irradiated samples after physiological salt sucrose centrifugation, lane 4 and 8 the supernatant "s" of the Protein A agarose beads and lane 5 and 9 the eluate "e" from those beads. Asterisks indicate crosslinks of C-99. The "X" refers to the radioactive Met-tRNA^{Met} (sample was not treated with RNaseA and EDTA). Molecular masses in kDa are indicated on the left.

Lane three of Figure 5.25 shows the crosslinked C-99 (asterisks) and lane four and five supernatant and eluate for the Protein A agarose beads. No immunoprecipitate was recovered with anti-Sec 61.

Lane seven shows the crosslinks of the 86mer of preprolactin (86aa pPL) to different proteins: since the 86mer derives from a truncated mRNA, it is stalled on the ribosome and should have the N-terminus within the translocon. The 86aa pPL contains also several modified lysine residues as the source of photoactivatable crosslinker, hence the higher amount and intensity of crosslinked bands. Lane nine shows the immunoprecipitated and eluted 86aa pPL x Sec 61 crosslink. As can be seen in lane eight, binding to the Protein A agaorose beads was not quantitatively.

A calibration of the gel using the relative mobility of known marker proteins reveals that the crosslink has an apparent molecular weight of ~46 kDa. Thus, C-99 is not crosslinked to Sec 61 because C-99 and the 86aa pPL have roughly the same size (14 kDa vs. 9 kDa respectively), but the apparent molecular weights of their respective crosslinks differ by more than 20 kDa and only 86aa pPL can be immunoprecipitated with anti-Sec 61.

5.6.5 Concluding remarks

Another complex of questions with regard to the activity of the γ-secretase arises from the controversial interpretations in studies on the presenilins, especially presenilin1 (PS1). At that time it seemed to be clear that presenilin1 is involved in the process of the cleavage of APP, but it was still under discussion whether it is a cofactor necessary for the cleavage, a regulatory element or the protease itself. It was the main suspect for being "the" γ-secretase and a crosslinked product with an apparent molecular weight corresponding to that of presenilin was found in this study.

Now it has been shown by reconstitution (99,100) that γ-secretase is indeed a heterotetrameric complex consisting of presenilin (~50 kDa), nicastrin (~75 kDa, although this does not take into account the heavy glycosylation), PEN-2 (~12 kDa), and APH-1 (~30 kDa).

The project was abandonmed when first reports suggested presenilin to be the protease in a larger γ-secretase complex (101,102).

6 Discussion

6.1 Interaction of the eukaryotic translation elongation factor 1A with nascent polypeptide chains

Macromolecular crowding in the cytosolic environment necessitates protection of the growing nascent chain as it is translated on the ribosome (103,104). In addition, some nascent chains require specific covalent modifications and/or targeting to an organelle such as endoplasmic reticulum, mitochondria, chloroplast, peroxisomes or the nucleus (105). Finally, although translation is remarkably error-free with one mistake in 10000 aa (106), rigorous quality control at the co- and post-translational stages is essential to remove protein that, for whatever reason, cannot attain its functional state. In fact, it has recently been found that in eukaryotic cells up to 50 % of newly translated proteins are immediately degraded (107,108). Many of the above functions are implemented by ribosome associated factors or RAFs. A physical association of nascent chains with several RAFs, including SRP, NAC and Ssb, was initially demonstrated by using in vitro transcription/translation systems in combination with a site-specific photo-crosslinking approach (for example see references (15,109,110)).

In this work a 50 kDa protein that crosslinked to a wide variety of nascent chains was identified and characterized as the eukaryotic translation elongation factor 1A or eEF1A, an elongation factor with a well-known function in translation, i.e. delivering aa-tRNA^{aa} to the A site at the ribosome. This work is the first to demonstrate that eEF1A binds to nascent chains and, in addition, to certain subset of released polypeptides. The latter point was demonstrated by direct physical association via crosslinking. Although eEF1A was found to bind to a variety of different nascent chains (Figure 5.5), its binding to released proteins was more selective. As assayed by crosslinking, eEF1A binds to pPL-M (Figure 5.7 B), a protein that cannot fold correctly under the conditions of the *in vitro* translation system, but not to ffLuc (Figure 5.7 A), a peroxisomal protein that does fold correctly. However, eEF1A is in contact with ffLuc nascent chains (Figure 5.5). It can be inferred from eEF1A stimulation of ffLuc refolding (see Figure 6 in reference (111)) that it also binds to unfolded ffLuc. In addition, a truncated form of β-actin released from the ribosome with puromycin, crosslinks to eEF1A (Figure 5.6). Taken together, this data suggests that eEF1A binds primarily to unfolded or not completely folded proteins.

A released polypeptide has previously (112) been observed to crosslink to a 50 kDa protein but the identity of the protein was not determined. In this study crosslinking experiments were performed using yeast prepro-α factor translated in a rabbit reticulocyte lysate supplemented with yeast microsomes. Prepro-α factor probably does not fold efficiently in the cytosol as it is translocated into microsomes post-

translationally. If the crosslinked 50 kDa protein in their experiments is indeed eEF1A then their result is an independent confirmation of this proposal that eEF1A binds to unfolded proteins.

It is worth noting that binding of eEF1A to nascent chains is clearly at a site distal from the peptidyl transferase center, where eEF1A is known to deliver charged aa-tRNA^{aa} necessary for elongation of the nascent chains. The experimental basis for this is as follows: (i) eEF1A crosslinks to both 86aa and 169aa pPL-MN which have lysines for crosslinking only at positions 4 and 9, over 76 aa and 159 aa away from the peptidyl transferase center (Table 7.1 and Figure 5.5 B), (ii) eEF1A crosslinks more efficiently to longer than shorter nascent chains (Figure 5.5) and (iii) full-length pPL-M, naturally released from the ribosome but unable to fold properly in an cytosol-like environment, also crosslinks to eEF1A (Figure 5.7 B). These results point to a novel function for eEF1A distinct from delivery of aa-tRNA^{aa}.

It has been shown before that EF1A, the bacterial homolog of eEF1A, has chaperone-like activity (113,114). We demonstrated that eEF1A also has chaperone-like activity and that half maximal refolding of denatured ffLuc occurs at a molar ratio of ca. 1:2 of substrate to eEF1A (see Figure 6 B in reference (111)). This compares well with ratios of 1:1 to 1:10 found for rhodanese to EF-Tu or citrate synthase to EF-Tu, respectively. In contrast Hsp 70 acts at a ratio of 1:50 (115).

Both, eEF1A and EF1A bind GTP, which must be hydrolyzed in order for bound aa-tRNA^{aa} to be released at the ribosome. Exchange of the bound GDP for a new molecule of GTP requires an accessory protein, eEF1Bα for the eukaryotic system and EF1B for prokaryotes. Our studies of eEF1A mediated refolding could not detect either a requirement for or inhibition by nucleotides, nucleotide analogs, or apyrase treatment. The findings on this for EF1A assisted refolding, however, are controversial. Caldas et al. (113) reported that the GDP bound form of EF1A is active in catalyzing refolding of citrate synthase and the GTP bound form inactive, although it is not clear from their data whether refolding requires GTP hydrolysis. In contrast, Kudlicki et al. (114) found increased refolding of rhodanese in the presence of GTP and inhibition by GDP or a non-hydrolyzable GTP analog. They further showed that EF1A assisted refolding is greatly stimulated by EF1B in the presence of GTP, to a maximum of 90 % of native activity. It is possible that in our experiments GTP and GDP had no effect on ffLuc refolding because all of the eEF1A used was already bound to nucleotide and our apyrase treatment was incomplete. It would then be necessary to supplement the reaction with eEF1Bα to fully resolve this question. However, we think it is not very likely that chaperone activity is a major function of either EF1A in bacteria or of eEF1A in eukaryotes. This is underlined for eEF1A by our finding that it stimulates a maximum refolding of ffLuc of ca. 30 % compared with 60 % obtained with rabbit reticulocyte lysate (see Figure 6 C in reference (111)). In agreement with this, studies by Frydman et al. (116), demonstrated that the majority of chaperone activity in reticulocyte lysate was due to Hsp 70. In the context of the present study, the

significance of eEF1A assisted refolding of a denatured protein is its demonstration that eEF1A binds to unfolded protein.

6.2 Competition of peptides with nascent polypeptide chains for binding to the eukaryotic translation elongation factor 1A

The initial experiments described in chapter 5 were all performed with rabbit reticulocyte lysate or factors isolated from it. However, purifying large quantities of e. g. eEF1A from this source is both, uneconomic and unreasonable, especially if better systems are available. An economic and time-saving way is the culture of the yeast *Saccharomyces cerevisiae*, sometime referred to as a "lower" eukaryote due to its cellular simplicity. Deploying *Saccharomyces cerevisiae* comes with two advantages: (i) it is a genetically easy to manipulate system, which could be used in further studies and (ii) the published crystal structure of eEF1A in complex with the catalytic moiety of eEF1Bα is known (53,54). The intellectual value of this model is its function as a potential guide in understanding results gained in biochemical *in vitro* experiments. However, a serious obstacle to this approach is the well known fact of probable incompatibilities between biological active entities from distant phylogenetic taxa. For example, ribosomes display kingdom-dependent accessebility for translation factors (117-119). Only when ribosomal proteins L10•L7/L12 and L11 of *E. coli* ribosomes were replaced by their counterparts P0•P1/P2 and RL12 from *Rattus norvegicus* the generated hybrid ribosomes were able to utilize the elongationfactors eEF1A and eEF2 from *Sus scrofa* in poly(U)-programmed translation (120). At the same time hybrid ribosomes lost the ability to utilize EF1A and EF2 from *E. coli*.

In analogy to this scenario, it cannot be assumed *bona fide* that eEF1A from a "lower" eukaryote will engage properly with e. g. ribosomes from a "higher" eukaryote. Despite a sequence identity of 81 % (34) between eEF1A from *Oryctolagus cuniculus* and *Saccharomyces cerevisiae*, two sequence patterns of the yeast eEF1A make it standing apart from all other mammalian eEF1As: it is missing the unique glycerylphosphorylethanolamine and it exhibits a different methylation pattern of its lysines (34).

In order to take advantage of the published structure of eEF1A•eEF1Bα, it was decisive to demonstrate the exchangeability of the eEF1A from *Saccharomyces cerevisiae* with the corresponding one from *Oryctolagus cuniculus*. The very same interaction of ribosomes isolated from rabbit reticulocyte lysate with eEF1A from *Oryctolagus cuniculus* and *Saccharomyces cerevisiae* (see 5.3.2 and 5.3.3) proved indeed that the elongation factors are functionally substitutive in the given experimental settings. It was, however, not investigated whether the two elongation factors are also functionally substitutive in the canonical translation events, because the interactions of eEF1A with nascent chains or released/unfolded proteins must clearly happen at places other than the ribosomal A site.

The initial set of peptides tested as described in section 5.3.2 and 5.3.3 contained the 36mer Sec 22 Cccp (z = +2, pI = 9.31) and the 29mer Gol (z = +1, pI = 8.29). This selection is not representative with respect to the chain length, charge, and isoelectric point. To secure a more unbiased view on the interaction of peptides with eEF1A, in a first assessment 30 previously synthesized peptides (Table 5.3) were chosen at random for use in competition assays. This set was to provide diversity with respect to amino acid composition (random peptides), chain length (from 8mer to 39mer), charge (from –6 to +7), and the isoelectric point (from 3.90 to 12.32). From this variety of peptides a surprising pattern emerged: apparently neither the overall charge nor the isoelectric point manifested a predominant feature for a peptides ability to compete with nascent chains for eEF1A. The C-terminal part of the coiled coil region of Gos 1 (pI = 12.32) competed as well as the 31mer Gonc (pI = 3.90) or peptides within this range. Mtj 1 (z = +7) is as efficiently as Rim (z = –6) in competition as are many peptides within this range. A view on Table 7.4, which provides additional information about the characteristics of the initial set of peptides as well as information about 34 more peptides used subsequently in this study, reveals that no sequence pattern can be inferred for the ability or inability of a peptide to compete with nascent chains for eEF1A.

The only conclusion to be drawn from these experiments is that there seems to exist a requirement for a certain minimum length of peptides in order to be able to compete. However, molecular chaperones have peptide binding sites which typically accommodate for up to seven to nine amino acids (78), similar to MHC molecules. The only exception is Hsp 47, which binds to peptides of about 30 aa, but this molecular chaperone binds specifically to procollagen and collagen during collagen biosynthesis (121,122). It was therefore unexpected to find a minimum length for peptides of 20-30 aa in competition experiments. The variety in the ability to compete for peptides longer than 20 but shorter than 30 aa is interpreted as a contribution of minor interactions in cases of interaction. It can be assumed that the peptide binding site on eEF1A is structurally different than the peptide binding site of a molecular chaperone which is usually a hydrophobic pocket.

Even though a total of 64 random peptides were tested in order to eliminate a potential sequence bias, this does not prove that there is no actual sequence bias by the peptides deployed. A more rigorous approach to consider with respect to a potential preference of eEF1A towards a peptide sequence pattern is the application of commercial peptide arrays.

The systematic approach using Gonc derivatives that covered peptide lengths from 13 to 31 amino acids demonstrated that a chain length of 31 amino acids has a dramatic effect on the crosslinking efficiency of nascent chains towards eEF1A. An important question arose as to what the oligomerization state of these peptides are. High speed centrifugation yielded neither visible pellets nor could any material be detected on stained PAGs.

Prelimnary NMR experiments (1D ^{1}H as well as HSQC) of the 29mer and 31mer Gonc suggested that both peptides are at least partially structured. Unfortunately, this does not exclude the possibility of aggregates in the samples, but the lack of pellets after high speed centrifugation speaks against it.

On the other hand, gelfiltration experiments illustrated that the 31mer of Gonc is present in a very large complex (~200-300 kDa), whereas the peptide that does not compete for binding to eEF1A has an apparent size only one-tenth of this complex. Interestingly, addition of eEF1A to the 31mer Gonc peptide changes the oligomerization state drastically and both, eEF1A and 31mer Gonc, co-migrate over a large range. It looks as if eEF1A has the ability to dissolve peptide complexes. It is interesting to note that this interaction does not require GTP and can be carried out at 4 ˚C. However the presence of aa-tRNA^{aa} is essential.

6.3 Competition of charged and uncharged tRNA^{aa} with nascent polypeptide chains for binding to for the eukaryotic translation elongation factor 1A

An interesting open question with respect to interactions of the nascent polypeptide chain to eEF1A is the actual location of the binding site. It is clear from the crystal structure and competition experiments that overlapping binding sites exist on eEF1A, because charged aa-tRNA^{aa} replaces eEF1Bα due to its higher affinity (53-55). As the results in section 5.3.7 clearly point out even small amounts of charged aa-tRNA^{aa} interfere strong with the ability of eEF1A to bind to nascent polypeptide chains. It is noteworthy to mention that the concentration of eEF1A was within the range of published cellular values and the amount of aa-tRNA^{aa} used was ten- and 100-fold higher than eEF1A, whereas in a cellular context the concentration of aa-tRNA^{aa} is about 20-fold higher (39-41). The uncharged tRNA^{aa} exhibited a trend towards the same effect, although less pronounced. This is in agreement with aa-tRNA^{aa} being the prime substrate for eEF1A in its canonical function.

It is reasonable to assume, that nascent polypeptide chains and aa-tRNA^{aa} have –partially– overlapping binding sites on eEF1A, similar as eEF1Bα and aa-tRNA^{aa} have. However, it is also entirely possible that aa-tRNA^{aa} induces upon binding to eEF1A a conformational change in eEF1A which eliminates the accessibility of or destroys the peptide binding site. This view is supported by a study in which eEF1A was found to have no fixed rigid structure in solution. It was speculated that this enables eEF1A to undergo large conformational changes upon interaction with partner molecules (61). In order to understand the underlying interaction(s), it was of great interest to identify the peptide binding site on eEF1A.

6.4 Elucidating the peptide binding site on the eukaryotic translation elongation factor 1A

Given the heterogenity of functions that eEF1A has been shown or suggested to be involved with (for references see section 3.3), it is beyond any reasonable doubt to assume at least one binding site for proteins or peptides. Reports on EF1A (77,113,114), on eEF1A (111) as well as the results presented in this study are indicative of the presence of a specific peptide binding site on these elongation factors.

In order to reveal the peptide binding site(s) on eEF1A it was attempted to attach several heterobifunctional crosslinkers to the well-competing 31mer Gonc peptide. Only one commercial crosslinker yielded a menaingful result. However, quite a few modifications had to be applied to the procedure provided by the manufacturer to be able to crosslink the peptide to eEF1A. The assay was so effective, that eEF1A could be completely crosslinked away. Unfortunately, this did not result in a single band of a higher apparent molecular weight, which could have been analyzed by mass spectroscopy. However, when this was eventually achieved by removing part of the crosslinker through reduction, mass spectroscopy of the trypsin digested sample yielded only inconclusive results. Although several unique masses were identified, non of them could be assigned to preidicted values.

An alternative way to investigate the peptide binding site of eEF1A in the future is by site directed crosslinking via the suppressor Tmd-Phe-tRNA^{Phe*} method (see chapter 5.6 for details). This method will circumvent potential problems rising from genetic approaches. To map the binding site of eEF1A a nascent chain is to be crosslinked to yeast eEF1A, RNCs are isolated and chains are released by RNase A and EDTA treatment. Then, nascent chains can be isolated over metal-affinity columns, if they carry an amino-terminal His-tag. The eluted nascent chains can be analyzed by SDS-PAGE. In a nearby lane, a similar crosslinking reaction that did not include ^{35}S-Met can be loaded. The radioactive part of the PAG can be dried and exposed to a film to determine the position of the crosslinked product. The section of the unlabeled gel can be excised, the protein eluted, digested with trypsin, and analyzed by mass spectroscopy.

6.5 Proposed model

The canonical function of eEF1A in protein biosynthesis is very well established. As diagrammed in Figure 6.2 in a simplistic way by the cycle of black arrows and described in great detail in sections 3.3.1 and 3.3.2, the ternary complex aa-tRNA^{aa}•eEF1A•GTP recruits the charged aa-tRNA^{aa} to the A site of ribosome. After delivery the binary complex of eEF1A•GDP disengages from the ribosome and eEF1A interacts with its guanine nucleotide exchange factor eEF1B in order to replace GDP by GTP. Subsequent interaction of eEF1A•GTP with aminoacyl-tRNA synthetases leads to a take up of another charged aa-tRNA^{aa} for the next delivery.

Based on the results presented in this work, a novel function for eEF1A is proposed, i. e. quality surveillance of nascent polypeptide chains. The proposal is also supportive towards an earlier suggestion (123) that uncharged $tRNA^{aa}$ is channeled back to aminoacyl-tRNA synthetases.

Channeling reactants

The rate of protein biosynthesis in diverse phylogenetic taxa can vary considerably. *E. coli* is reported to synthesize a protein with a speed of ~1000 aa per min (124), whereas *Saccharomyces cerevisiae* exhibits ~400 aa per min (125), and *in vitro* translation in reticulocyte lysate from *Oryctolagus cuniculus* proceeds with ~100 aa per min (126). This has intrinsic consequences with respect to the organizational level of these organisms. As a consequence, *E. coli* translocates secretory proteins mostly post-translational, *Saccharomyces cerevisiae* co- and post-translational and more complex cells of "higher" eukaryotes rely mostly on co-translational translocation.

In order to enable a cell to perform at these high synthesis rates, it is no big surprise that the translation elongation factors 1A (EF1A or eEF1A) in general are abundantly present in these cells. In eukaryotes, eEF1A is the second most abundant protein after actin, constituting with ~2 µM 1-2 % of the total protein in normal growing cells (36,37). But the protein biosynthetic machinery must also exhibit a high degree of spatial order and intricate interactions to guarantee these rates. As reported (35), there is for example only one amino acid-specific $tRNA^{aa}$ for every two ribosomes but there is 10-20 times more eEF1A than tRNA. It is known that there is neither free aa-$tRNA^{aa}$ nor free $tRNA^{aa}$ detectable in the cell (123), which hints to elaborated interactions between the ribosome as the producer of uncharged $tRNA^{aa}$ and aminoacyl-tRNA synthetases as the producer of aa-$tRNA^{aa}$. A convenient proposal, since economic for the cell, is that eEF1A not only delivers the charged aa-$tRNA^{aa}$ from the aminoacyl-tRNA synthetase towards the ribosomal A site, but also the uncharged $tRNA^{aa}$ from the ribosomal E site in the opposite direction.

Negrutskii and Deutscher tried to introduce labeled exogenous aa-$tRNA^{aa}$ into actively translating cells. Their conclusion was that the cycle described in Figure 6.2 as the canonical function of eEF1A is actually a closed cycle that prevents metabolites from diffusion. They based this on their finding that introduction of exogenously molecules was precluded.

In this study it was clearly demonstrated that charged aa-$tRNA^{aa}$ as well as uncharged $tRNA^{aa}$ competed with nascent polypeptide chains for binding on eEF1A and that both were able to stimulate the notoriously low GTPase activity of eEF1A considerably. It is important to note that the two assays are based on different principles, the first approach (photocrosslinking) indicative of direct physical contact, whereas the second measured a biochemical activity. Both methods provided dose-dependent impacts and revealed a trend, where charged aa-$tRNA^{aa}$ had a stronger effect than uncharged $tRNA^{aa}$. It is surprising

that without the relevant biological signal, the GTPase activity of eEF1A could be raised that much, but it is reasonable to assume, that the high concentration of aa-tRNA^{aa}/tRNA^{aa} in the *in vitro* experiments together with the use of purified components may have the potential to mimic the interaction of eEF1A with rRNA, hence triggering GTP hydrolysis.

However, this study contained no *in vivo* experiments, so it can not be said that the binding of tRNA^{aa} to eEF1A is indeed biological relevant. On the other hand, in the light of the results of Negrutskii, a biological relevance is possible entirely. If so, a complicated question to answer in this scenario is the exact sequence of events: to avoid diffusion of the tRNA^{aa} the guanine nucleotide exchange factor eEF1Bα can induce nucleotide exchange only after delivery of tRNA^{aa} to the aminoacyl-tRNA synthetase, which would mean that the exchange happens on the aminoacyl-tRNA synthetase. This should be a testable hypothesis.

Quality control of nascent polypeptide chains

It is well recognized that post-translational triage of unfolded or damaged protein can result in rescue by chaperones or in targeting for degradation by proteases (127). Previous studies showed that eEF1A could stimulate ubiquitin-dependent proteolysis of histone H2A, actin, and δ-crystallin (47). In general, the signals which trigger ubiquitination and/or protease degradation of newly synthesized proteins or nascent polypeptide chains stuck on the ribosome are not known. This is in stark contrast to bacterial systems. The bacterial tmRNA is so-named for its dual tRNA-like and mRNA-like nature (128). It's also known as 10Sa RNA or SsrA. The tmRNA engages in a remarkable *trans*-translation process, adding a C-terminal peptide tag to an unfinished protein on a stalled ribosome. The tmRNA-directed tag targets the unfinished protein for proteolysis via the protease Tsp. No homolog system to rescue stalled eukaryotic ribosomes is found yet.

In asking what requirements are necessary for a molecule to efficiently scan translating ribosomes for potential problems, two scenarios emerge with respect to the mechanical implications (in both scenarios it is assumed that the molecule in question interacts with the ribosome).

(i) If the number of scanning molecules is much less than the number of ribosomes, it requires these molecules to move quickly and directly from one ribosome to the next. It further necessitates that the scanning molecules make sure, that all ribosomes are visited on a even distribution, which needs a complicated regulation.

(ii) If the number of scanning molecules is at least equal or even (much) higher than the number of ribosomes to be scanned, both, the quick and direct searching as well as the complicated regulation are not required.

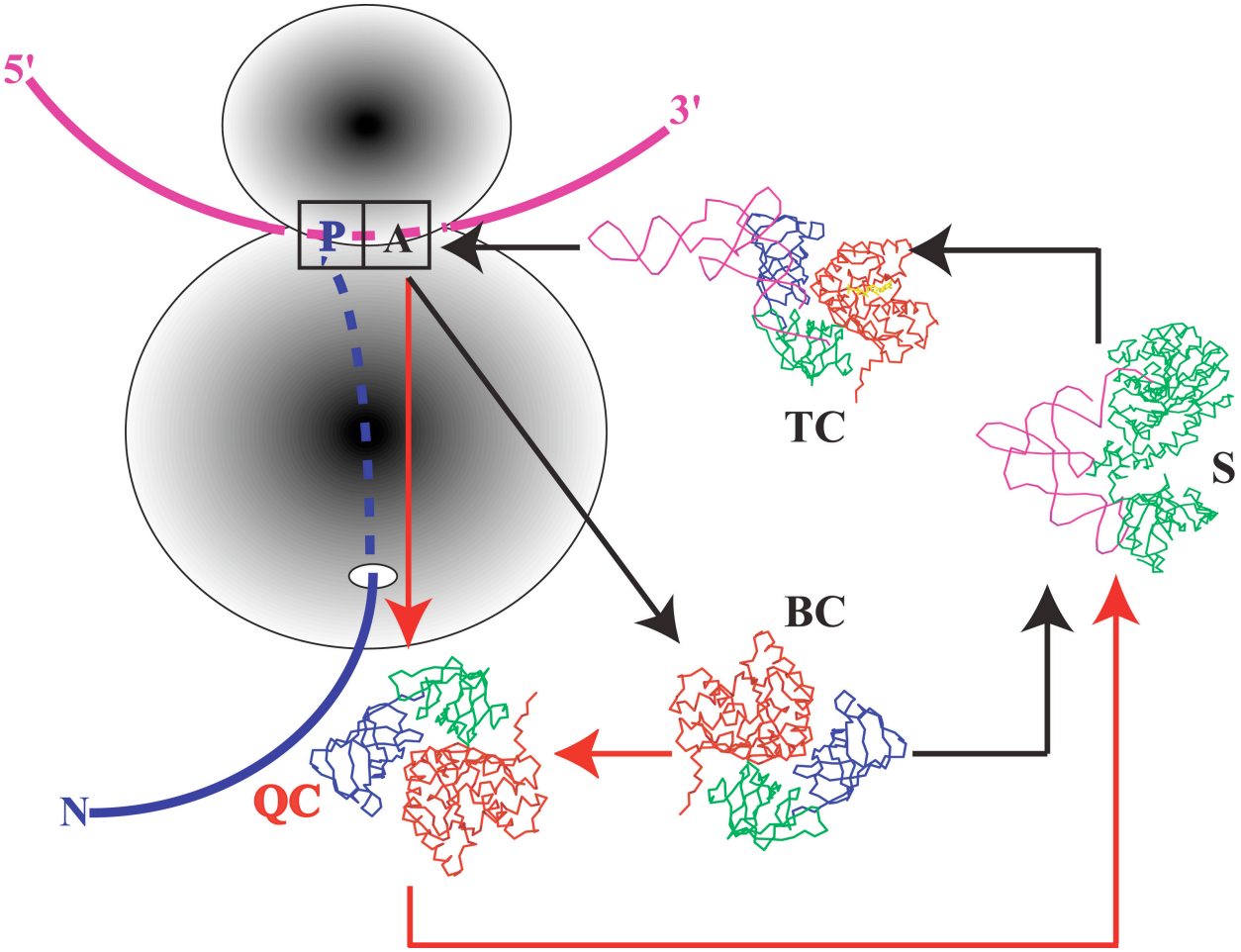

Figure 6.2: Established and proposed functions of the translation elongation factor 1A.
The small and large subunits of the ribosome are simplified by small and large circles. The mRNA is drawn in magenta and the 5' and 3' ends are indicated. The emerging nascent polypeptide chain is in blue, the N-terminus is marked by N. The intra-ribosomal parts of the mRNA as well as the nascent polypeptide chain are illustrated by a dashed line. Only the ribosomal P and A sites are shown for clarity. The ternary complex aa-tRNA^{aa}•eEF1A•GTP is marked by TC, the empty eEF1A itself as BC. Domain I of eEF1A is given in red, domain II is green and domain III is blue, GTP in the ternary complex is yellow and the aa-tRNA^{aa} is magenta. S indicates a aminoacyl-tRNA synthetase (green) with the aa-tRNA^{aa} in magenta. The cycle represented by black arrows describes the established function of eEF1A in translation, which is outlined in detail in section 3.3.1 and in short in the main text. The red arrows represent the proposed functions in quality control (QC) and channeling of tRNA^{aa} towards the aminoacyl-tRNA synthetase.

The eukaryotic translation elongation factor 1A is not only a ribosome associated factor, but it is present on the ribosome in high local concentrations. Furthermore, as was shown in this work, it is in physical contact with the nascent polypeptide chain, both, when arrested on the ribosome and when released from it. In this model it is proposed that eEF1A may function as a key component of such a quality control mechanism. Once eEF1A has released its cargo of charged aa-tRNA^{aa}, it is free to bind to the growing nascent chain. Its binding can be successfully competed by other ribosome associated factors, including NAC, SRP and Hsp 70/40. The high concentration of cytosolic eEF1A, especially close to the

ribosome, would ensure that a permanent scanning of the nascent chain is possible and eEF1A binding would then hasten the degradation of these proteins. The high level of empty eEF1A makes it an ideal sensor to check on the status of a growing nascent polypeptide chain; even in reticulocyte lysate about two eEF1A are generated per second.

This novel function for eEF1A is not in contrast to the non-canonical function mentioned before, rather these two mechanisms can compete with each other.

In this context a necessary question to ask is, how one single molecule can fulfull several distinctive functions (see section 3.3 for examples and references). Being able to solve the crystal structure of eEF1A in complex with the catalytic moiety of eEF1B from *Saccharomyces cerevisiae* indicates a unflexible constitution for most part of the molecule: amino acids 2-441 of eEF1A were modeled and only the last 17 amino acids were not resolved (53,54). From a theoretical point of view, though, one has to admit that the preparation and the handling of the samples do not represent conditions typical for a cytosolic environment. Moreover, it was reported (129) that disregarding structural heterogeneity of crystalls introduces – avoidable – degeneracy into the structure determination process. It was found that neglecting the structural heterogeneity is the reason why the accuracy of crystallographic structures has been widely overestimated.

In contrast to the described crystal structure a study based on physicochemical experiments (scanning microcalometry and neutron scattering) eEF1A was reported to exhibit an extended shape, enabling it to potentially perform large conformational changes upon binding with ligands (61). In order to get a clear picture about eEF1A's capabilities a solution-based approach like NMR spectroscopy would be very helpful.

7 Material and Methods

7.1 DNA and RNA techniques

7.1.1 Plasmid constructs

The truncated polypeptides and full-length proteins used in this study are summarized in Table 7.1, which notes the positions of all methionines and lysines and the restriction enzymes used to produce the truncated templates. Firefly luciferase (ffLuc) polypeptides are encoded by the plasmid pT3-Luc, a gift of Dr. M. Strauss. Wild-type bovine preprolactin (pPL) is encoded by pSPBP4 and pPL-M by pGEM4-PPL/SSKO and are gifts of Drs. P. Walter and B. Dobberstein, respectively. In pPL-M, the signal peptide has been altered by three amino acid substitutions (leucine 15 to proline, valine 19 to glutamic acid and leucine 23 to arginine) that destroy its ability to bind signal recognition particle. pPL-MN was constructed starting with pPL-N, the kind gift of Drs. W. Mothes and T. A. Rapoport. pPL-N encodes preprolactin in which every lysine codon has been mutated to an arginine or asparagine as follows: lysines 4, 9, 72 and 78 to arginine and lysines 99, 136, and 154 to asparagine. To make pPL-MN, the DNA encoding the signal sequence (aa 1-30) of pPL-N was excised and replaced with the corresponding sequence from pPL-M (thanks to Dr. Shu Wang for the plasmid construction). As seen in Table 7.1, this produced a plasmid encoding preprolactin with lysines only at positions 4 and 9 and, in addition, with a non-functional signal sequence.

Protein	Positions of		Restriction Enzyme
	Methionines	Lysines	
85 aa β-actin	1, 16, 44, 47, 82	18, 50, 61, 68, 84	Bgl II
133 aa β-actin	1, 16, 44, 47, 82, 119, 123, 132	18, 50, 61, 68, 84, 113, 118	SnaB I
221 aa β-actin	1, 16, 44, 47, 82, 119, 123, 132, 153, 190	18, 50, 61, 68, 84, 113, 118, 191, 213, 215	Xba I
77 aa ffLuc	1, 30, 59, 67	5, 8, 9, 28, 31, 68	Hinf I
197 aa ffLuc	1, 30, 59, 67, 90, 118, 152, 164, 196	5, 8, 9, 28, 31, 68, 130, 131, 135, 141, 142, 148, 155, 190	EcoR I
550 aa ffLuc-wt	1, 30, 59, 67, 90, 118, 152, 164, 196, 249, 265, 396, 398, 493	5, 8, 9, 28, 31, 68, 130, 131, 135, 141, 142, 148, 155, 190, 206, 281, 297, 303, 321, 329, 358, 364, 372, 380, 414, 439, 443, 445, 491, 496, 510, 511, 524, 529, 534, 541, 543, 544, 547, 549	*
229 aa pPL-M	1, 54, 66, 83, 111, 135, 160, 162	4, 9, 72, 78, 99, 136, 154, 172, 189, 211, 217	*
86 aa pPL-MN	1, 54, 66, 83	4, 9	Pvu II
169 aa pPL-MN	1, 54, 66, 83, 111, 135, 160, 162	4, 9	EcoR I
229 aa pPL-wt	1, 54, 66, 83, 111, 135, 160, 162	4, 9, 72, 78, 99, 136, 154, 172, 189, 211, 217	*

Table 7.1: Protein nomenclature and positions of relevant amino acids.
The restriction enzymes listed were used to generate the corresponding truncated polypeptides. An asterisk indicates full length of the protein.

7.1.2 Culturing of *E. coli* and isolation of plasmid DNA

In order to either mutate plasmid DNA or produce large amounts of plasmid DNA for subsequent use in *in vito* transcription assays, commercially available kits from Stratagene (La Jolla, CA) were employed. Epicurian Coli XL1-Blue Subcloning-Grade Competent Cells or Epicurian Coli BL21 (DE3) Competent Cells were used according to the instructions provided by the manufacturer.

Isolation of plasmid DNA on a small scale (~5 ml) followed the procedure described by Birnboim and Doly (130). Isolation of plasmid DNA on a large scale (500 ml) followed the procedure described by Sambrook et al. (131). Both procedures yield typically 3-5 µg plasmid DNA per ml culture.

7.1.3 Restriction digestion of plasmid DNA

A typical restriction digestion contained 50 µg purified plasmid DNA, 5 µl of corresponding commercial 10x buffer (New England Biolabs, Beverly, MA), an appropriate amount of restriction enzyme, additional factors as recommended by the manufacturers instructions (New England Biolabs, Beverly, MA) and water to reach a total volume of 50 µl. The restriction digest was carried out at the recommended temperature to ensure complete digestion. The amount of restriction enzyme needed (1 unit of restriction enzyme will digest 1 µg of DNA in a 50 µl reaction in 60 min) was calculated from the guidelines given by New England Biolabs, taking into account that the glycerol concentration in the digest must be kept under 5 % (v/v) to avoid inhibitory effects. Furthermore, restriction enzymes that generate 3' protruding ends had to be avoided because erraneous transcription will occur. The digested DNA was subjected to two rounds of phenol/chloroform extraction, 1 extraction with chloroform/isoamylalcohol and subsequent ethanol precipitation as described:

- add 450 µl H_2O to the 50 µl restriction digestion
- add 500 µl phenol/chloroform and mix well
- spin 2 min with 12000 rpm (Sorvall MC 12 V) at room temperature
- extract supernatant with 500 µl phenol/chloroform and mix well
- spin 2 min with 12000 rpm (Sorvall MC 12 V) at room temperature
- mix supernatant well with 500 µl chloroform/isoamylalcohol (24:1)
- spin 2 min with 12000 rpm (Sorvall MC 12 V) at room temperature
- mix supernatant well with 2 volumes of 100 % ice-cold EtOH and 0.01 volumes of 3 M NaAc
- place for 15 min at –20 ˚C
- spin 15 min with 14000 rpm (Eppendorf 5417R) at 4 ˚C
- aspirate supernatant
- wash pellet with 70 % ice-cold EtOH

- spin 15 min with 14000 rpm (Eppendorf 5417R) at 4 ˚C and aspirate supernatant and dry pellet
- add 50 µl H_2O to reach a final DNA concentration of 1 µg/µl
- run samples collected at various steps of the procedure on an 1 % (v/v) agarose gel to verify complete digestion and correct size of fragments

7.1.4 *In vitro* transcription of plasmid DNA

After linearization with the appropriate restriction enzyme and isolation of the digested plasmid DNA truncated mRNAs were produced by *in vitro* transcription with SP6 or T7 RNA polymerase (15,71). The composition of a typical 100 µl transcription mix was as follows:

	amount needed [µl]	Vendor
H_2O	43.5	-
5x Transcription Buffer	20.0	Promega
100 mM DTT	10.0	Promega
20 µg/µl BSA	0.5	Promega
50 mM each ATP, CTP, UTP	1.0	Sigma
$m^7G(5')ppp(5')G$	5.0	Boehringer Mannheim
40 U/µl RNasin	5.0	Promega
20 U/µl SP6 or T7 RNA-Polymerase	5.0	Promega
1 µg/µl DNA	10.0	-

Table 7.2: Compositon of a typical 100 µl transcription mix.
The mix can be scaled up linearly for larger transcriptions. The stock solution of the $m^7G(5')ppp(5')G$ Cap analog was prepared by dissolving 5 A_{250} units in 100 µl H_2O.

The transcription mix was incubated for 10 min at 37 ˚C, then 5 µl 10 mM GTP was added and the transcription mix was incubated for further 90 min at 37 ˚C. To stop the transcription, place the transcription mix for 5 min on ice.

7.1.5 Isolation of *in vitro* transcribed truncated mRNA

In order to isolate the truncated mRNA a nucleic acid extraction at an acidic pH was carried out twice. At an acidic to neutral pH DNA partitioned into the organic/interphase, whereas RNA separates into the aqueous phase.

To the transcription mix 1 volume phenol/chloroform/isoamylalcohol (25:24:1) pH 4.5 was added and mixed well. After a 2 min centrifugation step at 14000 rpm (Eppendorf 5417R) and 4 ˚C, the aqueous phase was combined with 1 volume of phenol/chloroform/isoamylalcohol (25:24:1) pH 4.5 and the extraction procedure was repeated. The aqueous phase is then extracted once with 1 volume chloroform/isoamylalcohol 24:1 and centrifuged again. The mRNA in the aqueous phase was then

precipitated by adding 2.5 volumes of 100 % ice-cold EtOH and 3 M NaAc pH 5.2 to reach a final concentration of 0.3 M NaAc. This solution was kept for at least 60 in at –20 ˚C. The precipitated mRNA was subjected to another centrifugation step for 15 min with 14000 rpm (Eppendorf 5417R) at 4 ˚C, was subsequently washed once with 70 % ice-cold EtOH and dryed at room temperature. After drying the mRNA it was resuspend in 50 µl H_2O and aliquots were stored at –80 ˚C.

As quality control samples were collected at various steps of the procedure and run on an 1 % (v/v) agarose gel to verify complete digestion, correct size of fragments, and successful *in vitro* transcription. Furthermore, a small test translation was carried out to establish the functionality of the newly generated mRNA.

7.2 Protein techniques

7.2.1 *In vitro* translation and crosslinking assay

In vitro translation was performed using rabbit reticulocyte lysate (97) for 20 min at 26 ˚C, a temperature that best preserves the RNC complexes while translation is still reasonable fast. Translation reactions included 1 mCi/ml ^{35}S-methionine (specific activity 1,000 Ci/mmol; Amersham Biosciences) and TDBA-Lys-tRNA^{Lys}. The preparation of the crosslinking agent TDBA-Lys-tRNA^{Lys} is described in great detail elsewhere (70).

When a synchronized *in vitro* translation was desired (Figure 5.7 A and B), translation initiation was allowed to proceed for 3 min (Figure 5.7 A) or 2 min (Figure 5.7 B), then blocked by addition of aurintricarboxylic acid and 7-methylguanosine 5'-monophosphate (Sigma, St. Loius MO) to 50 µM and 1.8 mM (Figure 5.7 A) or to 75 µM and 2 mM (Figure 5.7 B), respectively, followed by further incubation at 26 ˚C. This effectively synchronized the translations and uniformly produced nascent chains translated to the limit of the truncated mRNA. All other *in vitro* translations were unsynchronized. The reactions were stopped by either placing the reaction on ice or adding cycloheximide to a final concentration of 5 mM, then irradiated if necessary, treated with RNase A and EDTA and analyzed on a 10 % NuPAGE Bis-Tris gels in MES buffer and visualized by autoradiography, except as noted. Samples were irradiated on ice not more than 5 cm away from a high-intensity longwave UV lamp (UVP model B100AP, λ_{range} = 315 – 400 nm with λ_{max} = 365 nm).

7.2.2 Isolation of the high salt-stripped nascent polypeptide chains

To strip ribosome associated factors from ribosomes, translation reactions were diluted into 10 volumes of ice–cold high salt buffer (HSB: 50 mM Hepes/KOH pH 7.5, 700 mM potassium acetate, 5 mM magnesium acetate, 1 mM DTT, and 0.4 U/µl of placental RNase inhibitor). After 10 min incubation at 4 ˚C, samples were isolated by centrifugation (100000 rpm, 4 ˚C, 20 min, TLA 120.1 rotor, Beckman)

through a high-salt sucrose cushion (0.5 M sucrose in HSB). The ratio of the volumes of sucrose cushion to sample was ~2:1. Ribosome nascent chain complexes were resuspended in one volume translation blank buffer (TBB: 50 mM Hepes/KOH pH 7.5, 100 mM potassium acetate, 5 mM magnesium acetate, 1 mM DTT, protease inhibitor cocktail as described by Erickson and Blobel (98), and 0.4 U/µl of placental RNase inhibitor) and the high salt stripping was repeated as described above to completely remove associated proteins. The isolated high salt-stripped RNCs were incubated at 26 ˚C for 5 min with buffer A (50 mM Hepes/KOH pH 7.5, 50 mM potassium acetate, 5 mM magnesium acetate, 1 mM DTT), rabbit reticulocyte lysate (precipitated with 66 % ammonium sulfate and dialyzed against buffer A) or purified protein in buffer A supplemented with RNase inhibitor and protease inhibitors.

7.2.3 Release of truncated polypeptide chains from the ribosome

RNCs were incubated on ice for 30 min with 2 mM puromycin and then at 26 ˚C for 10 min with 0.1 mg/ml RNase A, to release the newly synthesized polypeptides. After treatment, the reaction mixture was centrifuged (100000 rpm, 4 ˚C, 20 min, TLA 120.1 rotor, Beckman) through a physiological salt sucrose cushion (0.5 M sucrose in TBB) to separate ribosomes (pellet) from released polypeptides and RAFs (supernatant).

7.2.4 Purification of the eukaryotic translation elongation factor 1A from rabbit and yeast

Rabbit (*Oryctolagus cuniculus*)

eEF1A was isolated from rabbit reticulocyte lysate prepared as described previously (98). After sedimentation of the ribosomes by centrifugation for 60 min at 100000 rpm in a Beckman rotor TLA 100.4, proteins were precipitated with 66 % ammonium sulfate, dialyzed against buffer A (50 mM Hepes/KOH pH 7.5, 50 mM KAc, 5 mM MgAc and 1 mM DTT) overnight, and applied to a Q-Sepharose column (Pharmacia, Uppsala Sweden). The flow through was applied to an S-Sepharose column (Pharmacia, Uppsala Sweden) and eluted with a linear gradient of 10-1000 mM potassium acetate in buffer A. A single protein was obtained at 390-450 mM potassium acetate concentration. The protein was dialyzed against 15 % glycerol in buffer A. From 35 ml of rabbit reticulocyte lysate, 200 µg of purified eEF1A was obtained. The columns were connected to a FPLC system from Pharmacia (Pump P500 and Controller LCC 501 Plus).

Yeast (*Saccharomyces cerevisiae* strain SKQN2)

eEF1A was isolated from yeast based on a modified version of a method described by Thiele et al. (76). Six liter YPD broth (Q-Biogene) was inoculated with *Saccharomyces cerevisiae* SKQN2, a strain low in endogenous proteases, and grown at 25 ˚C until $OD_{600} \approx 1.0$. Cells were harvested for 10 min at

4000 rpm and 4 ˚C in a Sorvall RC 12BP, washed with 500 ml H_2O, spun again under the same conditions, resuspended in extraction buffer A (100 mM Hepes/KOH pH 8.0, 1 mM DTT, 1 mM PMSF, 0.1 mM EDTA, 100 mM ammonium sulfate, 10 % w/v glycerol, 2 mM $MgCl_2$, 50 µM GDP) and spun again under the same conditions, typically yielding 40 – 50 g wet cells. After another resuspension in extraction buffer A (1 ml per 1 g cells) cells were homogenized under cooling passing twice a French Pressure Cell Press from SLM Instruments Inc. at 18000 psi. The cell extract was centrifuged in a SS34 rotor (Sorvall) for 20 min at 10500 rpm and 4 ˚C. The supernatant was centrifuged in a Beckman XL-90 Ultracentrifuge using a Ti90 rotor for 90 min at 50000 rpm and 4 ˚C.

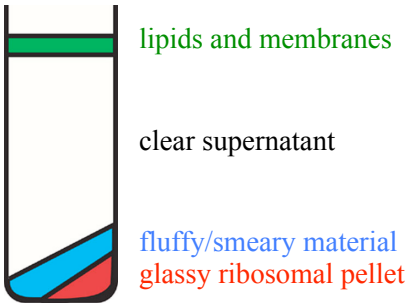

Figure 7.1: Supernatant after 90 min centrifugation at 50000 rpm.
Only the clear supernatant was processed in the batch process.

The purification continued with the clear supernatant only (Figure 7.1) in a batch process using the cation exchanger P11, a fibrous cellulose-based orthophosphate (Whatman, Maidstone/UK). 50 g P11 was equilibrated with 150 ml extraction buffer B (20 mM Hepes/KOH pH 8.0, 1 mM DTT, 1 mM PMSF, 0.1 mM EDTA, 100 mM ammonium sulfate, 10 % w/v glycerol, 2 mM $MgCl_2$, 50 µM GDP) and centrifuged at 2000 rpm for 3 min at 4 ˚C in a Beckman GS6KR. After two more washes the washed P11 was incubated with the clear supernatant in a ratio of 1 g P11 per 150 OD_{280} unit of the clear supernatant for 60 min at 4 ˚C on a rotator. The solution is centrifuged at 2000 rpm for 3 min at 4 ˚C in a Beckman GS6KR. The P11 matrix was washed with 2 volumes extraction buffer B and centrifuged again. This procedure was repeated until the supernatant exhibits $OD_{280} = 0$. Elution of eEF1A was reached by adding 2 volumes elution buffer (20 mM Hepes pH 8.0, 500 mM $(NH_4)_2SO_4$, 100 µM EDTA, 2 mM DTT, 50 µM GDP, 1 mM PMSF, and 10 % v/v glycerol) and collecting the supernatant after centrifugation as before. The P11 elution was diluted 1:5 with S-Sepharose buffer (20 mM Hepes pH 8.0, 100 µM EDTA, 2 mM DTT, 50 µM GDP, 1 mM PMSF, and 10 % v/v glycerol) and applied to a 2 ml S-Sepharose column equilibrated with the same buffer. The flow rate was controlled by gravitational force. After collecting the flow through, the column was washed with 2 ml S-Sepharose buffer. 15 ml S-Sepharose buffer containing 100 mM NaCl was applied to wash away unspecific bound material. Elution of eEF1A was achieved with 8•1 ml of S-Sepharose buffer containing 250 mM NaCl.

7.2.5 Recombinant protein expression and purification

A plasmid encoding a GST-eEF1A fusion protein was a generously provided by J. Condeelis (41). *E. coli* DH5α cells were transformed with this plasmid and a 2 liter culture in 2x YT was incubated at room temperature until it reached an optical density OD_{600} = 0.8. Protein expression was induced by addition of IPTG to a final concentration of 0.2 mM. After 7-8 hours, the cells were collected by centrifugation, resuspended in 100 ml of buffer (50 mM Tris/HCl pH 8.0, 300 mM KCl, 1 % Triton X-100, 15 % glycerol, 1 mM DTT, and protease inhibitor) and broken by one pass through an Avestin cell disrupter (Ottawa, Canada) at greater than 10000 psi. After centrifugation of the lysate at 12000 rpm for 10 min in a SA600 rotor (Sorvall), the resulting supernatant was spun at 35000 rpm in a Ti45 rotor (Beckman) for 60 min. The supernatant was then incubated overnight at 4 ˚C with 2 ml glutathione Sepharose 4B beads (Pharmacia). After centrifugation and wash, the beads were resuspended in 1 ml of glutathion elution buffer (Pharmacia), and incubated at room temperature for 10 min to elute the GST-eEF1A fusion protein from the beads. Finally, the beads were sedimented and the GST-eEF1A fusion protein was recovered from the supernatant. In order to cleave the GST-moiety from eEF1A, the GST-eEF1A protein was treated with thrombin (4 U/ml) and incubated at room temperature for 16 hours. Thrombin was inactivated by addition of 1 mM PMSF and 0.5 mM AEBSF for 30 min, followed by dialysis against buffer A containing 15 % glycerol. Recombinant eEF1A protein was recovered from the supernatant after incubation of the mixture with glutathione Sepharose 4B beads.

7.2.6 Immunoprecipitation

A 36 µl *in vitro* translation was pelleted through a physiological salt sucrose cushion and resuspended in 20 µl TBB. 12 µl of the resuspended pellet were diluted with 600 µl RIPA buffer (50 mM Tris/HCl pH 8.0, 150 mM NaCl, 1 % v/v Nonidet P-40, 0.5 % v/v Deoxycholate, 0.1 % v/v SDS) and split in two aliquots. One aliquot was incubated with 1 µl anti-Aβ 6E10 antibody, the other with 2 µl anti-presenilin1 antibody and subsequently incubated for 60 min at roomtemperatur on a rotator. 10 µl of three times RIPA-washed Protein G agarose beads or Protein A agaraose beads (Roche, Indianapolis IN) were added and continue incubation for another 60 min. After spinning down the beads (Eppendorf 5417R) and washing them three times with RIPA buffer, bound material was eluted with 20 µl two times concentrated sample buffer (Invitrogen, Carlsbad CA) containing 100 mM DTT.

7.2.7 NMR spectroscopy

NMR spectra were recorded on a Varian Inova 600 MHz spectrometer at 27 ˚C. The Data were processed with the corresponding software from Varian.

NMR studies were performed from the two longest Gonc peptides (29mer and 31mer). In a screening approach using 1 mM of each peptide in 20 mM Tris/HCl pH 7.8, 150 mM KCl, and 10 % v/v D_2O (99.9 atom % D) a 1D ^1H-spectra was recorded at 27 ˚C. Before recording the spectra the solutions were subjected to a centrifugation for 10 min at 100000 rpm and 4 ˚C in a Beckman ultracentrifuge (TLA120.1 rotor) and only the supernatant was used subsequently. No pelleted material was detected (visually and on a stained SDS-PAG).

In a second approach a 2D nuclear Overhauser effect spectroscopy (NOESY) spectrum was recorded from the same 31mer Gonc solution at the same temperature.

In a third set a 2D heteronuclear single quantum coherence (HSQC) spectrum was recorded from both peptides. The final concentration of the peptides in this experiment was 4.76 mM and the buffer was 50 mM Hepes pH 7.8, 10 % DMSO, and 10 % D_2O (99.9 atom % D). The rise in peptide concentration was necessary because the short peptides do not provide many naturally occuring ^{15}N nuclei, which this type of spectrum takes advantage of – ^{15}N abundance is 0.36 % among N isotopes. Before recording the spectra the solutions were subjected to a centrifugation for 10 min at 100000 rpm and 4 ˚C in a Beckman ultracentrifuge (TLA120.1 rotor) and only the supernatant was used subsequently. No pelleted material was detected (visually and on a stained SDS-PAG). The recording time was 17 h at 27 ˚C.

The experiments were kindly performed by Dr. Ananya Majumdar from the Structural Biology Department of the MSKCC, Nucleic Acid and Protein Structure Program (Dr. Dinshaw Patel).

7.2.8 Gel-filtration chromatography

Prepacked Superdex 75 and a Superdex 200 column (Pharmacia, Uppsala Sweden), both with a bed volume of 24 ml, were washed with at least 50 ml of the same buffer (50 mM Hepes pH 7.5, 150 mM KAc, 5 mM MgAc, 1 mM DTT, 2 % v/v DMSO) that was used to dissolve the standard proteins as well as the 29mer and 31mer Gonc peptides. The void volume of the column is approximately 1/3 of the bed volume, i. e. 8.0 ml. In case of the Gonc peptides 200 µl of a 1 mM peptide solution were loaded onto the column and eluted with a flow rate of 0.4 ml/min. Fractions of 0.36 ml (Superdex 75) and 1.0 ml (Superdex 200) were collected. The composition of the protein standards are given in Table 7.3 below.

Stock solutions of each protein standard were made from lyophilizate (Pharmacia, Uppsala Sweden) at a concentration of 25 µg/µl assumimg the lyophilizate to be 60 % w/w protein and 40 % w/w other material. Proteins were dissolved in 50 mM Hepes pH 7.5, 150 mM KAc, 5 mM MgAc, 1 mM DTT, 2 % v/v DMSO. Two standard mixes were composed: the first contained the five monomeric proteins only (five protein standard, each protein present at 5 µg/µl) and the second contained in addition the tetrameric catalase and the pentameric aldolase (seven protein standard, each protein present at 3.6 µg/µl).

Protein	Source	M_w [kDa] a	M_w [kDa] b	M_w [kDa] c	pI d	Stokes radius [Å] c
Serum albumin	*Bos taurus*, serum	69.29	66.43	66.43	5.60	35.5
Ovalbumin	*Gallus gallus*, egg white	42.75	42.75	42.75	5.19	30.5
Chymotrypsinogen A	*Bos taurus*, pancreas	25.67	-	-	8.52	20.9
A chain		-	1.25	1.25	5.52	
B chain		-	13.92	13.92	5.55	
C chain		-	10.07	10.07	9.17	
RNase A	*Bos taurus*, pancreas	16.46	13.69	13.69	8.64	16.4
Aprotinin	*Bos taurus*, lung	10.90	6.52	6.52	9.24	
Catalase	*Bos taurus*, liver	57.59	57.59	230.36	6.41	52.2
Aldolase	*Oryctolagus cuniculus*, muscle	39.21	39.21	156.84	8.40	48.1

Table 7.3: Protein standards for gel-filtration.
a: unprocessed monomeric chain; b: processed chain; c: under native conditions; d: pI refers to the monomer in a complex or to the –processed– monomer. The five protein standard contained the first five proteins of the list, the seven protein standard contained all seven proteins.

Prior to loading on the gel-filtration columns, standards as well as the different samples were spun for 5 min at 100000 rpm in a Beckham ultracentrifuge (TLA 120.1) at 4 ˚C. Only catalase seemed to have formed aggregates to a reasonable amount as judged by the the staining pattern on a SDS-PAG and the color of the pellet. The columns were connected to a FPLC system from Pharmacia (Pump P500 and Controller LCC 501 Plus).

7.2.9 Identification of the peptide binding site by a heterobifunctional crosslinking approach

The experiments described in 5.4 included the chemical crosslinkers SAND, EDC and APDP (all from Pierce, Rockford, IL). Since only APDP gave promising results, its use is described here in detail. The structure and some properties of APDP are shown in Figure 7.2, and Figure 7.3 explains the general reaction mechanism of APDP.

The following procedure is based on the original instruction of the manufacturer but underwent major modifications in order to optimize the result. The first step was the complete reduction of 500 µM 31mer-Gonc (see Tables 5.4 and 7.4) in 5 mM sodium phosphate pH 6.6 in a total volume of 80 µl. The reaction was kept for 60 min at 37 ˚C.

In a second step 40 µl of this reaction was incubated with 40 µl of 5 mM APDP, and the total volume was brought to 200 µl by adding 10 mM sodium phosphate pH 6.6. The reaction was kept for 60 min at 37 ˚C.

100 µl of the modified peptide was subsequently incubated with 60 µl 13.75 µM eEF1A and 40 µl of adjusting buffer (5 mM sodium phosphate pH 6.6, 10 mM Tris/HCl pH 7.5, 50 mM NaCl, 10 mM $CaCl_2$) to facilitate binding of the Gonc-peptide to the peptide binding site of eEF1A. The assay was incubated for 15 min at 37 ˚C and the assay concentrations were 4.125 µM eEF1A, 50 µM Gonc peptide,

500 µM APDP and 2 mM $CaCl_2$. After aliquoting the assay into samples for either – or + irradiation (15 min with λ_{range} = 315 – 400 nm and λ_{max} = 365 nm, UVP model B100AP), 70 µl of the the assay was incubated with 6 µl 2.5 M DTT at room temperature for 3 h in order to break the disulfide bridge between the Gonc peptide and the crosslinker. This left the phenyl azide moiety and the spacer arm attached to eEF1A. Since this part of the molecule has a molecular weight of 308, it should be easily recognizeable in a mass spectroscopic analysis. Bands were excised from a Coomassie stained 8 % SDS-PAG, the eluted protein was trypsin digested and fragments analyzed by mass spectroscopy by the Targeted Proteomics Group of MSKCCs Molecular Biology Program.

Figure 7.2: Structure of APDP.
The pyridyldisulfide moiety (blue) is connected via a 2.11 nm long spacer arm to the hydroxyphenyl azide. It reacts first with a sulfhydryl containing ligand via disulfide exchange. Irradiation of the hydroxyphenyl azide group creates a reactive arylnitrene. The hydroxyphenyl azide group can be radioiodinated (light blue) in the meta position. The molecular weight is 446.55 Da for the non-iodinated molecule.

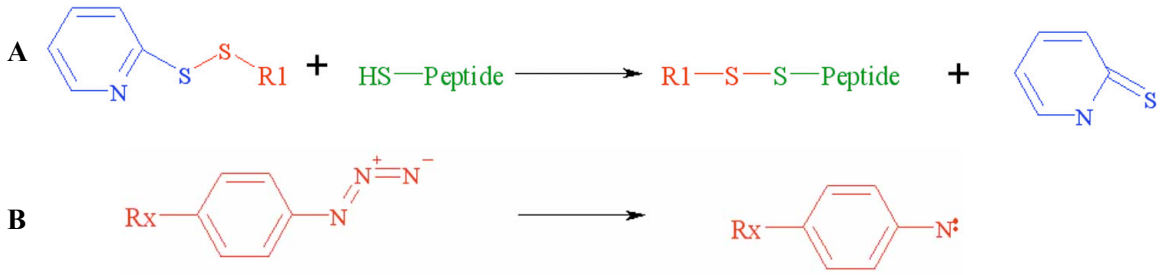

Figure 7.3: Reaction scheme of APDP.
A: Pyridyldisulfide (blue) reacts towards a sulfhydryl-group of a peptide (green) via disulfide exchange. This generates an aryl azido peptide and pyridine-2-thione (M_w = 110.2). The remaining part of the crosslinker has a molecular weight of 336.4. **B:** The photolysis of aryl azide can be reached with λ_{range} = 250 – 460 nm. The actual wavelength range applied was λ = 315 – 400 nm with λ_{max} = 365 nm. Photolysis creates an arylnitrene, which reacts non-specifically to form a covalent bond. Possible resultant reactions include insertion into an alkane or amine group, addition into an alkene, condensation reactions or re-arrangements to other products. The arylnitrene moiety has a molecular weight of 308. See references (132,133) and *http://www.piercenet.com*

7.2.10 GTPase assay for the eukaryotic translation elongation factor 1A

The GTPase assay developed for this study is based upon publications by Randerath and Randerath (134) and Schiedel et al. (135). An assay of 50 µl size typically contained 2.5 µM eEF1A and 5.0 µl 10x incubation buffer (500 mM Tris/HCl pH 7.8, 20 mM EDTA, 10 mM DTT, 1 mM GTP, and 100 µCi/ml α-^{32}P-GTP). In dependence of the actual experiment carried out, $tRNA^{aa}$ or $aa\text{-}tRNA^{aa}$ were

titrated as described elsewhere (5.5.1). The assays were supplemented with adjusting buffer (20 mM Tris/HCl pH 7.8 and 150 mM KCl) to reach the final volume of 50 µl. When not incubated during the reaction, samples were kept on ice in order to keep (auto-)hydrolysis of GTP at a minimum. Charging of yeast $tRNA^{aa}$ (Boehringer Mannheim) was performed as described (70).

After pipetting the components together, the samples were preincubated for 3 min on ice in the absence of Mg^{2+} to facilitate complex formation. The zero time point (start of the GTPase reaction) is defined by the addition of Mg^{2+} to a final concentration of 12.5 mM. Aliquots of 5 µl were taken at various time points from the assays during incubation at 37 ˚C, and the reactions were stopped by adding an equal volume of stop solution (50 mM Tris/HCl pH 7.8, 5 mM EDTA, 0.2 % w/v SDS, 50 mM GDP, and 50 mM GTP). The probes were heated at 70 ˚C for 2 min in order to remove protein bound nucleotides.

A closed double-trough glass development chamber (27 cm•24cm•7cm) was equilibrated with developing solvent (1 M HCOOH, 1 M LiCl, adjusted with 10 N NaOH to pH = 2.0) for at least an hour to guarantee proper saturation of the gaseous space in the development chamber.

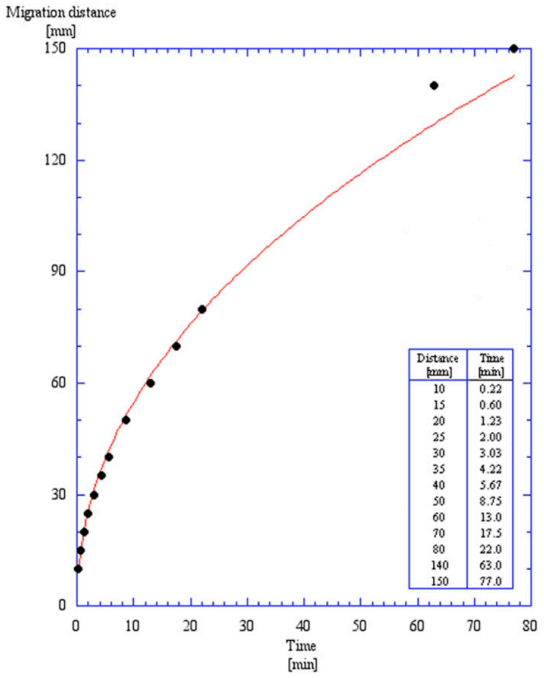

Figure 7.4: Migration distance of the mobile phase front in dependence of time.
The migration distance of the front of the mobile phase was measured at various time points. A power law according to $f(x) = 18.55 \bullet x^{0.4698}$ and a correlation coefficient of R = 0.9986 yielded the best fit (red line).

1 µl of each of the inactive samples was spotted about 1 cm from the edge of a Cellulose PEI sheet (~4.5 mm in diameter) and samples were immediately dried on a handwarm heating block. The Cellulose PEI sheet was placed in the dry half of the closed development chamber for 15 min to guarantee equilibration of the solid with the gaseous phase. Inserting the Cellulose PEI sheet almost vertically into the developing solvent started the ascending chromatography. The level of developer was not to reach the line where the dried samples were spotted. Development of the Cellulose PEI lasted until the front line of the mobile phase reached the top end of the strip. It was empirically determined that a strip length of about 8 cm (7 cm migration distance) is a reasonable length with respect to the need of a good nucleotide separation and the time required for the development (Figure 7.4).

The dried chromatograms were exposed overnight to a KODAK Biomax XR films. After developing the films, the radioactive spots were localized with the help of a handheld UV lamp (UVGL-25 from UVP, Upland CA), marked, cut out, and measured in a scintillation counter.

7.3 Data processing

A Power Mac G4 version 2.1 from Apple Computer Inc. (Cupertino, CA) with the System Software Mac OS X 10.2.8 (6R73) was the source of pleasure to perform almost all computer related work.

Images of stained gels and autoradiographic films were digitalized using Photoshop version 5.0 LE from Adobe in connection with the ScanWizard Controller version 3.2.4 from Microtek Lab and the ScanMaker 4 from Microtek. Image handling was performed with Photoshop version 7.0 from Adobe.

Adobe Illustrator version 10 and Macromedia Freehand version 8.0.1 were used to assemble compound figures.

For quantification of band intensities of radioactive gels, the gels were dried on paper and exposed to a phosphor screen. The screen was then subjected to a scan with a Storm840 PhosphorImager and the exposure was analyzed with the corresponding ImageQuant software version 1.1.1. All equipment was from Molecular Dynamics, a Division of Amersham Bioscience (Piscataway, NJ).

Kaleidagraph version 3.08d from Synergy Software and Microsoft Excel version X for Mac were used for data processing and graphic representations.

For text processing Word X for Mac from Microsoft and Endnote 6.0.1 from Thomson ISI ResearchSoft were in use. Original files were converted into pdf-files and assembled to the final document using Acrobat version 6.0 and Acrobat Distiller version 6.0, both from Adobe.

Chemical structures were generated with either the software CS ChemDraw Pro version 4.5 from CambridgeSoft (Cambridge, MA) or ISIS/Draw version 2.2 from MDL Information Systems Inc. (San Leandro, CA).

7.4 Miscellaneous

All bulk chemicals were purchased from Sigma (St. Louis, MO) and common lab equipment was from Fisher Scientific (Pittsburgh, PA).

Restriction enzymes were obtained from New England Biolabs (Beverly, MA).

Plasmids were isolated either according to the alkaline lysis method from Birnboim and Doly or using the Plasmid Midi Kit from Qiagen (Valencia, CA) according to the manufacturers instructions.

DNA sequencing was performed by the DNA Sequencing Resource Center of the Rockefeller University (New York, NY).

Radioactive labeled amino acids were purchased from Amersham Bioscience (Piscataway, NJ) and radioactive labeled γ-^{32}P-GTP was from NEN Life Science Products (Boston, MA). This supplier also provided the Enlightning – Rapid Autoradiography Enhancer solution.

Autoradiographic films (BioMax MR and X-Omat AR) were purchased from the Eastman Kodak Company (Rochester, NY).

Flexible Cellulose PEI sheets for thin layer chromatography were purchased from J. T. Baker (Phillipsburg, NJ).

Peptide	Sequence	Residue	length [aa]	M_W [Da]	pI	z	©	Comments	¶
1 Bet 1	NQTIDQLGDTFHNTSVKLKRTFGNMMEMARRSGIS	87-121	35	3985.5	9.98	+2	+	Protein transport protein Bet 1, a v-SNARE, C-terminal half	Sc
2 Gos 1	SNVLNTANNKVLQTLQRIPGVNQLIMKINTRR	170-201	32	3648.2	12.32	+5	+	Golgi v-SNARE protein 1, C-terminal half	Sc
3 Nyv 1	SDIGDATEDQIKDVIQIMNDNIDKFLER	163-190	28	3236.5	3.98	-5	+	Vacuolar v-SNARE, N-terminal half	Sc
4 Sec 22 Cccp	GDSLDKMSDMSSSLKETSKRYRKSAQKINFDLLISQ	158-193	36	4108.6	9.31	+2	+	Protein transport protein Sec 22, C-terminal half	Sc
5 Sft 1	SSVINQMTDSLGSMFTDIKNSSSRLTRSLKAGNSIW	47-77	36	3933.4	9.98	+2	w	Intra Golgi transport v-SNARE, C-terminal half	Sc
6 Snc 1	YALSEHDEERPQNVQSKSRTAELQAEIGGTVGIMRD	10-45	36	4016.3	4.84	-3	w	Synaptobrevin homolog 1, N-terminal half	Sc
7 Snc 1	GERLTSIEDKADNLAVSAQGFKRGANRVRKAMWYKD	54-89	36	4082.6	9.82	+3	w	Synaptobrevin homolog 1, C-terminal half	Sc
8 Snc 2	YVPPEESNSGANPNSQNKTAALRQEIDDTVGIMRDN	10-45	36	3932.2	4.30	-3	+	Synaptobrevin homolog 2, N-terminal half	Sc
9 Syntaxin 1A	C TGRTTTSEELEDMLES	156-171	17	1902.0	3.91	-4	-	Synaptotagmin associated protein	Rn
10 Syntaxin 1A	KQALSEIETRHSEIIKLENSIRELHDMFMDMAMLVESQ	189-226	38	4504.1	4.82	-4	w	Synaptotagmin associated protein, N-terminal half	Rn
11 Syntaxin 1A	GEMIDRIEYNVEHAVDYVERAVSDTKKAVKYQSKARRKK	227-265	39	4612.2	9.46	+3	+	Synaptotagmin associated protein, C-terminal half	Rn
12 Tlg 1	GQLLDNMDEGMDGVVNKLARGRRQLEWVYEKNKEKY	167-202	36	4283.8	6.35	0	+	t-SNARE of late Golgi compartment, C-terminal half	Sc
13 Vamp 2	NLTSNRRLQQTQAQVDEVVDIMRVNVDKVLERDQK	24-58	35	4139.6	6.27	0	+	Vesicle associated membrane protein, N-terminal half	Rn
14 Vamp 2	LSELDDRADALQAGASQFETSAAKLKRKYWWKNLK	59-94	35	4039.5	9.31	+2	w	Vesicle associated membrane protein, C-terminal half	Rn
15 Vam 7	NELLTALEDDVDNTGRRLQIANKKARHFNNSA	285-316	32	3624.9	6.77	0	w	Vacuolar morphogenesis protein 7, C-terminal half	Sc
16 Vti 1	RETLENARQTLFQADSYVDKSIKTLKTMTRRLVA	159-192	34	3984.5	9.98	+3	+	Vesicle transport protein, C-terminal half	Sc
17 Canx	DTSAPTSPKVTYKAPVPTG C	50-68	20	2020.2	8.18	+1	-	Calnexin precursor, PP90	Cf
18 Canx	C AEEDEILNRSPRNRKPRRE	573-591	20	2468.7	8.22	+1	-	Calnexin precursor, PP90	Cf
19 □-Crystallin	MDIAIHHPWIRRPFFPFHSPSRLF	1-24	24	3005.5	11.7	+5	-	B chain	Hs
20 DLG 4	SPAHLPNQANSPPVI C	25-39	16	1644.8	6.45	0	-	Presynaptic density protein 95	Rn
21 DLG 4	NEISHSSYLGTDYPT C	270-284	16	1786.8	4.35	-1	-	Presynaptic density protein 95	Rn
22 FLAG	DYKDDDDK	1-8	8	1012.9	3.97	-3	-	artificial sequence	-
23 Lox	C YLRPSIVENSVAI	650-662	14	1563.8	5.99	0	-	Arachidonate 12/15-lipoxygenase	Oc
24 Lysozyme	LRLKIYKDTEGYY	13-25	13	1661.9	8.38	+1	e	Lysozyme	T4
25 Mtj 1	ELLGRKKRERKKKTGSK	177-193	17	2042.4	11.17	+7	+	DnaJ homolog Mtj1	Mm
26 Psb 7	RRNAVLEADFAKRGYK C	20-35	17	1997.3	9.78	+3	-	Proteasome subunit □ type 7 precursor	Hs
27 Psb 7	C LEIEVLEETVQTMDTS	262-277	17	1940.1	3.45	-5	-	Proteasome subunit □ type 7 precursor	Hs
28 RAG 1	AASLPSTLSFFSSAPDE C *additional F*	2-18	18	1830.0	3.67	-2	-	V(D)J recombination activating protein 1	Mm
29 RAG 1	C EDSLESQDSMEF	1029-1040	13	1519.5	3.39	-5	-	V(D)J recombination activating protein 1	Mm
30 RAG 2	SLGMVTVGHN C *G should be Q*	2-11	11	1117.3	6.45	0	-	V(D)J recombination activating protein 2	Mm
31 RAG 2	C PAKKSFLRRLFD	516-527	13	1580.9	10.05	+3	-	V(D)J recombination activating protein 2	Mm
32 Rim	C LTEEERNIIMAVMDRQKEEEEKEE	28-51	25	3082.4	4.36	-6	+	Rab3-interacting molecule 1	Rn
33 S 3	C GKPEPPAMPQPV	229-240	13	1350.6	5.99	0	-	40S ribosomal protein	Hs
34 Sec 61 □	AIKFLEVIKPFC	1-12	12	1407.7	8.24	+1	-	Protein transport protein Sec61□	Cf
35 Sec 61 □	C KEQSEVGSMGALLF	462-475	15	1598.8	4.53	-1	-	Protein transport protein Sec61□	Cf
36 Sec 61 □	PGPTPSGTN C	1-9	10	930.0	5.91	0	-	Protein transport protein Sec61□	Cf
37 Sec 63 L	MAGQQFQYDDSGN C	(-1)-12	14	1563.6	3.56	-2	-	Translocation protein Sec63 homolog	Hs
38 Sec 63 L	C PRDQNAEQIRLKNIR	35-49	16	1954.2	9.50	+2	-	Translocation protein Sec63 homolog	Hs
39 Sec 63 L	C KVSKTDREYQEYN	91-103	14	1762.9	6.17	0	-	Translocation protein Sec63 homolog	Hs
40 Sec 63 L	C QYNKDATSRPTDNIL	258-272	16	1839.0	5.95	0	-	Translocation protein Sec63 homolog	Hs
41 Sec 63 L	C DEDQEDSEGFEDSFEE	735-750	17	2009.8	3.28	-10	-	Translocation protein Sec63 homolog	Hs
42 SRP 14	MDGLKKRDKKNKTKK	91-105	15	1818.2	10.39	+6	w	Signal recognition particle 14 kDa subunit	Hs
43 SRP R □	KKFEDSEKAKKPVR C	137-150	15	1793.1	9.52	+3	-	Signal recognition particle receptor □ subunit	Cf
44 SRP R □	EKELNTLRVTRSAA C	196-209	15	1690.9	8.32	+1	-	Signal recognition particle receptor □ subunit	Hs
45 Tom 40	GTKQLSPTEAFPVLVGD C	135-151	18	1862.1	4.37	-1	-	Translocase of outer membrane 40 kDa subunit	Mm
46 Tom 40	C AFLNHRKNKFL	340-350	12	1490.7	10.06	+3	-	Translocase of outer membrane 40 kDa subunit	Mm
47 M-Tomosyn	PYRREPRSPRKSRQ C	678-691	15	1916.1	11.44	+5	-	Syntaxin 1 binding protein	Rn
48 M-Tomosyn	GELARARLALDERG C	1064-1077	15	1629.8	6.18	0	-	Syntaxin 1 binding protein	Rn
49 M-Tomosyn	DERGQKLSDLEER C	1074-1086	14	1677.8	4.51	-2	-	Syntaxin 1 binding protein	Rn
50 Unc 18	C SQMLKKMPQYQKEL	328-341	15	1855.2	9.11	+2	-	Syntaxin binding protein 1, N-Sec 1	Mm

Peptide	Sequence	Residue	length [aa]	M_W [Da]	pI	z	©	Comments	¶
51 VDAC 1	AVPPTYADLGKSARDVFTK C	1-19	20	2139.4	8.22	+1	-	Voltage-dependent anion channel protein 1	Rn
52 Gol	AVMGMVRRAIPNLIAFDICGVQPMNSPTG	94-122	29	3059.6	8.29	+1	+	Major capsid protein gene product 23	T4
53 Gonc 31mer	MDIAIFDICGVQPMNSPTGEDQVDPRLIDGK	-	31	3375.8	3.90	-4	+	self designed peptide	-
54 Gonc 29mer	IAIFDICGVQPMNSPTGEDQVDPRLIDGK	-	29	3129.6	4.04	-3	-	self designed peptide	-
55 Gonc 27mer	IFDICGVQPMNSPTGEDQVDPRLIDGK	-	27	2945.3	4.04	-3	-	self designed peptide	-
56 Gonc 25mer	DICGVQPMNSPTGEDQVDPRLIDGK	-	25	2685.0	4.04	-3	-	self designed peptide	-
57 Gonc 23mer	CGVQPMNSPTGEDQVDPRLIDGK	-	23	2456.7	4.23	-2	-	self designed peptide	-
58 Gonc 21mer	VQPMNSPTGEDQVDPRLIDGK	-	21	2296.5	4.23	-2	-	self designed peptide	-
59 Gonc 19mer	PMNSPTGEDQVDPRLIDGK	-	19	2069.3	4.23	-2	-	self designed peptide	-
60 Gonc 17mer	NSPTGEDQVDPRLIDGK	-	17	1841.0	4.23	-2	-	self designed peptide	-
61 Gonc 15mer	PTGEDQVDPRLIDGK	-	15	1639.8	4.23	-2	-	self designed peptide	-
62 Gonc 13mer	GEDQVDPRLIDGK	-	13	1441.6	4.23	-2	-	self designed peptide	-
63 Prol	EDQVDPRLIDGKPNLIAFDICGVQPMNSPTG	-	31	3340.7	4.04	-3	e	self designed peptide	-
64 Senc	MDIAISLKETSCRYRKSAQKEDQVDPRLIDGK	-	32	3695.2	7.90	+1	e	self designed peptide	-

Table 7.4: Complete list of peptides used in this work.

Peptide names are given in commonly used abbreviations. N or C for the peptides # 1-15 denotes the N- or C-terminal half of the coiled coil region of the peptide derived from the corresponding SNARE protein. Several peptides were designed to raise antibodies and contain therefore a cysteine at either terminus. In cases where this amino acid is not part of the original sequence, the C is separated from the rest of the sequence. The length of the peptides are given by their number of amino acids. The molecular weight M_W, the isoelectric point pI, and the charge z were calculated using the the sequence analysis tool "ProtParam" from the ExPASy Molecular Biology Server at *http://us.expasy.org/tools/protparam.html*; the charge is calculated as $z = (-1)\bullet\{\Box(D + E)\} + (+1)\bullet\{\Box(R + K)\}$, not considering the contribution of the N- and C-termini, since only the overall charge is given. The strength of the competition © is based on visual comparisons between titrations for each peptide and therefore only of qualitative nature. A "+" indicates competition, a "-" indicates no competition, a "w" is indicative of a weak competition and an "e" indicates even an enhancement in crosslinking.

¶: abbreviations of taxonomic terms are *Bacteriophage T4* (T4), *Canis familiaris* (Cf), *Homo sapiens* (Hs), *Mus musculus* (Mm), *Oryctolagus cuniculus* (Oc), *Rattus norvegicus* (Rn), and *Saccharomyces cerevisiae* (Sc).

The color code for the artificial peptides (number 53-64) is as follows: sequences derived from Gol are in blue, from Sec 22 Cccp in green, the Protein C tag is in red, and the N-acetylation recognition sequence in magenta. Mistakes in the sequences of the peptides are in orange.

I thank Drs. Colin Kleanthous, Tom Melia, Ouathek Ouerfelli, Fabienne Paumet, Thomas Söllner, Oleg Varmalow, and Richard Zimmermann for their kind provision of the majority of oligopeptides. The peptides Gonc, Prol and Senc were initially ordereded from SynPep (Dublin, CA). In later experiments Gonc and its derivatives were ordered from Dr. Jan Pohl (Emory University Microchemical Facility, Atlanta GA). T4 Lysozyme was ordered from Sigma Genosys (The Woodlands, TX).

8 Abbreviations

’	prime end
*	indicates in connection with Phe or Lys a photoactivatable crosslinker
°C	degree Celsius
1D	one dimensional NMR
2D	two dimensional NMR
aa	amino acid(s) with respect to proteins or aminoacyl with respect to tRNA
APDP	N-[4-(p-Azidosalicylamido)butyl]-3’-(2’-pyridyldithio)propionamide
APP	amyloid precursor protein
APS	ammonium peroxodisulfate
Amp	ampicillin
A site	aminoacyl-tRNA-binding site
ATP	adenosine 5’-triphosphate
bp	basepair(s)
BSA	bovine serum albumin
c	concentration
Ci	Curie
cpm	counts per minute
CTP	cytidine 5’-triphosphate
D_2O	deuterium oxide, heavy water
d	path length [cm]
δ	chemical shift [ppm]
Da	Dalton
DTT	1,4-dithiothreitol
DMSO	dimethyl sulfoxide
DNA	deoxyribonucleic acid
E. coli	*Escherichia coli*
EDTA	ethylenediaminetetraacetic acid
eEF1A	eukaryotic translation elongation factor 1A, formerly known as eEF1α or EF1α
EF1A	prokaryotic translation elongation factor 1A, formerly EF-Tu (thermal unstable)
ER	endoplasmic reticulum
E site	tRNA-exit site
EtOH	ethanol

ffLuc	luciferase from the firefly *Photinus pyralis*
FPLC	fast performance liquid chromatography
g	gram or centrifugal force
GDP	guanosine 5'-diphosphate
Gonc	derived from the Gol peptide (growth on Lit) and the Protein C
GST	glutathione S-transferase
GST-eEF1A	GST-eEF1A fusion protein
GTP	guanosine 5'-triphosphate
h	hour
Hepes	4-(2-hydroxyethyl)piperazine-1-ethanesulfonic acid
HSQC	heteronuclear single quantum coherence
IPTG	Isopropyl □-D-1-thiogalactopyranoside
KAc	potassium acetate, CH_3COOK
kDa	kilodalton
□	wavelength in [nm], an index may indicate a specific wavelength or a range
LB	Luria-Bertani media
M	molar
MES	2-morpholinoethanesulfonic acid monohydrate
^{35}S-Met	methionine radiolabeled with ^{35}S
MgAc	magnesium acetate tetrahydrate, $(CH_3COO)_2Mg \bullet 4H_2O$
MHC	major histocompatability complex
min	minute(s)
mol	mole
M_W	molecular weight in [Da] or [kDa]
NaAc	sodium acetate, CH_3COONa
NAC	nascent polypeptide-associated complex
NMR	nuclear magnetic resonance
NOESY	nuclear Overhauser effect spectroscopy
NTPase	nucleoside triphosphatase
$OD_{□}$	optical density at the wavelength □, □ in [nm]
P_i	inorganic phosphate, orthophosphate, HPO_4^{2-}
PAG	polyacrylamide gel
PAGE	polyacrylamide gel electrophoresis
PDB	protein data bank at *http://www.rcsb.org/pdb/*

PEG	polyethylene glycol (subsequent number refers to the average molecular weight)
pI	isoelectric point
pPL	preprolactin
ppm	parts per million
P site	peptidyl-tRNA-binding site
RAF	ribosome associated factor
RNA	ribonucleic acid
	(i) mRNA is messenger RNA
	(ii) aa-tRNA^{aa} is transfer RNA charged with amino acids in general,
	specifically charged populations are marked by the three letter amino acid
	(iii) tRNA^{aa} is transfer RNA that is not charged with amino acids
	(iv) rRNA is ribosomal RNA
RNC	ribosome nascent chain complex
rpm	revolutions per minute
s	second(s)
SDS	sodium dodecyl sulfate
Sec 22 Cccp	C-terminal coiled coil part of the SNARE protein Sec 22
S_N2	nucleophilic substitution of second-order
SRP	signal recognition particle
t	time
T	temperature [°C]
TDBA	4-(3-trifluoromethyldiazirino) benzoic acid
TEMED	N,N,N',N'-tetramethylethylenediamine
Tris	tris(hydroxymethyl)-aminomethane
U	unit
UTP	uridine 5'-triphosphate
UV	ultraviolet
V	volt
v/v	volume per volume ratio
w/v	weight per volume ratio
z	charge

Inorganic substances (e. g. sodium chloride) are generally written in their elements (NaCl) according to the current IUPAC-nomenclature. Amino acids are written either in their standard one-letter or three-letter code.

9 Literature

9.1 Publications

Hotokezaka, Y., Többen, U., Hotokezaka, H., van Leyen, K., Beatrix, B., Smith, D. H., Nakamura, T., and Wiedmann, M. (2002) *J Biol Chem* **277**, 18545-18551

9.2 References

1. Claude, A. (1938) *Proc Soc Exp Biol med* **39**, 1
2. Claude, A. (1941) *Cold Spring Harbor Symp Quant Biol* **9**, 263
3. Roberts, R. B. (1958) (Roberts, R. B., ed), *Microsomal particles and protein synthesis*, Pergamon Press, New York
4. Jeener, R., and Brachet, J. (1942) *Acta Biol Belg* **2**
5. Luria, S. E., Delbrück, M., and Anderson, T. F. (1943) *J Bacteriol* **46**, 57
6. Palade, G. E. (1955) *J Biophys Biochem Cytol* **1**, 59-68
7. Palade, G. E., and Siekevitz, P. (1956) *J Biophys Biochem Cytol* **2**, 171-200
8. Littlefield, J. W., Keller, E. B., Gross, J., and Zamecnik, P. C. (1955) *J Biol Chem* **217**, 111-123
9. Keller, E. B., and Littlefield, J. W. (1957) *J Biol Chem* **224**, 13-30
10. Nomura, M., and Erdmann, V. A. (1970) *Nature* **228**, 744-748
11. Ban, N., Nissen, P., Hansen, J., Moore, P. B., and Steitz, T. A. (2000) *Science* **289**, 905-920
12. Cate, J. H., Yusupov, M. M., Yusupova, G. Z., Earnest, T. N., and Noller, H. F. (1999) *Science* **285**, 2095-2104
13. Spahn, C. M., Beckmann, R., Eswar, N., Penczek, P. A., Sali, A., Blobel, G., and Frank, J. (2001) *Cell* **107**, 373-386
14. Woolhead, C. A., McCormick, P. J., and Johnson, A. E. (2004) *Cell* **116**, 725-736
15. Wiedmann, B., Sakai, H., Davis, T. A., and Wiedmann, M. (1994) *Nature* **370**, 434-440.
16. Nissen, P., Hansen, J., Ban, N., Moore, P. B., and Steitz, T. A. (2000) *Science* **289**, 920-930
17. Cech, T. R. (2000) *Science* **289**, 878-879
18. Ramakrishnan, V. (2002) *Cell* **108**, 557-572
19. Youngman, E. M., Brunelle, J. L., Kochaniak, A. B., and Green, R. (2004) *Cell* **117**, 589-599
20. Wimberly, B. T., Brodersen, D. E., Clemons, W. M., Jr., Morgan-Warren, R. J., Carter, A. P., Vonrhein, C., Hartsch, T., and Ramakrishnan, V. (2000) *Nature* **407**, 327-339

21. Barta, A., Dorner, S., and Polacek, N. (2001) *Science* **291**, 203
22. Berg, J. M., and Lorsch, J. R. (2001) *Science* **291**, 203
23. Polacek, N., Gaynor, M., Yassin, A., and Mankin, A. S. (2001) *Nature* **411**, 498-501
24. Muth, G. W., Ortoleva-Donnelly, L., and Strobel, S. A. (2000) *Science* **289**, 947-950
25. Thompson, J., Kim, D. F., O'Connor, M., Lieberman, K. R., Bayfield, M. A., Gregory, S. T., Green, R., Noller, H. F., and Dahlberg, A. E. (2001) *Proc Natl Acad Sci U S A* **98**, 9002-9007
26. Moazed, D., and Noller, H. F. (1989) *Cell* **57**, 585-597
27. Moazed, D., and Noller, H. F. (1989) *Nature* **342**, 142-148
28. Bretscher, M. S. (1968) *Nature* **218**, 675-677
29. Carter, A. P., Clemons, W. M., Brodersen, D. E., Morgan-Warren, R. J., Wimberly, B. T., and Ramakrishnan, V. (2000) *Nature* **407**, 340-348
30. Moore, P. B., and Steitz, T. A. (2002) *Nature* **418**, 229-235
31. Kisselev, L. L., and Buckingham, R. H. (2000) *Trends Biochem Sci* **25**, 561-566
32. Janosi, L., Hara, H., Zhang, S., and Kaji, A. (1996) *Adv Biophys* **32**, 121-201
33. Selmer, M., Al-Karadaghi, S., Hirokawa, G., Kaji, A., and Liljas, A. (1999) *Science* **286**, 2349-2352
34. Cavallius, J., Zoll, W., Chakraburtty, K., and Merrick, W. C. (1993) *Biochim Biophys Acta* **1163**, 75-80
35. Condeelis, J. (1995) *Trends Biochem Sci* **20**, 169-170
36. Dharmawardhane, S., Demma, M., Yang, F., and Condeelis, J. (1991) *Cell Motil Cytoskeleton* **20**, 279-288
37. Slobin, L. I. (1980) *Eur J Biochem* **110**, 555-563
38. Demma, M., Warren, V., Hock, R., Dharmawardhane, S., and Condeelis, J. (1990) *J Biol Chem* **265**, 2286-2291
39. Edmonds, B. T., Bell, A., Wyckoff, J., Condeelis, J., and Leyh, T. S. (1998) *J Biol Chem* **273**, 10288-10295
40. Edmonds, B. T., Murray, J., and Condeelis, J. (1995) *J Biol Chem* **270**, 15222-15230
41. Liu, G., Tang, J., Edmonds, B. T., Murray, J., Levin, S., and Condeelis, J. (1996) *J Cell Biol* **135**, 953-963
42. Kuriyama, R., Savereide, P., Lefebvre, P., and Dasgupta, S. (1990) *J Cell Sci* **95 (Pt 2)**, 231-236
43. Ohta, K., Toriyama, M., Miyazaki, M., Murofushi, H., Hosoda, S., Endo, S., and Sakai, H. (1990) *J Biol Chem* **265**, 3240-3247
44. Durso, N. A., and Cyr, R. J. (1994) *Plant Cell* **6**, 893-905
45. Shiina, N., Gotoh, Y., Kubomura, N., Iwamatsu, A., and Nishida, E. (1994) *Science* **266**, 282-285

46. Gonen, H., Schwartz, A. L., and Ciechanover, A. (1991) *J Biol Chem* **266**, 19221-19231
47. Gonen, H., Smith, C. E., Siegel, N. R., Kahana, C., Merrick, W. C., Chakraburtty, K., Schwartz, A. L., and Ciechanover, A. (1994) *Proc Natl Acad Sci U S A* **91**, 7648-7652
48. Hopfield, J. J. (1974) *Proc Natl Acad Sci U S A* **71**, 4135-4139
49. Ninio, J. (1975) *Biochimie* **57**, 587-595
50. Saraste, M., Sibbald, P. R., and Wittinghofer, A. (1990) *Trends Biochem Sci* **15**, 430-434
51. Sprang, S. R. (1997) *Annu Rev Biochem* **66**, 639-678
52. Andersen, G. R., Nissen, P., and Nyborg, J. (2003) *Trends Biochem Sci* **28**, 434-441
53. Andersen, G. R., Pedersen, L., Valente, L., Chatterjee, I., Kinzy, T. G., Kjeldgaard, M., and Nyborg, J. (2000) *Mol Cell* **6**, 1261-1266
54. Andersen, G. R., Valente, L., Pedersen, L., Kinzy, T. G., and Nyborg, J. (2001) *Nat Struct Biol* **8**, 531-534
55. Janssen, G. M., and Moller, W. (1988) *J Biol Chem* **263**, 1773-1778
56. Kjeldgaard, M., Nissen, P., Thirup, S., and Nyborg, J. (1993) *Structure* **1**, 35-50
57. Kjeldgaard, M., and Nyborg, J. (1992) *J Mol Biol* **223**, 721-742
58. Berchtold, H., Reshetnikova, L., Reiser, C. O., Schirmer, N. K., Sprinzl, M., and Hilgenfeld, R. (1993) *Nature* **365**, 126-132
59. Nissen, P., Kjeldgaard, M., Thirup, S., Polekhina, G., Reshetnikova, L., Clark, B. F., and Nyborg, J. (1995) *Science* **270**, 1464-1472
60. Andersen, G. R., Thirup, S., Spremulli, L. L., and Nyborg, J. (2000) *J Mol Biol* **297**, 421-436
61. Budkevich, T. V., Timchenko, A. A., Tiktopulo, E. I., Negrutskii, B. S., Shalak, V. F., Petrushenko, Z. M., Aksenov, V. L., Willumeit, R., Kohlbrecher, J., Serdyuk, I. N., and El'skaya, A. V. (2002) *Biochemistry* **41**, 15342-15349
62. Wiberg, N. (1985) *Hollemann-Wiberg: Lehrbuch der Anorganischen Chemie*, 91-100 Ed., Walter de Gruyter, Berlin
63. Leipe, D. D., Koonin, E. V., and Aravind, L. (2003) *J Mol Biol* **333**, 781-815
64. Leipe, D. D., Wolf, Y. I., Koonin, E. V., and Aravind, L. (2002) *J Mol Biol* **317**, 41-72
65. Goldberg, J. (1998) *Cell* **95**, 237-248
66. Boriack-Sjodin, P. A., Margarit, S. M., Bar-Sagi, D., and Kuriyan, J. (1998) *Nature* **394**, 337-343
67. Worthylake, D. K., Rossman, K. L., and Sondek, J. (2000) *Nature* **408**, 682-688
68. Wang, Y., Jiang, Y., Meyering-Voss, M., Sprinzl, M., and Sigler, P. B. (1997) *Nat Struct Biol* **4**, 650-656
69. Kawashima, T., Berthet-Colominas, C., Wulff, M., Cusack, S., and Leberman, R. (1996) *Nature* **379**, 511-518

70. Görlich, D., Kurzchalia, T. V., Wiedmann, M., and Rapoport, T. A. (1991) *Methods Cell Biol* **34**, 241-262

71. Gilmore, R., Collins, P., Johnson, J., Kellaris, K., and Rapiejko, P. (1991) *Methods Cell Biol* **34**, 223-239

72. Brunner, J. (1993) *Annu Rev Biochem* **62**, 483-514

73. Laemmli, U. K. (1970) *Nature* **227**, 680-685

74. Blum, H., Beier, H., and Gross, H. J. (1987) *Electrophoresis* **8**, 93-99

75. Hendrick, J. P., Langer, T., Davis, T. A., Hartl, F. U., and Wiedmann, M. (1993) *Proc Natl Acad Sci U S A* **90**, 10216-10220

76. Thiele, D., Cottrelle, P., Iborra, F., Buhler, J. M., Sentenac, A., and Fromageot, P. (1985) *J Biol Chem* **260**, 3084-3089

77. Bingham, R., Ekunwe, S. I., Falk, S., Snyder, L., and Kleanthous, C. (2000) *J Biol Chem* **275**, 23219-23226

78. Flynn, G. C., Pohl, J., Flocco, M. T., and Rothman, J. E. (1991) *Nature* **353**, 726-730

79. Coleman, D. E., Berghuis, A. M., Lee, E., Linder, M. E., Gilman, A. G., and Sprang, S. R. (1994) *Science* **265**, 1405-1412

80. Cool, R. H., and Parmeggiani, A. (1991) *Biochemistry* **30**, 362-366

81. Scheffzek, K., Ahmadian, M. R., Kabsch, W., Wiesmuller, L., Lautwein, A., Schmitz, F., and Wittinghofer, A. (1997) *Science* **277**, 333-338

82. Selkoe, D. J. (1998) *Trends Cell Biol* **8**, 447-453

83. Selkoe, D. J. (1999) *Nature* **399**, A23-31

84. Buxbaum, J. D., Liu, K. N., Luo, Y., Slack, J. L., Stocking, K. L., Peschon, J. J., Johnson, R. S., Castner, B. J., Cerretti, D. P., and Black, R. A. (1998) *J Biol Chem* **273**, 27765-27767

85. Marcinkiewicz, M., and Seidah, N. G. (2000) *J Neurochem* **75**, 2133-2143

86. Hussain, I., Powell, D., Howlett, D. R., Tew, D. G., Meek, T. D., Chapman, C., Gloger, I. S., Murphy, K. E., Southan, C. D., Ryan, D. M., Smith, T. S., Simmons, D. L., Walsh, F. S., Dingwall, C., and Christie, G. (1999) *Mol Cell Neurosci* **14**, 419-427

87. Lin, X., Koelsch, G., Wu, S., Downs, D., Dashti, A., and Tang, J. (2000) *Proc Natl Acad Sci U S A* **97**, 1456-1460

88. Sinha, S., Anderson, J. P., Barbour, R., Basi, G. S., Caccavello, R., Davis, D., Doan, M., Dovey, H. F., Frigon, N., Hong, J., Jacobson-Croak, K., Jewett, N., Keim, P., Knops, J., Lieberburg, I., Power, M., Tan, H., Tatsuno, G., Tung, J., Schenk, D., Seubert, P., Suomensaari, S. M., Wang, S., Walker, D., John, V., and et al. (1999) *Nature* **402**, 537-540

89. Vassar, R., Bennett, B. D., Babu-Khan, S., Kahn, S., Mendiaz, E. A., Denis, P., Teplow, D. B., Ross, S., Amarante, P., Loeloff, R., Luo, Y., Fisher, S., Fuller, J., Edenson, S., Lile, J., Jarosinski, M. A., Biere, A. L., Curran, E., Burgess, T., Louis, J. C., Collins, F., Treanor, J., Rogers, G., and Citron, M. (1999) *Science* **286**, 735-741

90. Yan, R., Bienkowski, M. J., Shuck, M. E., Miao, H., Tory, M. C., Pauley, A. M., Brashier, J. R., Stratman, N. C., Mathews, W. R., Buhl, A. E., Carter, D. B., Tomasselli, A. G., Parodi, L. A., Heinrikson, R. L., and Gurney, M. E. (1999) *Nature* **402**, 533-537

91. Wolfe, M. S., Xia, W., Ostaszewski, B. L., Diehl, T. S., Kimberly, W. T., and Selkoe, D. J. (1999) *Nature* **398**, 513-517

92. Wolfe, M. S., and Selkoe, D. J. (2002) *Science* **296**, 2156-2157

93. Steiner, H., and Haass, C. (2000) *Nat Rev Mol Cell Biol* **1**, 217-224

94. Rawson, R. B., Zelenski, N. G., Nijhawan, D., Ye, J., Sakai, J., Hasan, M. T., Chang, T. Y., Brown, M. S., and Goldstein, J. L. (1997) *Mol Cell* **1**, 47-57

95. Baldini, G., Martoglio, B., Schachenmann, A., Zugliani, C., and Brunner, J. (1988) *Biochemistry* **27**, 7951-7959

96. Graf, R., Brunner, J., Dobberstein, B., and Martoglio, B. (1998) in *Cell Biology: A Laboratory Handbook* Vol. 4, 2nd Ed., pp. 495-501, Academic Press

97. Jackson, R. J., and Hunt, T. (1983) *Methods Enzymol* **96**, 50-74

98. Erickson, A. H., and Blobel, G. (1983) *Methods Enzymol* **96**, 38-50

99. Edbauer, D., Winkler, E., Regula, J. T., Pesold, B., Steiner, H., and Haass, C. (2003) *Nat Cell Biol* **5**, 486-488

100. Yu, G., Nishimura, M., Arawaka, S., Levitan, D., Zhang, L., Tandon, A., Song, Y. Q., Rogaeva, E., Chen, F., Kawarai, T., Supala, A., Levesque, L., Yu, H., Yang, D. S., Holmes, E., Milman, P., Liang, Y., Zhang, D. M., Xu, D. H., Sato, C., Rogaev, E., Smith, M., Janus, C., Zhang, Y., Aebersold, R., Farrer, L. S., Sorbi, S., Bruni, A., Fraser, P., and St George-Hyslop, P. (2000) *Nature* **407**, 48-54

101. Kimberly, W. T., LaVoie, M. J., Ostaszewski, B. L., Ye, W., Wolfe, M. S., and Selkoe, D. J. (2003) *Proc Natl Acad Sci U S A* **100**, 6382-6387

102. Esler, W. P., Kimberly, W. T., Ostaszewski, B. L., Ye, W., Diehl, T. S., Selkoe, D. J., and Wolfe, M. S. (2002) *Proc Natl Acad Sci U S A* **99**, 2720-2725

103. Ellis, R. J. (2001) *Trends Biochem Sci* **26**, 597-604.

104. Naylor, D. J., and Hartl, F. U. (2001) *Biochem Soc Symp*, 45-68.

105. Blobel, G. (1980) *Proc Natl Acad Sci U S A* **77**, 1496-1500

106. Stryer, L. (1995) *Biochemistry*, 4th Ed., W. H. Freeman and Company, New York

107. Turner, G. C., and Varshavsky, A. (2000) *Science* **289**, 2117-2120
108. Schubert, U., Anton, L. C., Gibbs, J., Norbury, C. C., Yewdell, J. W., and Bennink, J. R. (2000) *Nature* **404**, 770-774.
109. Kurzchalia, T. V., Wiedmann, M., Girshovich, A. S., Bochkareva, E. S., Bielka, H., and Rapoport, T. A. (1986) *Nature* **320**, 634-636
110. Pfund, C., Lopez-Hoyo, N., Ziegelhoffer, T., Schilke, B. A., Lopez-Buesa, P., Walter, W. A., Wiedmann, M., and Craig, E. A. (1998) *Embo J* **17**, 3981-3989
111. Hotokezaka, Y., Többen, U., Hotokezaka, H., van Leyen, K., Beatrix, B., Smith, D. H., Nakamura, T., and Wiedmann, M. (2002) *J Biol Chem* **277**, 18545-18551
112. Plath, K., and Rapoport, T. A. (2000) *J Cell Biol* **151**, 167-178.
113. Caldas, T. D., El Yaagoubi, A., and Richarme, G. (1998) *J Biol Chem* **273**, 11478-11482
114. Kudlicki, W., Coffman, A., Kramer, G., and Hardesty, B. (1997) *J Biol Chem* **272**, 32206-32210
115. Frydman, J., Nimmesgern, E., Erdjument-Bromage, H., Wall, J. S., Tempst, P., and Hartl, F. U. (1992) *Embo J* **11**, 4767-4778
116. Frydman, J., Nimmesgern, E., Ohtsuka, K., and Hartl, F. U. (1994) *Nature* **370**, 111-117
117. Nathans, D., and Lipmann, F. (1961) *Proc Natl Acad Sci U S A* **47**, 497-504
118. Parisi, B., Milanesi, G., Van Etten, J. L., Perani, A., and Ciferri, O. (1967) *J Mol Biol* **28**, 295-309
119. Rendi, R., and Ochoa, S. (1962) *J Biol Chem* **237**, 3707-3710
120. Uchiumi, T., Honma, S., Nomura, T., Dabbs, E. R., and Hachimori, A. (2002) *J Biol Chem* **277**, 3857-3862
121. Dafforn, T. R., Della, M., and Miller, A. D. (2001) *J Biol Chem* **276**, 49310-49319
122. Tasab, M., Batten, M. R., and Bulleid, N. J. (2000) *Embo J* **19**, 2204-2211
123. Negrutskii, B. S., and Deutscher, M. P. (1991) *Proc Natl Acad Sci U S A* **88**, 4991-4995
124. Forchhammer, J., and Lindahl, L. (1971) *J Mol Biol* **55**, 563-568
125. Waldron, C., Jund, R., and Lacroute, F. (1974) *FEBS Lett* **46**, 11-16
126. Bergmann, J. E., and Lodish, H. F. (1979) *J Biol Chem* **254**, 11927-11937
127. Wickner, S., Maurizi, M. R., and Gottesman, S. (1999) *Science* **286**, 1888-1893
128. Keiler, K. C., Waller, P. R., and Sauer, R. T. (1996) *Science* **271**, 990-993
129. DePristo, M. A., De Bakker, P. I., and Blundell, T. L. (2004) *Structure (Camb)* **12**, 831-838
130. Birnboim, H. C., and Doly, J. (1979) *Nucleic Acids Res* **7**, 1513-1523
131. Sambrook, J., Fritsch, E. F., and Maniatis, T. (1989) *Molecular cloning - a laboratory manual*, 2nd Ed., Cold Spring Harbor Laboratory Press, Cold Spring Harbor
132. Zecherle, G. N., Oleinikov, A., and Traut, R. R. (1992) *Biochemistry* **31**, 9526-9532

133. Rinke, J., Meinke, M., Brimacombe, R., Fink, G., Rommel, W., and Fasold, H. (1980) *J Mol Biol* **137**, 301-304

134. Randerath, K., and Randerath, E. (1964) *J Chromatogr* **16**, 111-125

135. Schiedel, A. C., Barnekow, A., and Mayer, T. (1995) *FEBS Lett* **376**, 113-119